

JAANUS LIIGAND

Standard substance free quantification
for LC/ESI/MS analysis based on
the predicted ionization efficiencies



JAAANUS LIIGAND

Standard substance free quantification
for LC/ESI/MS analysis based on
the predicted ionization efficiencies



Institute of Chemistry, Faculty of Science and Technology, University of Tartu,
Estonia

The dissertation was accepted for the commencement of the degree of *Doctor philosophiae* in Chemistry at the University of Tartu on June 20th, 2019 by the Council of Institute of Chemistry, Faculty of Science and Technology, University of Tartu.

Supervisor: Assoc. Prof. Anneli Kruve-Viil, Institute of Chemistry,
University of Tartu, Estonia, Department of Environmental
Science and Analytical Chemistry, Stockholm University,
Sweden

Opponent: Prof. Jonathan Martin, Stockholm University, Sweden

Commencement: Room 1021, Chemicum, 14A Ravila Street, Tartu,
on August 22nd in 2019, at 13.15.

Graduate School on Functional Materials and Technologies (GSFMT), Univer-
sity of Tartu and Tallinn University of Technology, EU Social Funds project
1.2.0401.09-0079



European Union
European Regional
Development Fund



Investing
in your future

ISSN 1406-0299

ISBN 978-9949-03-104-7 (print)

ISBN 978-9949-03-105-4 (PDF)

Copyright: Jaanus Liigand, 2019

University of Tartu Press
www.tyk.ee

CONTENTS

LIST OF ORIGINAL PUBLICATIONS	7
Author's contribution	7
ABBREVIATIONS.....	8
INTRODUCTION.....	9
REVIEW OF LITERATURE.....	11
Properties of compounds that affect ionization efficiency	11
Solvent effects on ionization efficiency	13
Solvent type.....	13
Additives	15
Concentration of additives.....	17
Previous ionization efficiency models.....	17
The benefit of ionization efficiency model	19
EXPERIMENTAL	21
Chemicals	21
Equipment	21
Ionization efficiency measurement.....	23
Descriptor calculation.....	24
Data pre-processing.....	25
Ionization efficiency prediction model development	26
Concentration from predicted ionization efficiency	26
Green tea data treatment.....	27
Sample preparation for cereal samples.....	28
Statistical tests	28
Ionization degree measurement.....	28
Discriminant analysis for pH effect.....	29
RESULTS AND DISCUSSION	31
Solvent effects publication	31
Comparison with earlier results.....	33
The impact of organic modifier.....	33
The impact of organic modifier percentage.....	33
The impact of eluent pH.....	34
The interplay between the effect of compound properties and eluent pH on ionization efficiency	35
Processes occurring in the ESI	39
Effect of water phase additives to ionization efficiency.....	40
Properties of compound affecting the pH dependency.....	41
Transferability between instruments	43
Electrospray source design and solution properties	45
Mass spectrometer properties	46
The usefulness of ionization efficiency scales	47

Independent validation	47
Standard substance free quantification.....	48
Predicting ionization efficiencies	48
Quantifying pesticides in cereals.....	50
Different matrices.....	51
Quantifying metabolites in green tea.....	53
Different instruments and labs	54
Retrospective analysis	55
SUMMARY	57
SUMMARY IN ESTONIAN	59
REFERENCES.....	61
ACKNOWLEDGMENTS.....	71
APPENDIX	72
PUBLICATIONS	121
CURRICULUM VITAE	241
ELULOOKIRJELDUS.....	243

LIST OF ORIGINAL PUBLICATIONS

- I. Liigand, J., Kruve, A., Leito, I., Girod, M., Antoine, R. Effect of Mobile Phase on Electrospray Ionization Efficiency. *J. Am. Soc. Mass Spectrom.* 25(11), 1853–1861 (2014)
- II. Liigand, J., Kruve, A., Liigand, P., Laaniste, Asko, Girod, M., Antoine, R., Leito, I. Transferability of the Electrospray Ionization Efficiency Scale between Different Instruments. *J. Am. Soc. Mass Spectrom.* 26(11), 1923–1930 (2015)
- III. Liigand, J., Laaniste, A., Kruve, A. pH effects on Electrospray Ionization Efficiency. *J. Am. Soc. Mass Spectrom.* 28, 461–469 (2017)
- IV. Liigand, J., de Vries, R., Cuyckens, F. Optimization of flow splitting and make-up flow conditions in liquid chromatography-electrospray ionization-mass spectrometry *Rapid. Commun. Mass Spectrom* 33(3), 314–322 (2018)
- V. Liigand, J., Wang, T., Kellogg, J. J., Smedsgaard, J., Cech, N. B., Kruve, A. Quantifying the unquantifiable: Quantification for non-targeted LC/MS screening without standards. *Submitted to Nat Methods*

Author's contribution

- Paper I: Main person responsible for planning and writing the manuscript. Performed all the experimental work.
- Paper II: Main person responsible for planning and writing the manuscript. Performed all the experimental work.
- Paper III: Main person responsible for planning and writing the manuscript. Performed all the experimental work.
- Paper IV: Main person responsible for planning and writing the manuscript. Performed all the experimental work.
- Paper V: Main person responsible for planning and writing the manuscript. Performed the majority of the experimental work.

ABBREVIATIONS

α – ionization degree in solution
ANN – artificial neural network
APCI – atmospheric pressure chemical ionization
DMS – differential mobility spectrometry
ESI – electrospray ionization
HILIC – hydrophilic interaction liquid chromatography
HOMO – highest occupied molecular orbital
HPLC – high-performance liquid chromatography
HRMS – high-resolution mass spectrometry
 $\log IE$ – ionization efficiency value
 $\log P$ – octanol-water partition coefficient
LC – liquid chromatography
MLR – multiple linear regression
MS – mass spectrometry
PLS – partial least squares regression
QDA – quadratic discriminant analysis
RMSE – root-mean-square error
RPLC – reversed-phase liquid chromatography
TFA – trifluoroacetic acid
VIP – variable importance in projection
WANS – weighted average negative sigma, the charge delocalization parameter

INTRODUCTION

Liquid chromatography electrospray ionization mass spectrometry (LC/ESI/MS) is a widely applied high-performance analytical chemistry technique and it is a golden standard for trace analysis of organic compounds.

The targeted LC/ESI/MS analysis does not see the forest behind the trees: it focuses on the analysis of a preselected list of compounds with the aid of standard substances and neglects any further information retrievable from the analysis. The awareness of possible pollutants in the environment is widening, as is the number of small molecules known to direct the life in living organisms. This, on the other hand, increases the number of standard substances required, which is economically unfeasible. Recent developments in hardware and software have made non-targeted analysis feasible and over a couple of last years, it is becoming more and more popular. Non-targeted analysis can detect thousands of molecular features in a single run and identify compounds based on these features. Unfortunately, standard substances are still needed to obtain quantitative information about the detected compounds as the ionization efficiency of electrospray is compound dependent and varies strongly. Standard substances may not be always available.

The ultimate aim of my doctoral thesis is to provide a solution to overcome the need of standard substances and to quantify compounds detected and identified with LC/ESI/MS. I propose an approach of estimating the concentration of detected and identified compounds in LC/ESI/MS analysis using predicted electrospray ionization efficiencies and using the ionization efficiency to convert LC/ESI/MS signals to the concentrations of compounds.

To develop an electrospray ionization efficiency prediction model, it is necessary to understand the mechanism and study the causes. In the chair of analytical chemistry, there is an established approach to measure ionization efficiencies of small singly charged compounds using relative measurements, which gives quantitative insight to processes occurring during the electrospray ionization. I measured the effect of compound structure, eluent and instrument to ionization efficiency to collect meaningful data for model development.

Up to now, the studies in the literature have investigated the ESI process using relatively small sets of compounds and often the studied compounds are from a narrow chemical space. Moreover, the majority of studies are conducted in single eluent composition and on one instrumental setup. There is no guideline to apply this knowledge to different eluent compositions and different instrumental setups. Also, though predicted, the ionization efficiencies have not been used for the quantification purposes in the non-targeted LC/ESI/MS analysis.

The aim of my thesis is to enable standard substance free quantification in LC/ESI/MS analysis. To achieve this, I studied the influence of compound structure to ionization efficiency on a large set of compounds. Furthermore, I studied the effect of chromatographic eluent to ionization efficiency covering

most widely used organic modifiers, additives and pH. Thirdly, the effect of instrumentation on ionization efficiency was studied and finally the model was developed. Moreover, I developed an approach named shortly Quantem to provide standard substance free quantification in LC/ESI/MS analysis that accounts for specific sample (analytes and matrix) and specific method (eluent used, gradient program and instrumentation). The developed Quantem approach is made available as a software to LC/ESI/MS community.

REVIEW OF LITERATURE

Electrospray ionization (ESI) source is used to introduce samples to mass spectrometry (MS) or to connect high-performance liquid chromatography (HPLC) with mass spectrometry. LC/ESI/MS nowadays is the most popular analytical method for metabolomics,¹ drug development and metabolism studies,² environmental screening,³ and food safety analyses⁴ to name some. The scientific audience has described the processes occurring during electrospray ionization with three models: ion evaporation model^{5,6} for small molecules (< 1500 Da), charge residue model⁷ for large molecules, and chain ejection model⁸ for linear intermediate size molecules. This work focuses on the small molecules thus on the ion evaporation model.

Electrospray ionization can be used in positive as well as in negative mode to generate positive or negative gas-phase ions respectively and to introduce these to the mass spectrometer. This work focuses mainly on ESI positive mode. In the positive ionization mode, the ions are intrinsically charged,⁹ formed by protonation^{10,11} or adduct formation with cations such as sodium,^{12,13} potassium,¹⁴ ammonium¹⁵ or formed by electrochemical oxidation in the electrospray needle.¹⁶ Furthermore, the ions may be multiply charged. This work focuses on singly charged ions either intrinsically or formed by protonation.

Although LC/ESI/MS is widely applied, the method is not considered as inherently quantitative as ionization efficiencies, the efficiency of generating gas-phase ions from analyte molecules or ions in the ESI source, of different compounds, may vastly differ. In our group, several orders of magnitude differences in ionization efficiencies have been observed in positive ionization mode.¹⁰ Additionally, ion transport efficiency depends on instrument and source design,^{17,18} and strong matrix effects may affect the analyses.^{19,20} Therefore, calibration with standard substances is needed to get quantitative results of the concentration of the compound of interest in the sample of interest. As standard substances are not always available nor possible to synthesize there is a need for approaches to estimate the concentration of studied analytes with reasonable reliability. First steps to develop new approaches for quantification is to understand which parameters and how these affect the ionization efficiency.

Properties of compounds that affect ionization efficiency

Several groups have studied the physicochemical properties of compounds that affect the ionization efficiency (Table S 1).^{11,21-28} The reported parameters affecting electrospray ionization were gas-phase basicity, basicity in solution (pK_b), hydrophobicity ($\log P$), adjusted mass (hydrogen and carbon ratio in the molecule), and molecular volume.

Amad et al.²² studied the gas phase basicities of used solvents and analytes and found that solvents with higher proton affinities in the gas phase suppress the ionization of analytes. On the other hand, results of Ehrmann et al.²³ show

that gas-phase basicity does not show significant correlation with ionization efficiency, but the pK_b of analytes in solution does affect ionization efficiency. Additionally, they showed that it is not possible to describe ESI as solely a transfer of protonated analyte into the gas phase. For some analytes with very high pK_b values the predicted concentration of the protonated species in solution is significantly below the detection limit; however, these compounds were still detectable in mass spectra.

Oss et al.¹⁰ studied small organic bases in ESI positive mode. The ionization efficiencies were correlated with different molecular properties and significant correlation was observed with molecular volume and with basicity of the molecules.

Henriksen et al.²⁵ studied negative ionization and their results showed that ionization efficiency dependence on pK_a is more complex. Highly acidic compounds would be assumedly most responsive for the analysis due to their tendency to form negative ions. However, for the compounds studied the effect of acidity was not consistent. Many highly acidic compounds were polar and poorly responsive. Furthermore, compounds with very high pK_a values, which would not form anions in bulk solution were still detectable. Additionally, they observed a positive correlation between hydrophobicity ($\log P$) and the negative ion response in ESI/MS. This is expected as more hydrophobic compounds have a higher affinity towards the droplet surface.

Huffman et al.²⁶ extended the study of Henriksen et al.²⁵ They observed that compounds with electron-withdrawing groups and extended conjugation ionized best due to resonance and inductive effects. Additionally, they observed that in general, the ionization efficiency increases when in the homological compound set the alkyl chain length increases. Furthermore, in the family of phenols, introducing electron acceptor substituent increases the ionization efficiency.

Nguyen et al.²⁷ studied organic acids in ESI positive mode. They observed a positive correlation between adjusted mass and response of ion in ESI/MS. The adjusted mass was defined as a product of the molecular mass and the H/C ratio in the molecule.

Chalcraft et al.¹¹ studied zwitterionic and cationic metabolites in ESI positive mode. They observed a positive correlation between molecular volume, $\log P$, absolute mobility and effective charge and cation response in ESI/MS.

Also, Cech and Enke²⁹ observed the tendency of increasing response in ESI/MS with increasing hydrophobic character of oligopeptide. They studied oligopeptides of 3 amino acids with a different amino acid as C-terminus. The trend is explained with the increasing affinity towards the droplet surface.

These findings demonstrate that several physicochemical parameters have shown correlation with ionization efficiency. The studied parameters can be divided into two groups: firstly, parameters describing the hydrophobicity of the compound and, secondly, parameters explaining the charging of the compound. However, contradictory observations e.g. importance of hydrophobicity ($\log P$) or basicity (GB, pK_b) are present in the literature. Thus, a broader set of compounds may give more insight into the effect of compound properties.

Solvent effects on ionization efficiency

Next to properties of compounds also the eluent is affecting the response in ESI/MS. Kostiainen and Kauppila³⁰ and Gao et al.³¹ have reviewed the effect of eluent on ionization efficiency in ESI.

Solvent type

The conductivity of the solvent must be sufficient for efficient charge separation if high sensitivity and good stability are desired. Solvents suitable for ESI vary from polar to medium polar, the most widely used being water, methanol and acetonitrile. Non-polar solvents with low conductivity are not favourable and are used in LC/ESI/MS mainly with a post-column addition of a polar solvent compatible with ESI.³² Neat water is considered a poorer solvent for conventional ESI than are organic solvents such as methanol and acetonitrile.³³ This is partly because the viscosity of water is higher and, therefore, the electrophoretic mobility of ions is lower, leading to inefficient charge separation and difficulties in producing a stable spray. Moreover, higher surface tension needs higher voltage applied to capillary to achieve stable spray.³⁴ Additionally, the water vapour pressure is lower thus formed droplets do not dry as quickly and fewer ions are ejected into the gas phase.³⁵ Hence, the ESI response is lower when water alone or highly aqueous eluent is used.³⁶ Therefore, to increase the response of analyte stronger retention in reversed-phase would be beneficial as compounds will elute with higher organic modifier content hence have higher ionization efficiency.³⁷ However, pneumatically assisted and thermal focusing is often used in commercial sources on the market in which spray stability in case of pure water does not differ from other eluent compositions.³⁸ Cech and Enke²⁸ suggest in their review to use at least 50% of organic (moderately polar) modifier to achieve a stable spray in ESI. In commercially available ESI sources the stability of the spray is often ensured throughout the HPLC gradient when using pneumatically assisted and especially additionally thermally focused ionization sources as shown for example by Krueve³⁸ in negative mode and by Periat et al.³⁹ in positive mode. The most popular organic modifiers in LC/ESI/MS are methanol and acetonitrile. There is no clear conclusion that one of them outperforms the other.

Huffman et al.²⁶ studied neat methanol, acetonitrile, acetone and water as eluents in negative ESI/MS. They found that for 2/3 of studied compounds (48) exhibited greater response in methanol than in other eluent compositions. As a class of compounds, the steroids gained the most when methanol was used as eluent. Generally, responses followed the order methanol > water > acetonitrile \geq acetone for most test compounds. They explained it that polar protic eluents stabilize the charge separation thus the spray and solvate better the formed ions.

Silvester⁴⁰ also studied the effect of organic modifier on the response of analytes in both ESI positive and negative mode in chromatographic analysis.

According to his results in both ESI positive and negative mode over a broad range of eluent pH values ($3 < \text{pH} < 10$) the methanol outperforms acetonitrile (signal increase up to 500%). However, the effect can be quite small (20%) in the example of rosuvastatin. One additional explanation of why methanol outperforms acetonitrile was the fact that due to the lower eluotropic strength of methanol retention times of analytes were longer. Therefore, the organic modifier percentage was higher at retention time enhancing the signal observed in case of methanol.

Thacker and Schug⁴¹ studied solvent effects on glucose response in ESI/MS and also found that methanol-water mixture (80/20) outperforms acetonitrile-water mixture (80/20) in both ESI positive and negative mode. They observed for a methanol-water mixture that in both modes the higher the methanol percentage the higher the response. Surprisingly, for acetonitrile-water mixture in ESI positive mode, the response decreased remarkably with increasing acetonitrile percentage. In ESI negative mode the signal increased with increasing acetonitrile percentage up to 60% of acetonitrile, plateaued up to 80% of acetonitrile and decreased sharply if acetonitrile percentage was further increased.

Periat et al.⁴² compared HILIC and RPLC with MS detection. HILIC turned out to be a more sensitive approach. The main explanation for that was that higher acetonitrile percentage was required in case of HILIC separation to elute all 56 test compounds. Again, showing that higher organic modifier percentage results in higher ionization efficiency hence more sensitive method.

Gao et al.⁴³ reviewed the alternatives of acetonitrile in bioanalysis in light of acetonitrile shortage between 2008 and 2009. In addition to previous findings, they pointed out that one disadvantage of methanol over acetonitrile is its reactivity. It is observed that some metabolites react with methanol during analysis hence changing the structure and thus ionization efficiency of the analyte.

Steiner and Hassel⁴⁴ studied different solvents in non-aqueous capillary electrophoresis-mass spectrometry for basic analytes and in terms of limit of detection they observed hardly any difference between methanol and acetonitrile.

Monnin et al.⁴⁵ studied effects of eluent additives to lipidomic analysis. In the example of studied compounds, there are no significant differences in relative intensities of compounds between methanol and acetonitrile containing eluents.

Maragou et al.⁴⁶ studied the effect of eluent on response factors in ESI positive mode. They concluded that the differences between methanol and acetonitrile are not remarkable except for 3,4-dichloroaniline. In case of 3,4-dichloroaniline, 60-fold higher response factor was observed in case of acetonitrile containing eluent. Such findings address that there can be compound specific effects of eluent on ionization efficiency.

Campbell et al.⁴⁷ studied the protomers of 4-aminobenzoic acid and the distribution of two forms in different eluent compositions. They compared

acetonitrile/water mixtures with methanol/water mixture. It was evident that O-protomer is dominant in differential mobility spectrometry (DMS) ionogram in case of methanol containing eluent whereas N-protomer is dominant in case of acetonitrile rich eluent. They concluded that protic solvent stabilizes preferably O-site and acetonitrile amine group. The amine group is in the liquid phase more basic than the carboxylic group. This means in case of protic eluent the charge can travel from N-site to O-site during the ESI process.

Additives

Additives and buffers are used in LC eluents to improve resolution and reproducibility. Chemical properties and concentration of the additive, as well as pH, have a significant effect on analyte response in ESI. Unfortunately, many of the additives and buffers, especially non-volatile ones, commonly used in LC are not compatible with ESI/MS. In general, non-volatile buffers such as phosphate and borate tend to cause increased background, signal suppression, and rapid contamination of the ion source resulting in decreased sensitivity and stability.³⁰ Although various volatile additives have been employed in LC/ESI/MS, the most widely used are acetic acid, formic acid, ammonium hydroxide, ammonium acetate and ammonium formate.^{48,49} In addition trifluoroacetic acid (TFA) is used. The performance of TFA is somewhat controversial. In one hand it is volatile and more acidic ($pK_a = 0.3$) than formic acid ($pK_a = 3.75$) which is very favourable for ESI, on the other hand, several groups have observed suppressive effects on the signal of analytes caused by TFA.

Often the best sensitivity in ESI positive mode is achieved when the analyte is ionized already in the liquid phase. Therefore, acidic eluents in ESI positive are preferred for basic analytes, such as amines. In ESI negative mode basic conditions are preferable for acidic analytes, such as carboxylic acids and phenols.³¹ On the other hand, often the best chromatographic performance in reversed-phase LC, with good retention factors and resolution, is achieved by adjusting the pH so that the acidic or basic analytes are neutral in the eluent.³⁰ However, there are some studies showing that increasing the ionization degree (α) in solution could result in a decrease in sensitivity because of the properties of corresponding eluent composition. Kamel et al.⁴⁸ studied the effect of TFA, acetic acid, ammonia, and sodium acetate on the sensitivity of antiviral agents using ESI positive mode. They observed that TFA suppresses and acetic acid enhances the signal in ESI. Additionally, they observed that the addition of ammonia to the aqueous phase significantly enhances analyte response. A significant conclusion drawn from that work⁴⁸ was that the major processes for the formation of ions from pyrimidines occurred via gas phase ion/molecule reactions and not through solution phase reactions. The effects of TFA and acetic acid on the sensitivity of basic drugs in ESI positive mode were also studied by Mallet et al.⁵⁰. Dams et al.⁵¹ observed, similarly to Kamel et al.⁴⁸, that

TFA has a suppressive effect and added that other acids with higher concentrations, as well, have a suppressive effect. They reported the suppressive effect of volatile acids (formic and acetic acid) on morphine analysis, with the most suppression observed at acid concentrations 0.03–0.04% (v/v); higher concentration did not yield further suppression.⁵¹

The signal reduction and spray instability caused by TFA has been explained by either the high conductivity or surface tension of the aqueous eluent containing TFA^{52,53} or strong ion-pairing between the TFA-anion and the protonated molecule. The ion-pairing process is described as masking the protonated molecules and thereby decreasing the efficiency of the ESI droplet to emit protonated molecules to the gas phase.⁵⁴ Ion-pairing may also lead to reduced charge separation at the tip of the ESI sprayer and thereby to decreased ionization efficiency.^{51,55}

Silvester⁴⁰ observed the highest responses in positive mode ESI for various analytes (propranolol, rosuvastatin, and drug AZ-X) in basic solutions (ammonium acetate buffer, pH = 9.9), for which the analytes were expected to be in a neutral form. Additionally, Rainville et al.⁵⁶ studied the effect of acidic and basic eluent on the sensitivity of 24 pharmaceuticals. They observed that for 87% of compounds the basic eluent resulted in an increase in the peak area. Additionally signal-to-noise ratio increased for 70% of compounds. They showed that the phenomenon is not explained by later elution as for 70% of compounds the retention time did not increase. Mansoori et al.⁵⁷ first observed, and Zhou and Cook⁵⁸ later studied in detail, “the wrong-way-round ionization” this means that analytes give a high response in conditions where the analyte is not expected to ionize according to solution phase chemistry (pK_a and pH). They explained the phenomenon by gas-phase reactions occurring with precursors either present in solution or induced by corona discharge. Hua and Jenke⁵⁹ showed that some compounds form ammonium adducts in the droplet that may lead to increased protonated analyte signals. Peng and Farkas⁶⁰ also showed that a high eluent pH is suitable for analysis of basic analytes.

The pH effect on ESI efficiency becomes even more complex if changes in solution pH during the ESI process are considered.^{61–63} Van Berkel et al.⁶¹ showed that electrochemistry occurring on the needle tip changes the pH of the solution remarkably. In unbuffered solutions, the pH decreases in positive ion mode by as much as 1.8 pH units in case of low flow rates (0.008 mL/min) and 0.6 pH units using typical chromatographic flow rates (0.2 mL/min). Additionally, Zhou et al.⁶³, Girod et al.⁶² and Liigand et al.⁶⁴ have shown that the pH of droplets decreases along the ESI plume by approximately 0.6 pH units.

Next, to pH effects, the compound-specific effects may arise. Park and Jung⁶⁵ observed that adding small amount (0.05 mM) ammonium formate to the water-phase containing formic acid as eluent additive resulted in an increase of signal of protonated species compared to sodiated ion in case of gingerols. Surprisingly just increasing the formic acid concentration (from 0.1% to 2.0%) did not show any significant increase in signal of protonated species. Additionally, Yuan et al.⁶⁶ have shown that oxalic acid as an additive is most

efficient to suppress sodium adduct formation thus enhancing the protonated signal in case of oligopeptides. Krue and Kaupmees¹² have recently also shown the same effect on small molecules.

Concentration of additives

The concentrations of additives required in LC are often at the level of 100 mM that is too high for ESI. In practice, usually, the additive concentrations should not exceed 10 mM in order to avoid ionization suppression.³⁰ Constantopoulos et al.⁹ presented an equilibrium partitioning model, which predicts that analyte response is proportional to concentration at electrolyte concentrations below 1 mM. At higher concentrations, the analyte response decreases. The decrease may be explained by the repulsive forces caused by the increased charge density at high buffer concentrations and these repulsive forces cause spreading of the spray. The density of ions at the centre of the spray is then reduced, and fewer ions are collected by the ESI source for mass analysis. Spreading of the spray at higher salt concentrations has been visually observed.⁹ The decreased sensitivity at high buffer concentrations may also be due to the competition of ions for a site at the surface of the ESI droplet or due to the formation of a solid residue.⁶⁷ The suppression effect may also depend on the surface activity of an additive^{28,67-69} so that electrolytes with higher surface activity can be expected to suppress ionization of an analyte more than those with lower surface activity.

Previous ionization efficiency models

Proposed models describing the ionization process during ESI have been accepted in the mass spectrometric audience and several groups have observed a correlation between physicochemical parameters of compounds and their ionization efficiencies. Models have been proposed attempting to predict ionization efficiency from physicochemical parameters of compounds.^{10,11,21,24,71-75} To make different studies comparable the input data and results are compared quantitatively. If needed and possible the performance of the model is re-evaluated to compare the results using root-mean-square error (RMSE).

$$RMSE = 10^{RMSE_{log}},$$
$$RMSE_{log} = \sqrt{\frac{\sum_{i=1}^n (\log IE_{pred} - \log IE)^2}{n}} \quad \text{Eq. 1}$$

Where $\log IE_{pred}$ is predicted ionization efficiency, $\log IE$ denotes measured ionization efficiency and n is a number of ionization efficiencies in a particular study.

Caetano et al.⁷² studied 170 molecules with different chemometric tools with the main aim to identify whether one ionization technique outperforms the other in comparison of APCI and ESI. To hold some parameters constant, they used source parameters optimized for cocaine and studied the corrected response in one eluent composition. They studied different algorithms and partial least squares regression (PLS) outperformed stepwise multiple linear regression (MLR) for predicting the corrected response in ESI. The developed model covered ionization efficiency values of 2.4 orders of magnitude. The RMSE of the training set was 1.8 times and RMSE of the test set was 2.2 times.

Chalcraft et al.¹¹ developed relative response factor prediction model for ESI positive mode. They used an MLR algorithm and the significant parameters in their model were molecular volume, $\log P$ and absolute mobility. The 48 metabolites used in training set covered ionization efficiency values of 2.8 orders of magnitude. Validation set consisted of 10 compounds. The model was developed for one eluent composition. The average error was 1.4 times. And RMSE was 1.6 times.

Oss et al.¹⁰ studied 62 of nitrogen and oxygen bases covering ionization efficiencies 6 orders of magnitude in ESI positive mode in one eluent composition. They also developed an MLR model to predict ionization efficiencies. The most significant parameters were molecular volume and aqueous pK_a . Standard residual error for the training set was 6.5 times and for test set 7.2 times. The obtained RMSE of the model was 6.3 times.

Wu et al.²⁴ studied ESI negative mode. They developed a model using MLR algorithm based on 20 organic acids covering ionization efficiencies of 1.3 orders of magnitude and validated it with 17 compounds on another mass spectrometric setup. Five significant parameters in their model were: hydrogen bond acidity, HOMO energy, the number of hydrogen bond donating group, the ratio of organic modifier, and the polar solvent accessible surface area. RMSE for the training set was 1.2 times.

Gioumouxouzis et al.⁷⁴ studied ESI negative mode in case of 110 druglike compounds in one eluent composition. As all the compounds were studied at the same concentration the problem arises that some studied compounds may not be in the dynamic range rather in saturation. They developed a model using the PLS algorithm. RMSE of the developed model was 1.5 times.

Alymatiri et al.⁷¹ studied the response of steroids in ESI/MS. They used 30 steroids to develop a model to predict response in ESI/MS. The studied compounds covered 1.8 orders of magnitude of ionization efficiency in ESI positive mode and 3.2 orders of magnitude in ESI negative mode. Again, the PLS algorithm was used for model development. The most significant parameter according to VIP plot was gas phase basicity. It was not possible to obtain information about the performance of the developed model based on the data available in the publication.

Golubovic et al.²¹ studied ESI positive mode in the example of seven sartans. For model development, artificial neural network (ANN) algorithm was used. The significant parameters for model were methanol percentage, flow rate, pK_a ,

$\log P$, molecular volume and number of hydrogen bond acceptor sites. The RMSE of the model was 1.5 times.

Cramer et al.⁷³ studied 77 pharmaceuticals and developed a model based on 66 compounds using MLR algorithm. The significant parameters were aqueous proton affinity and total surface area of the molecule in its conjugate base form. The model was developed in ESI positive mode for one eluent composition. The studied compounds covered 3.7 orders of magnitude in ionization efficiency. RMSE of the model was 4.0 times.

Hermans et al.⁷⁵ studied free and derivatized amino acids. Altogether 84 different compounds were under investigation in ESI positive mode. For model development, MLR algorithm was used. The studied compounds covered 3.5 orders of magnitude of ionization efficiencies. The significant parameters for the model were SPAN and BIC0. BIC0 is the bonding information content index proposed by Basak et al.⁷⁶ and generally describes the diversity of atomic composition and structural groups. The SPAN geometrical index is a simple size descriptor. It is the radius of a sphere centred in the molecule centre of a mass enclosing the entire molecule.⁷⁷

The comparison of abovementioned reveals promising prediction accuracy but also low universality arising from the limited scope. Namely, the similarity of studied analytes in one set is high. Mainly only one eluent composition has been studied, or the number of analyte eluent compositions is small. However, some groups use LC separation with gradient elution, which increases the number of eluent conditions used but does not increase the number of analyte and eluent combinations. The last is important to effectively model the influence of both analyte properties and eluent properties. Next, the accuracy of the models is also influenced by the measurement technique: often ionization efficiency is determined on a single concentration level without verifying linearity.

Shortcomings of the modelling approaches also limit the domain of application. Often the studies and proposed models are instrumentation specific and there is no guidance on how to transfer these approaches and especially models to other instrumentations in other labs. Additionally, the studies are prevalently in positive mode and there are few examples of application in real samples.^{24,78} Even more so, the predicted ionization efficiencies have been rarely used to estimate the real concentrations of the compounds detected in LC/MS analysis. All in all, the ionization efficiencies have potential in making analysis quantitative even without the availability of standard substances, but this potential is until now strongly underdeveloped.

The benefit of ionization efficiency model

LC/MS has become the most versatile analytical tool to discover and detect metabolites,¹ pharmaceuticals and their transformation products,² environmental contaminants,³ and food contaminants⁴ with non-targeted⁷⁹ analysis. To better

understand the chemical and mechanistic dynamics of a system, a quantitative approach is preferred, which requires two main elements: identification and quantification of each compound of interest (determining the concentration of compounds within the dataset). Currently, accurate mass measurements from high-resolution mass spectrometry (HRMS), together with relevant data analysis,^{80,81} is increasingly able to assign structures to the features detected.⁸² Quantification, however, remains a primary challenge. For example, out of 114 100 compounds in the Human Metabolome Database, only ca. 21 000 have been detected and identified.⁸³ Currently, the ability to get quantitative information from LC/MS is almost exclusively limited by the availability of standard substances as different compounds ionize in a different extent in ESI source. The response of the compounds in LC/MS is influenced by the properties of the compound, eluent composition, and instrument. Thus, quantifying all detected compounds with a targeted analysis is exceedingly difficult, as standard substances (to match retention time, mass fragmentation pattern, and provide a calibration curve) are not available for most of the compounds.

Additionally, the results of most LC/MS analyses conducted in different laboratories can currently only be compared based on qualitative data, as the measurement conditions and instruments used vary strongly and quantitative data are not available.⁷⁹ The lack of facile quantification also represents an obstacle to longitudinal studies, as samples collected over a long period of time must be stored and analysed all together in the same laboratory with the same methods. This raises concerns about sample preservation, stability, and delays in information dissemination, especially in cases where fast interventions may be crucial.

EXPERIMENTAL

Chemicals

The compounds for which ionization efficiency values were measured and/or collected from previous studies for model development are listed in Table S 2. Acetonitrile (Chromasolv® Plus for HPLC, $\geq 99.9\%$ Sigma-Aldrich, USA), methanol (Chromasolv® Plus for HPLC, $\geq 99.9\%$ Sigma-Aldrich, USA), acetone (puriss. p.a. $\geq 99.5\%$ Sigma Aldrich, USA), 2-propanol (for HPLC, 99.9% , Sigma Alrich, USA), ultra-pure water (purified with Millipore Advantage A10 MILLIPORE GmbH, Molsheim, France), formic acid (98% , Fluka USA), oxalic acid ($\geq 99.0\%$, Fluka, USA), propionic acid ($\geq 99.5\%$, Fluka, USA), trifluoroacetic acid ($99+\%$, Aldrich, USA), ammonia solution (25% , Lach:Ner, Czech Republic), ammonium fluoride ($\geq 98.0\%$, Fluka USA), ammonium formate ($\geq 99.0\%$, Fluka, USA), ammonium bicarbonate ($\geq 99.0\%$, Fluka, USA), and ammonium acetate ($\geq 99.0\%$, Fluka, USA) were used as eluent components. Studied eluent compositions are listed in Table S 3.

Equipment

The ionization efficiency measurements were carried out in the positive ion mode on 7 different mass spectrometers.

- I. An Agilent XCT ion trap mass spectrometer (Agilent Technologies, Santa Clara, CA, USA) with an Agilent 1100 series HPLC (Agilent Technologies, Santa Clara, CA, USA) was used. The measurements were carried out in flow injection mode. For instrument control, an Agilent ChemStation for LC (Rev. A. 10.02) and MSD Trap Control (Version 5.2) were used. The following MS and ESI parameters were used for commercial ESI source: nebulizer gas pressure, 15 psi; drying gas flow rate, 7 L/min; drying gas temperature, $300\text{ }^{\circ}\text{C}$. For in-house developed 3R sprayer nebulizer⁸⁴ following parameters were used: gas pressure 2 psi, drying gas flow rate 10 L/min, drying gas temperature $350\text{ }^{\circ}\text{C}$, and inner capillary gas pressure 12 bar. For both setups the needle voltage was 3500 V. Additionally, only the target mass (TM) was optimized.¹³
- II. A Varian J-320 (Varian Inc., Walnut Creek, CA, USA) triple quadrupole mass spectrometer. For the instrument control, MS Workstation was used. Used ESI source has an angular geometry and used parameters were: needle voltage 3500 V, drying gas 10 psi, drying gas temperature $300\text{ }^{\circ}\text{C}$, and shield voltage 300 V. The signal was recorded with capillary voltages 30 V, 40 V, 50 V, 60 V, 70 V. The highest obtained signal was used.
- III. An Agilent Single Quad 6100 (Agilent Technologies, Santa Clara, CA, USA) equipped with the modified⁸⁵ Agilent Jet Stream (AJS) ESI

Source (Agilent Technologies, Santa Clara, CA, USA). Used ESI parameters were: capillary voltage 3500 V, nozzle voltage 600 V, nebulizer gas pressure 15 psi, drying gas flow rate 7 L/min, drying gas temperature 300 °C, sheath gas flow rate 1 L/min and sheath gas temperature 80 °C.

- IV. An Agilent 6495 Triple Quadrupole (Agilent Technologies, Santa Clara, CA, USA) with conventional ESI source or Agilent Jet Stream ESI Source and iFunnel ion funnel (Agilent Technologies, Santa Clara, CA, USA). In case of conventional ESI source parameters used were: capillary voltage 4000 V, nebulizer gas pressure 14 psi, drying gas flow rate 15 L/min, drying gas temperature 200 °C. For Jet Stream parameters used were: capillary voltage 3000 V, nebulizer gas pressure 20 psi, drying gas flow 12 L/min, drying gas temperature 200 °C, sheath gas flow 11 L/min and sheath gas temperature 250 °C. For instrument control, Agilent MassHunter Workstation Data Acquisition was used.
- V. An LTQ Ion trap (Thermo Fisher Scientific, San Jose, USA) with a standard ESI source or heated HESI-II source was used. For standard ESI source following settings were used: sheath gas flow rate 35 psi, auxiliary gas flow 10 a.u., sweep gas flow rate 5 a.u., spray voltage 3.5 kV and a capillary temperature of 275 °C. A heated electrospray HESI-II source was used under the same settings except for the capillary temperature that was set at 350 °C. An ACCELA liquid chromatograph (Thermo Fisher Scientific) was used for flow injection analysis. Xcalibur software was used for data processing.
- VI. A Synapt G2 (Waters, Wilmslow, UK) quadrupole time-of-flight hybrid mass spectrometer with a Z-Spray ESI source. The source parameters were: source temperature 120 °C, desolvation gas temperature 450 °C, desolvation gas flow rate 800 L/h, capillary voltage 1 kV, sample cone 35 V, extraction cone 7.0 V, cone gas 50 L/h. An Acquity UPLC (Waters, Milford, MA, US) with ctc-PAL autosampler was used for flow injection analysis. MassLynx software was used for data processing.
- VII. An API 4000 (Sciex, Concord, Canada) triple quadrupole with TurboSpray ESI source was used with following parameters: Ionspray Voltage 5.5 kV, curtain gas 10 psi, nebulizer gas (Ionspray gas1) 40 psi, heater gas (Ionspray gas2) 40 psi, and heater gas temperature 425 °C. An Acquity UPLC (Waters) was used for flow injection analysis. Analyst software was used for data processing.

For all measurements in flow injection mode, the flow rate was set at 0.2 mL/min. Measurements in the publication I and II also used direct infusion experiments and the flow rate used was 0.008 mL/min. The measurement results for flow injection analysis and direct infusion analysis were consistent⁸⁶ and, therefore, the majority of the measurements were conducted in flow injection mode.

For the ionization degree measurements, UV-Vis spectra were recorded with a PerkinElmer Lambda 2S UV/Vis spectrometer (PerkinElmer, Massachusetts, USA). Spectra were recorded from 190–750 nm using 1 cm cuvettes.

For chromatographic experiments, an Agilent XCT ion trap mass spectrometer (Agilent Technologies, Santa Clara, CA, USA) with an Agilent 1100 series HPLC (Agilent Technologies, Santa Clara, CA, USA) was used. As the column, a Zorbax Eclipse XDB-C18 column (5 μm , 250 \times 4.6 mm) was used. Isocratic elution with 80% acetonitrile was used for chromatographic ionization degree determination in the corresponding eluent.

The aqueous phase pH was measured with pH-meter (Evikon pH Meter E6115) using a glass electrode (Evikon pH631).

Ionization efficiency measurement

For the evaluation of $\log IE$ values, the responses of $[\text{M}+\text{H}]^+$ were recorded in an MS1 scan mode in ESI positive mode. In case in source fragmentation of the compounds occurred, the intensities of the fragment ion peaks were added to the intensity of the molecular ion peak. Six dilutions of the analyte stock solutions were made (1-, 1.25-, 1.67-, 2-, 2.5-, and 5-fold) with the corresponding eluent by the autosampler and delivered to MS in flow injection mode. All measurements were conducted in the linear range.

The absolute ionization efficiency values tend to vary significantly depending on the ionization source geometry, ion optics, day, cleanliness of the ionization source, etc. Therefore, we measured the relative ionization efficiency (RIE) of a compound M_1 relative to anchor compound (M_2)⁸⁷ according to the following equation:

$$RIE(M_1/M_2) = \frac{\text{slope}(M_1)}{\text{slope}(M_2)} \quad \text{Eq. 2}$$

where the slope of the analyte signal versus concentration is estimated via linear regression in the linear range of the signal-concentration plot. As isotopologues abundance in mass spectrum depends on the compound, isotope correction was used to correct the signal. In our measurements anchor compound in positive mode is tetraethylammonium. To make the data easier to present and analyse, the logarithmic scale ($\log IE$) was used. The scale in positive mode was anchored to $\log IE$ of tetraethylammonium, taken as 3.95 in the acetonitrile/0.1% formic acid(aq) 80/20 as previously stated.¹⁰

$$\log IE_{M_1} = \log RIE(M_1/M_2) + \log IE_{\text{anchor}} \quad \text{Eq. 3}$$

To minimize the influence of possible differences in conditions when measuring M_1 and anchor compound, two steps were taken: (1) each compound was measured on at least three different runs (on three different days) and the results

were averaged, and (2) anchor compound was measured in the beginning and end of each run on each day. To anchor the scales of other eluent compositions, the MS signal intensities of anchor compound in all eluents were measured in the same day and the $\log IE$ value of anchor compound in an eluent n was calculated using Eq. 4:

$$\log IE_{S_n} = \log \left(IE_{S_1} \cdot \frac{Signal_{S_n}}{c_{S_n}} \cdot \frac{c_{S_1}}{Signal_{S_1}} \right) \quad \text{Eq. 4}$$

where the $Signal_{S_n}$ and $Signal_{S_1}$ are the signal intensities in eluent n and 1 and C_{S_1} and C_{S_n} are the corresponding concentrations of benzoic acid in the respective eluents. In the main text of this thesis, the ionization efficiency values may differ from the ones presented in the publications. As for publication I anchoring over tetrapropylammonium was conducted. In proceeding publications, the anchoring over tetraethylammonium was performed. To make the results from different publications numerically consistent reanchoring of the results was performed so that $\log IE$ value of tetraethylammonium always corresponds to 3.95 in acetonitrile/0.1% formic acid(aq) 80/20.

The reproducibility of measurements was calculated as a pooled standard deviation (Eq. 5):

$$s_{pooled} = \sqrt{\frac{\sum_i^k (n_i - 1) \cdot s_i^2}{\sum_i^k n_i - k}} \quad \text{Eq. 5}$$

Where s_i is the standard deviation of an analyte in one eluent, n is the number of measurements performed on an analyte in one eluent and k is the number of different analytes in the corresponding eluent.

Descriptor calculation

For analysing the correlation between $\log IE$ values and physicochemical properties of compounds two approaches COSMO-RS and PaDEL were used to calculate physicochemical properties.

COSMO-RS^{88,89} method was used for calculating various parameters: aqueous pK_a , $\log P$, charge delocalization parameters ($WANS$ and Klamt parameters). Ionization degree (α) of the compounds was calculated from the pK_a values calculated with $COSMOtherm$.⁹⁰ $WANS$ parameter describes charge delocalization. Klamt parameters include molecular area and volume of the molecule (for neutral form and cationic form), $sig2$ and $sig3$ describe polarity and polarizability of the molecule, $Hacc3$ describes the hydrogen bond accepting capacity and $Hdon3$ hydrogen bond donating capacity.

For general ionization efficiency prediction model development, 1D and 2D PaDEL descriptors⁹¹(1444 descriptors) were calculated for every compound using ChemDes calculator.⁹² Additionally, five empirical eluent descriptors

(viscosity⁹³, surface tension⁹⁴, polarity index⁹⁵, pH, NH₄ presence) were added to the dataset.

The viscosity of organic modifier water binary mixture^{93,96,97} was calculated using the general model:

$$\text{viscosity} = A \cdot (\text{org}\% \cdot 100)^2 + B \cdot \text{org}\% \cdot 100 + C \quad \text{Eq. 6}$$

The surface tension of organic modifier water binary mixture^{94,98} was calculated using the general model:

$$\begin{aligned} \text{surface tension} &= \sigma_1 + D \cdot \sigma_1 \cdot \text{org}\% \\ &+ (E \cdot \sigma_2 - D \cdot \sigma_1 - \sigma_1) \cdot \text{org}\%^2 \\ &+ (\sigma_2 - D \cdot \sigma_2) \cdot \text{org}\%^3 \end{aligned} \quad \text{Eq. 7}$$

Polarity index of organic modifier water binary mixture⁹⁵ was calculated using the general model:

$$\text{polarity index} = F \cdot \text{org}\% + G \cdot (1 - \text{org}\%) \quad \text{Eq. 8}$$

NH₄ presence parameter was 1 if the additive included either ammonia or ammonium salt (ammonium acetate, ammonium formate, ammonium bicarbonate, ammonium fluoride), otherwise, it was kept 0.

Table 1 Parameters used to calculate eluent descriptors.

	acetonitrile	methanol	isopropanol	acetone	water
A	-1.04·10 ⁻⁴	-3.59·10 ⁻⁴	-4.74·10 ⁻⁴	-3.13·10 ⁻⁴	–
B	4.36·10 ⁻³	3.20·10 ⁻²	5.89·10 ⁻²	2.47·10 ⁻²	–
C	8.84·10 ⁻¹	9.03·10 ⁻¹	7.88·10 ⁻¹	9.02·10 ⁻¹	–
D	-2.91	-2.24	-3.89	-2.54	–
E	7.14	5.62	15.56	6.84	–
F	5.80	5.10	3.92	5.10	–
G	–	–	–	–	10.20
σ₁	–	–	–	–	71.76
σ₂	27.86	22.12	16.98	22.16	–

Data pre-processing

As PADEL descriptor calculation of some descriptors fails for some compounds, the descriptors with NA (not available values) were removed from the dataset. Next, all the descriptors with had the same value for > 95% of compounds were eliminated from the dataset. As the third cleaning step, the pairwise correlation of descriptors was considered. If the R² was higher than 0.8

the former descriptor was removed from the dataset. After data pre-processing for ESI positive mode 1086 descriptors were left in the dataset and for ESI negative mode 822 descriptors were left in the dataset.

Ionization efficiency prediction model development

Different machine learning algorithms (MLR, support vector machine (SVM) regression, ANN and random forest regression) were tested for model development. Regularized random forest regression algorithm⁹⁹ from library RRF in R turned out to yield best performing models. For ESI negative and positive mode, individual models were developed. For model development, dataset was randomly split into two sets. 80% of observations were used for developing the model and 20% of observations were used as a validation set. The number of trees used in the random forest was optimized and the optimal number was 100 decision trees. The regularization isotherm selected 450 significant descriptors for ESI positive mode and 145 significant descriptors in ESI negative mode.

Concentration from predicted ionization efficiency

As the model output is in universal $\log IE$ values and not instrumentation specific a set of compounds is used to transform the universal predicted $\log IE$ values to instrumentation specific values. The workflow is presented in Figure 1.

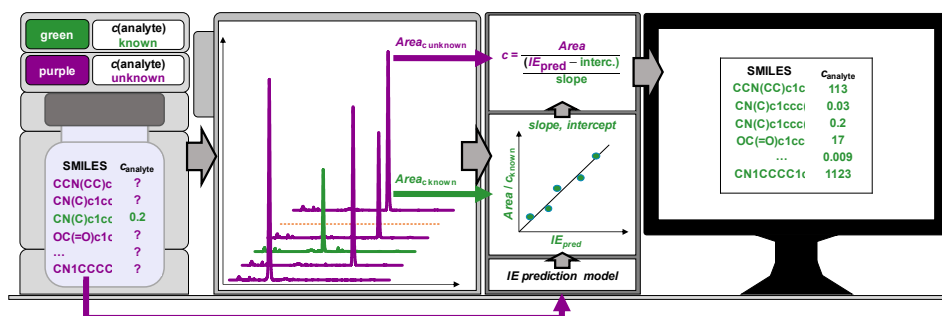


Figure 1 Flow chart of the Quantem approach to apply ionization efficiency prediction to estimate concentration. Purple is used for compounds of interest and green is used for compounds with known concentration; the latter is used to account for instrument-specific effects in the prediction model.

For transforming the predicted $\log IE$ values the set either spiked to the matrix or as a standard solution was measured in dynamic range with the same method as analytes. From the analysis results logarithmic response factors ($\log RF$) were calculated:

$$\log RF = \frac{\text{Signal}}{\text{concentration}} \quad \text{Eq. 9}$$

$$\log RF_{\text{pred}} = \text{Slope} \cdot \log IE_{\text{pred}} + \text{intercept} \quad \text{Eq. 10}$$

where the signal is recorded as a peak area in scan mode and corrected with isotope correction factor. Molar concentrations are used for calculation of response factor. $\log RF$ values were correlated with predicted $\log IE$ values to obtain parameters necessary for transforming the predicted $\log IE$ values. For studied pesticides in cereals and metabolites in green tea, these obtained parameters were used to transform predicted $\log IE$ values to $\log RF$ values. Knowing the scan mode peak areas of compounds of interest and predicted response factors it is possible to predict concentration (Eq. 11). Slope and intercept values in Eq. 10 were calculated based on the coefficients of the linear regression curve between $\log RF$ and $\log IE_{\text{pred}}$ values in the calibration set.

$$c = \frac{\text{Signal}}{10^{\log RF_{\text{pred}}}} \quad \text{Eq. 11}$$

In order to validate the obtained results, the prediction errors between real concentration and predicted concentration in both cereal matrices and green tea samples were calculated as follows.

$$\text{prediction error} = \max \left\{ \begin{array}{l} \frac{\text{predicted concentration}}{\text{measured concentration}} \\ \frac{\text{measured concentration}}{\text{predicted concentration}} \end{array} \right. \quad \text{Eq. 12}$$

Green tea data treatment

For validation of the developed model, the approach was applied for previously collected data on different instrumentation in the different research group. Data from the study of Kellogg et al.¹⁰⁰ was used to compare the performance of the model. Ionization efficiencies were predicted for 14 metabolites (Table S 4) that were quantified with a targeted method. To transfer the predicted $\log IE$ values to response factor specific to this instrumentation and experiment a transformation with six compounds has been performed. These six compounds were chosen as 20% percentiles and response factors were calculated for the NIST green tea reference material (sample T26). The concentrations of these 14 compounds were predicted in 38 samples.

Sample preparation for cereal samples

All of the cereal samples were prepared by Tingting Wang according to the QuEchERS extraction method, described elsewhere.¹⁰¹ In short, the blank samples (pesticides free) were obtained from proficiency test material for the six EUPTs: EU-PT-CF8 (wheat), -C3 (oat), -CF10 (rye), -C6 (barley), -CF9 (maize), and -SRM6 (rice). Two grams of homogenized cereal samples were soaked with 10 mL acidified Milli-Q water containing 0.2% formic acid. Next, the sample was extracted with 10 mL of acetonitrile. Thereafter, 4 g of magnesium sulfate and 1 g of sodium chloride were added, and the tube was shaken for 1 min followed by centrifugation. The organic upper layer (2 mL) was removed and shaken with 0.1 g of Bondesil-C18 and 0.3 g of magnesium sulfate for 2 min followed by centrifugation. Then 1.5 mL of purified extract was removed into a vial with insert and spiked with different concentration of tested compounds (Table S 4) prior to injection on the LC/MS system.

Statistical tests

T-test and *F*-test were carried out as statistical tests for data analysis and treatment. All statistical tests were carried out at 95% confidence level and using R software.

Ionization degree measurement

Ionization degree (α) of an analyte is calculated as follows:

$$\alpha = \frac{[AH^+]}{[AH^+] + [A]} = \frac{1}{1 + \frac{K}{[H^+]}} \quad \text{Eq. 13}$$

where $[AH^+]$ denotes the concentration of a protonated analyte, $[A]$ denotes the concentration of analyte and K the constant of protonation of the analyte.

For measurements of α , solutions of the analyte with different aqueous phase pH were made. The pH ranged from pH = 1.0 (0.1 M hydrochloric acid) to pH = 13.0 (0.1 M sodium hydroxide). The intermediate pH values were obtained by titrating 5 mM ammonium acetate with formic acid or ammonia.

The absorbances at the corresponding wavelengths were recorded, and the α was calculated as follows:

$$\alpha = \frac{A_{pH(i)} - A_{cation}}{A_{neutral} - A_{cation}} \quad \text{Eq. 14}$$

where $A_{pH(i)}$ is absorbance at particular pH and $A_{neutral}$ and A_{cation} are the absorbances corresponding to the purely neutral and purely cationic form,

respectively. The absorbance maxima with the largest difference in absorbance between neutral and cationic forms of an analyte were used for calculations.

Compounds without chromophores (trizma base) could not be studied with UV-Vis spectroscopy; for these compounds, HPLC measurements were performed.¹⁰² For three analytes, the HPLC measurements were used to confirm the results obtained with UV-VIS spectroscopy. For chromatographic ionization degree measurements, the analytes were analyzed after isocratic elution with two different aqueous phase pH values: 0.1% TFA (pH = 2.1) and 0.1% ammonia (pH = 10.7). The eluent consisted of 80% acetonitrile and 20% buffer (v/v). The change in retention times at different pH values was an indicator of change in α .

Discriminant analysis for pH effect

Ions are known to escape droplets as solvent clusters or as associates of eluent modifiers or combined.¹⁰³ However, there is no certainty in which extent the escaping ions are clustered under specific conditions used in experiments. Therefore, we use molecular parameters calculated for ions without a solvent shell. The eligibility of this approach has also been demonstrated before by successfully modelling the ionization efficiencies of various compounds by parameters calculated for analyte ion.^{10,11,87}

Various physicochemical properties of the analytes in the solvent phase were calculated with COSMO-RS method to determine the appropriate analyte form (neutral or ionic) for linear discriminant analysis (LDA) and quadratic discriminant analysis (QDA). The calculated parameters were: aqueous pK_a , $\log P$, *WANS* parameter, and the Klamt parameters (molecular area, molecular volume, *sig2* and *sig3* that describe polarity and polarizability, respectively, and *Hbdon3* and *Hbacc3*, which are quantitative measures of hydrogen bonding donor and acceptor capacities, respectively). These parameters were calculated for both neutral and cationic forms of an analyte. Additionally, parameters such as a change in α , and a number of potential charge centres were used.

To conduct linear discriminant analysis, the analytes were randomly divided into training and validation sets. In the validation set, there were 9 compounds: *N,N*-diphenylbispidine, 2,4-dinitroaniline, 2,6-dimethylpyridine, *N,N*-dimethylaniline, acridine, 2,4,6-trinitroaniline, 3-hydroxypyridine, quinoline, and 3-aminobenzoic acid. The other 19 compounds were used for developing a linear discriminant function. The modelling was first performed using a one-parameter-at-a-time approach and the subsequent steps were performed using up to five parameters. All possible combinations were considered in discriminant function development. First, the models were generated with either one, two, three, four or five parameters for the training set (including leave-one-out cross-validation step). For validation, the best models (for each number of parameters) were also tested on a validation set (Figure S 1). In case of a small number of compounds (size of the training set and validation set), it is possible

that overfitting of the LDA model occurs. Using training set results, a model with the smallest number of parameters having sufficient prediction precision was chosen (Figure S 1). It was observed that more than two parameters in the LDA model do not significantly improve the prediction precision neither for training nor for the validation set. Therefore, it is possible that models with a higher number of parameters give small improvement by chance. The two-parameter model was considered the best added that both parameters alone also gave good prediction precisions. For quadratic discriminant analysis, all 28 compounds were used to study the relationship. The quadratic discrimination analysis was not used to make any prediction but to describe the observed phenomena.

RESULTS AND DISCUSSION

To enable rapid developments in biology, food safety and environmental analyses there is a great need for increasing the amount of quantitative data obtained from LC/MS measurements. In my doctoral project, I hypothesized that it is possible to predict ionization efficiencies and use predicted ionization efficiencies to estimate the concentration of compounds of interest in LC/ESI/MS analysis. Such an approach would enable standard substance free quantification in LC/ESI/MS analysis. To develop the model, I determined the parameters of analysis that affect the ionization of particular analyte in a specific analysis method. At the beginning of the studies first, the effect of eluent on ionization efficiency was studied using a set of 10 compounds covering a wide range of physicochemical properties ($-4.2 < \log P < 6.1$ and $3.9 < \text{p}K_{\text{a}}(\text{aq}) < 11.3$). In the study, 7 eluents covering acetonitrile percentage from 20% to 80% and pH from 2.7 to 9.8 were investigated. Furthermore, the change of composition of droplets in ESI plume was studied using online fluorescence spectroscopy.

Solvent effects publication

The results of the $\log IE$ measurements and comparison with the previous study¹⁰ are presented in Table S 5 and Figure 2. Altogether 120 relative measurements with the 10 compounds were carried out during 7 months in 7 eluents. In each eluent, an ionization efficiency scale was constructed. The widest of the resulting scales have a span around 5 orders of magnitude. To assign $\log IE$ values to the analytes in the scale of the main eluent composition (acetonitrile/ 0.1% formic acid(aq) 80/20) the results were anchored to the $\log IE$ value of tetraethylammonium in the scale obtained by Oss et al.¹⁰ The other scales were anchored to the scale of the main eluent composition, taking into account the differences in $\log IE$ values of tetraethylammonium between the different eluents. This way of anchoring the scales have the advantage that the $\log IE$ values in different eluents become numerically comparable. The results are presented together with pooled standard deviation in Figure 2.

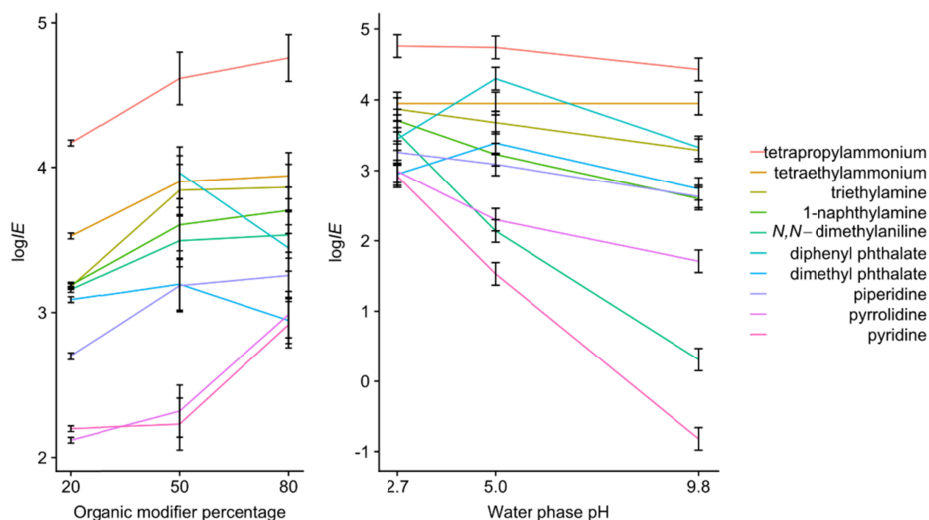


Figure 2 The positive mode ESI ionization efficiency ($\log IE$) values in different solvent compositions. Error bars correspond to s_{pooled} (Eq. 5). On the left hand side graph water phase is 0.1% formic acid(aq) and organic modifier percentage is 80% on the right-hand side graph.

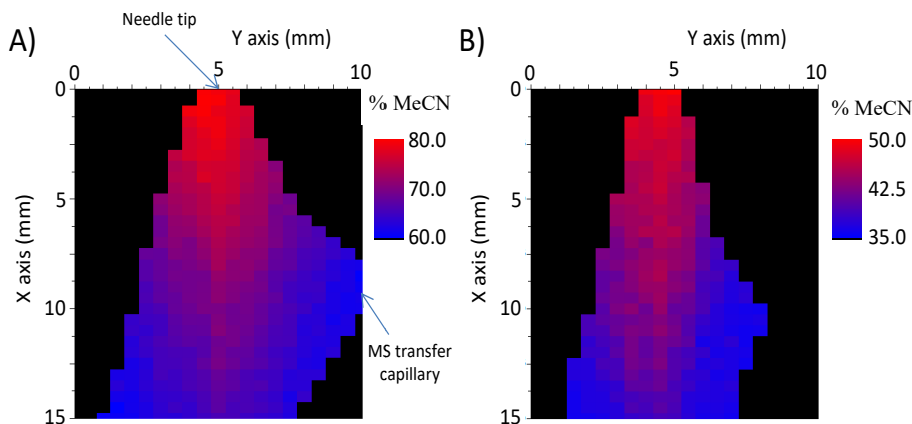


Figure 3 XY image of solvent fractionation in the plume (% of acetonitrile) from the fluorescence signal of 20 μM of Nile Red in A) eluent composition acetonitrile/1 mM ammonia(aq) 80/20, B) eluent composition acetonitrile/1 mM ammonia(aq) 50/50. Eluent flow rate 1 mL/h.

The evolution of the acetonitrile percentage in the electrospray plume decreases along the plume due to the solvent fractionation (Figure 3). It is seen that in case of acetonitrile/1 mM ammonia(aq) 80/20 the acetonitrile percentage decreases from 80% (needle tip, X; Y = 0; 5) to 61% (MS transfer capillary, X; Y = 8.8; 10). For acetonitrile/1 mM ammonia(aq) 50/50, it is not possible to determine

the acetonitrile percentage at the MS transfer capillary because not enough fluorescence signal was observed at this point. Indeed, the fluorescence of Nile Red in more than 65% water (in which it is only slightly soluble) is strongly quenched.¹⁰⁴ If the intersection of two eluent compositions acetonitrile percentage evolution pictures are compared it is seen that by acetonitrile/1 mM ammonia(aq) 80/20 the initial concentration of acetonitrile (80%) (X; Y = 0; 5.5) decreases to 63% (X; Y = 10; 8.5) and by acetonitrile/1 mM ammonia(aq) 50/50 the acetonitrile percentage decreases from 50% to 36%.

Comparison with earlier results

Comparing the $\log IE$ values between this study and study by Oss et al.¹⁰ with the t -test the differences are statistically insignificant. Therefore, the previous study¹⁰ remains valid even in the context of improved ion optics parameters implemented in this study. This shows on one hand that the previously established scale is sufficiently universal and on the other hand gives evidence that the scales established in this study are valid.

The impact of organic modifier

In a later study (IV publication) different organic modifiers were compared. Independent from the acidic modifier used, isopropanol as organic modifier gave the lowest ionization efficiencies with on average 6.6 times lower ionization efficiencies compared to methanol/10 mM formic acid(aq) 90/10 (Table S 6). This result is not unexpected since, among the studied organic modifiers, isopropanol is the least volatile, the most viscous and has the highest surface tension which results in larger droplets and, therefore, fewer ions are ejected into the gas phase and directed into the mass spectrometer.

The observed $\log IE$ values increased according to the used organic modifier as follows: isopropanol < acetone < acetonitrile < methanol. When formic acid was applied as a modifier, methanol gave statistically significantly higher (on average 1.5 times) $\log IE$ values than acetonitrile. In case of oxalic acid and propionic acid, there was no statistically significant difference in $\log IE$ values between methanol and acetonitrile. Acetonitrile provided higher $\log IE$ values than acetone.

The impact of organic modifier percentage

Comparison of the ionization efficiencies in different eluent compositions reveals that the $\log IE$ values depend on the organic modifier percentage. In general, the higher organic modifier content increases the ionization efficiency (Figure 2, Table S 5).

The ionization efficiency is a joint property of the analyte and the eluent. The organic modifier percentage affects the droplet “drying” rate. We know from the fluorescence measurements, that acetonitrile percentage decreases by at least 20% if the initial acetonitrile percentage is 80% and by at least 15% or slightly more in case of 50% initial acetonitrile percentage. Girod et al.⁸⁵ have shown that faster evaporation results in a quicker decrease of droplet radius. Iribarne et al.⁵ suggested that there is a crossing point in droplet radius when Coulomb fission is taken over by ion evaporation. Therefore, when the droplet radius decreases faster, the crossing point is achieved earlier, and the ions have more time to evaporate resulting in higher ionization efficiency. The solvent’s ability to support ionization largely compensates for the low extent of protonation of the weakly basic compounds. The decrease of organic percentage from 80% to 50% decreases the $\log IE$ values statistically significantly for pyrrolidine, pyridine and diphenyl phthalate in case of 0.1% formic acid(aq) as water phase. The same is observed for diphenyl phthalate, 1-naphthylamine, dimethyl phthalate, diphenyl phthalate, piperidine and pyridine in case of 5 mM ammonium acetate buffer pH = 5.0 as water phase and for diphenyl phthalate, dimethyl phthalate, *N,N*-dimethylaniline, pyrrolidine and pyridine in case of 1 mM ammonia(aq) as water phase. The organic modifier percentage change influences the eluent pH and the pK_a values of the bases and, therefore, affect the ionization degree of bases.¹⁰⁵ This could be the reason why the $\log IE$ values of weak bases decrease with decreasing acetonitrile percentage. Additionally, in case of 50% organic modifier the organic modifier content decreases to 36% and, therefore, the analyte ions with lower hydrophobicity are better solvated and their evaporation decreases. The precise reasons for the change of $\log IE$ values for phthalates are not clear but one possibility could be that the solubility of phthalates decreases with decreasing organic modifier content.

The impact of eluent pH

The ionization efficiency of a compound depends on the eluent composition and varies from compound to compound. Comparing scales of different eluent compositions and the pK_a values of the analytes it is seen that there are three kinds of analytes: analytes which $pK_a \gg \text{pH}(\text{aq})$, $pK_a \ll \text{pH}(\text{aq})$ and $pK_a \sim \text{pH}(\text{aq})$.

The calculated α in solution (Table S 5) were compared with ionization efficiency values. In case of analytes for which α in solution does not change significantly from eluent to eluent, either being 1 or approximately zero, $\log IE$ values do not depend significantly on the $\text{pH}(\text{aq})$. In case of analytes with α in solution varying significantly between eluents, the $\log IE$ values depend on the $\text{pH}(\text{aq})$. It is seen that there are three compounds for which the α changes in the aqueous phases of the 7 eluents: pyridine, *N,N*-dimethylaniline and 1-naphthylamine. Comparing the $\log IE$ values of pyridine in these eluents 2.92, 1.53 and -0.82 (80% acetonitrile and the corresponding aqueous phase composition: 0.1%

formic acid, pH = 5.0 buffer, 1 mM ammonia(aq)) and the corresponding α in solutions: 1.00, 0.67 and 0.00, we can see that the lower the α in solution the lower the $\log IE$ value. Similar relationships are seen by *N,N*-dimethylaniline and 1-naphthylamine. The change of $\log IE$ values in eluents with 80% organic modifier and different aqueous phase compositions is statistically significant in case of *N,N*-dimethylaniline, pyridine and occasionally 1-naphthylamine (Table S 7). On the other hand, the analytes with α in solution nearly zero can still give relatively high $\log IE$ value, as is seen on the example of diphenyl phthalate and dimethyl phthalate. Their α -s are nearly zero in all eluents but the $\log IE$ values in the used eluents are in the range of 4.56 to 3.33 for diphenyl phthalate and 3.90 to 2.74 for dimethyl phthalate. The possible reason is that although the concentration of protonated phthalate esters in the droplets is very small they are ejected from the droplet very efficiently because they are (1) hydrophobic and (2) the chelated proton is poorly accessible for solvent molecules hindering efficient solvation of the ion. Another possibility is the existence of highly acidic (possibly super acidic) conditions in some of the droplets, possibly caused by several H^+ ions in the droplet and an insufficient number of solvent molecules to properly solvate them, leading to the high activity of protons.¹⁰⁶

The interplay between the effect of compound properties and eluent pH on ionization efficiency

In order to study the co-effect of pH and compounds physicochemical properties on the ionization 28 analytes in 22 different eluents (all containing acetonitrile and buffer) with aqueous phase pH ranging from 2.1 to 7.0 and acetonitrile percentages of 20% and 80% were used. The studied analytes covered a wide range of $pK_a(aq)$ values from -15.2 to 9.5, and a wide hydrophobicity range: $\log P$ values from -2.0 to 5.0. The ESI results were compared with the α in solution, estimated by UV-Vis spectrophotometric measurements or from chromatographic data.

The results of the $\log IE$ measurements for different eluents are presented in Table S 8. The pooled standard deviation of the results (Eq. 5) in case of acetonitrile/buffer 80/20 was 0.14 $\log IE$ units and in case of acetonitrile/buffer 20/80, 0.23 $\log IE$ units. All 28 analytes were measured in both eluent compositions with pH = 2.1 and pH = 7.0 and if the difference between $\log IE$ values was larger than 0.5 $\log IE$ unit (the threshold for statistical significance, calculated based on the reproducibility of the results), the compound was placed in a pH-dependent group. Analytes with statistically insignificant $\log IE$ change were grouped into the pH-independent group. The $\log IE$ values determined for the analytes in both eluent compositions and both pH values studied are listed in Table 2. All measured $\log IE$ values are listed in Table S 8.

Table 2 The $\log IE$ values of analytes in both eluents (80% and 20% (v/v) acetonitrile) with two different aqueous phases: pH = 2.1 and pH = 7.0. Grey shading indicates that analyte ionization efficiency is dependent on aqueous phase pH.

Analyte	Acetonitrile/buffer			
	80/20		20/80	
	pH = 2.1	pH = 7.0	pH = 2.1	pH = 7.0
2,6-(NO ₂) ₂ -C ₆ H ₃ -P(pyrr)	5.27	5.22	4.62	4.84
<i>N,N</i> -diphenylbispidine	4.63	4.84	4.13	4.28
acridine	4.20	4.17	3.90	2.88
3-methoxy- <i>N,N</i> -dimethylaniline	3.93	2.70	3.62	2.06
4-dimethylamino- <i>N,N</i> -dimethylaniline	3.82	3.68	3.56	3.19
8-aminoquinaldine	3.74	3.46	3.55	1.52
<i>N,N</i> -dimethylaniline	3.74	1.81	3.31	2.46
quinoline	3.65	2.61	3.29	1.98
2,6-dimethylpyridine	3.60	2.34	3.19	1.84
2-aminobenzimidazole	3.60	3.42	3.14	3.30
1-naphthylamine	3.49	2.85	3.01	1.95
4-amino- <i>N,N</i> -dimethylaniline	3.44	3.17	2.73	2.75
2,6-diaminopyridine	3.32	3.06	3.10	2.63
2-aminopyridine	3.20	2.85	2.32	2.36
aniline	3.12	0.92	2.92	0.78
3-hydroxypyridine	2.92	2.64	2.27	1.67
2-aminophenol	2.92	2.32	2.82	2.18
3-nitroaniline	2.85	0.57	2.23	-0.31
pyridine	2.76	1.03	2.48	1.00
3-aminobenzoic acid	2.70	1.74	2.08	1.23
4-aminobenzoic acid	2.68	1.73	1.94	1.29
3-aminophenol	2.66	2.34	2.94	2.56
3-dimethylaminobenzoic acid	2.64	2.67	3.16	2.41
4-nitroaniline	2.59	2.56	2.15	2.08
trizma base	2.53	2.16	2.66	1.64
2-nitroaniline	2.48	1.92	1.89	0.86
2,4-dinitroaniline	1.39	-0.53	0.41	NA ^a
2,4,6-trinitroaniline	1.27	0.96	NA ^a	NA ^a

^a not possible to measure

The largest decrease in $\log IE$ with a pH change from 2.1 to 7.0 was observed for 3-nitroaniline (2.3 $\log IE$ units) and smallest statistically significant $\log IE$ decrease was observed for 2-nitroaniline (0.6 $\log IE$ units) in case of acetonitrile/buffer 80/20. The average decrease of $\log IE$ in the pH-dependent group was 1.2 $\log IE$ units. Similarly, in case of acetonitrile/buffer 20/80, the largest decrease was observed for 3-nitroaniline (2.5 $\log IE$ units) and the smallest for 2-nitroaniline (0.6 $\log IE$ units) with a pH change from 2.1 to 7.0.

Out of the 28 studied analytes, 13 were pH-dependent and 15 were pH-independent.

The change in $\log IE$ values was studied in detail for compounds in the pH-dependent group (pH from 2.1 to 7.0). The flow rate effect on pH dependency was determined for three compounds: *N,N*-dimethylaniline, pyridine, 1-naphthylamine. The pH dependence of the $\log IE$ values of these compounds was evident and numerically consistent at flow rates of 0.008 mL/min and 0.2 mL/min. The $\log IE$ change has the same profile and change occurs at the same aqueous phase pH (Figure S 2). The obtained $\log IE$ values with both flow rates at corresponding eluent compositions were in a good correlation ($0.84 < R^2 < 0.99$). Therefore, it can be assumed that ionization efficiency change with pH is a flow rate independent effect. Typical behaviour of a pH-dependent analyte is presented in Figure 4 for the case of *N,N*-dimethylaniline.

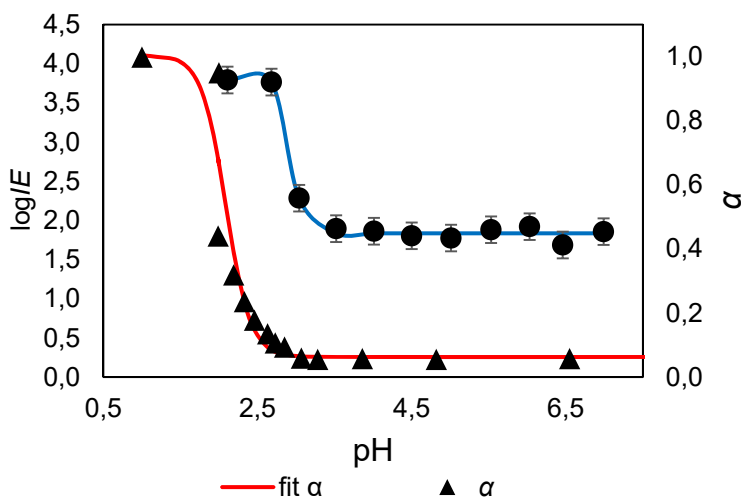


Figure 4 The $\log IE$ values and degree of ionization (α) values of *N,N*-dimethylaniline in acetonitrile/buffer 80/20 and pH 2.1–7.0. The blue and red lines are fitted curves.

In addition to the change in the ionization efficiency, the degree of ionization (α) in the solution phase was determined for all analytes. The results of corresponding changes in α in solution are indicated in Table 3. Based on the results of α measurements in solution and the corresponding $\log IE$ values, analytes were divided into four groups: (I) compounds for which both the $\log IE$ and α changes (10 compounds); (II) compounds for which α changes but the $\log IE$ does not change (13 compounds); (III) compounds for which α does not change but $\log IE$ changes (3 compounds); and (IV) compounds for which neither α nor $\log IE$ changes (2 compounds) (Table 3). However, it is possible that for some analytes, the $\log IE$ change occurs but is too small to be statistically significant.

Table 3 The distribution of analytes according to the behaviour of $\log IE$ values in ESI and α in the solution for acetonitrile/buffer 80/20.

α \ $\log IE$	Dependent	Independent
Dependent	pyridine 2-aminophenol 3-aminobenzoic acid aniline 2,6-dimethylpyridine quinoline 3-methoxy- <i>N,N</i> -dimethylaniline <i>N,N</i> -dimethylaniline 1-naphthylamine 4-amino benzoic acid	acridine <i>N,N</i> -diphenylbispidine 3-aminophenol 4-amino- <i>N,N</i> -dimethylaniline 8-aminoquinaldine 2,6-diaminopyridine 2-aminopyridine 2-aminobenzimidazole 3-dimethylaminobenzoic acid 3-hydroxypyridine 2,6-(NO ₂) ₂ -C ₆ H ₃ -P(pyrr) trizma base 4-dimethylamino- <i>N,N</i> -dimethylaniline
independent	3-nitroaniline 2-nitroaniline 2,4-dinitroaniline	4-nitroaniline 2,4,6-trinitroaniline

Three analytes – acridine, 8-aminoquinaldine and trizma base – had ionization efficiencies independent of pH in an eluent containing 80% acetonitrile but, in an eluent, containing 20% acetonitrile, their ionization efficiency depended significantly on pH. For other compounds, the ionization efficiencies were independent of the eluent acetonitrile composition.

To explain the pH-dependence in ESI source, an LDA was conducted based on physicochemical parameters calculated via the COSMO-RS method and on measured solution phase α . For acetonitrile/buffer 80/20 eluent, the best accuracy was achieved with equation 15.

$$-1.501 \cdot N_{\text{charge centers}} - 0.210 \cdot HBacc3_n + 2.211 \quad \text{Eq. 15}$$

where $N_{\text{charge centers}}$ is the number of potential charge centres, $HBacc3_n$ is the hydrogen bonding acceptor capacity of the neutral form of the analyte. If $F > 0$, then the analyte was considered to be in a pH-dependent group; if $F < 0$, then the analyte was considered to be in the pH-independent group. The prediction precision of this model was 84.2% in the training set and 66.7% in the validation set. This means that 16 compounds out of 19 were grouped correctly into corresponding groups in the training set and 6 of 9 correspondingly in the validation set. If three parameters were used the prediction precision increased in the validation set (Figure S 1) but the functions had the same precision using any of the parameters as the third parameter. It shows additionally that two parameter function describes the behaviour sufficient.

The best discrimination in case of acetonitrile/buffer 20/80 was achieved using equation 16:

$$F = -0.186 \cdot pK_a - 0.030 \cdot sig2_n + 3.500 \quad \text{Eq. 16}$$

Where $sig2_n$ is the polarity of the neutral form of the analyte. The prediction precision was 78.9% for the training set and 77.8% for the validation set. If $F > 0$, then the analyte was considered to be in a pH-dependent group; if $F < 0$, then the analyte was considered to be in the pH-independent group.

Processes occurring in the ESI

In a previous part of this study, we observed that ionization efficiencies of analytes with pK_a values in the range of studied aqueous phase pH were pH-dependent. In this part, we focus on analytes with different $\log P$ (-1.5 to 5.1 calculated with COSMO-RS method) and $pK_a(\text{aq})$ values, mostly in the range of studied aqueous phase pH. The analytes with these particular pK_a values divide into two groups based on ESI response behaviour (Table 3). However, the reasoning for such grouping is not self-explanatory: it cannot be determined solely based on pK_a values of compounds or α determined in a particular eluent. LDA (Eq. 15 and Eq. 16) was used to explain the grouping of analytes based on their pH-(in)dependence in ESI source and the best fit was achieved by using two parameters: number of potential charge centres and hydrogen bonding acceptor capacity (in case of 80% acetonitrile) or polarity and pK_a (in case of 20% acetonitrile). These parameters can be related to three stages occurring during electrospray ionization: (1) protonation of analyte in the droplet interior, K_{a_i} , and on the droplet surface, K_{a_s} , (Figure 5), (2) ejection of charged analyte from the droplet and (3) protonation of analyte in the gas phase, K_{a_g} . The possible processes occurring in the droplet are shown in Figure 5.

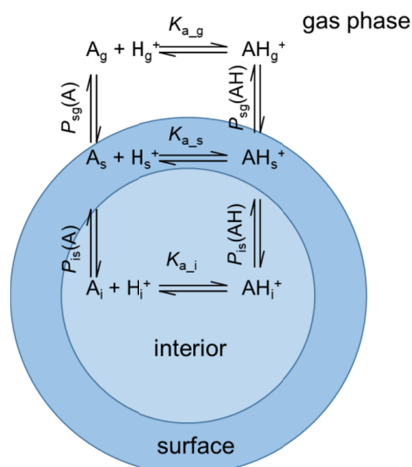


Figure 5 The possible processes affecting the formation of a charged analyte. K_a denotes equilibrium constant of protonation, P denotes the partition between two phases and subscripts i, s and g stand correspondingly for the interior of the droplet, the surface of the droplet and the gas phase.

The number of potential charge centres and pK_a can be related to the process of ionization in solution. Analyte polarity and possibility to accept hydrogen bonds influence the ability to move to the droplet surface and eject from the droplet. The number of potential charge centres describes the analyte probability of becoming charged in the solution phase. Analytes with more than one potential charge centre tend to be in the pH-independent group; however, this group also contains compounds that have only one charge centre. The analytes with more than one potential charge centre are more likely to be ionized, as these compounds have more possibilities to become protonated. Similar observations have been made by Wang et al.¹⁰⁷ who observed that the fragmentation spectra of drugs with two basic functional groups may be significantly different at various pH. They explained this phenomenon by the change in the location of the charge on the molecule. This effect suggests that attaching the proton maybe the limiting stage in ESI ionization for pH-independent compounds.

Effect of water phase additives to ionization efficiency

In publication IV I extended the number of water phase additives with oxalic acid and propionic acid. Among the studied conditions formic acid showed the highest $\log IE$ values. Surprisingly stronger acid oxalic acid did not outperform formic acid. However, the compounds with lower $\log IE$ values profit most (on average 7 times) in $\log IE$ values if oxalic acid is used as an additive. Previously, Yuan et al.⁶⁶ have shown that oxalic acid as an additive is most efficient to suppress sodium adduct formation thus enhancing the protonated signal in case

of oligopeptides. Kruve and Kaupmees¹² have recently also shown the same effect on small molecules. In the mass spectra generated in this particular study, there were no signs of sodium adducts under any conditions. Propionic acid as weaker acid gave unsurprisingly lower $\log IE$ values for studied compounds. Additionally, a higher concentration in formic acid does not statistically significantly increase the $\log IE$ values.

Comparing 10 mM formic acid with 0.1% formic acid (26 mM) in case of methanol/aqueous phase 90/10, it can be noted that ionization efficiencies did in general not increase statistically significantly with higher acid concentration. Low responders benefitted from higher concentrations of acid giving an average 4.4 times increase in $\log IE$ values, whereas high responders lost on average 1.4 times in $\log IE$ values.

Comparing acetonitrile/10 mM formic acid(aq) 90/10 with acetonitrile 0.1% formic acid(aq) 80/20 it was seen that increasing the acid concentration (overall formic acid concentration in the former eluent is 1 mM and, in the latter, it is 5.2 mM) the ionization efficiencies enhanced on average 1.5 times but are lower than in methanol/10 mM formic acid 90/10. The difference between the two acetonitrile containing compositions can be explained by the difference in acidity. The higher acid concentration, as well as lower acetonitrile concentration at the same time, result in higher acidity.¹⁰⁵ Additionally, as acetonitrile is an aprotic solvent the higher content of water results in a more stable spray.³⁸

Properties of compound affecting the pH dependency

The effect of multiple charge centres on pH-dependence can be followed in the example of pyridine (one charge centre), 2-aminopyridine (two charge centres) and 2,6-diaminopyridine (three charge centres); of these, only pyridine is in the pH-dependent group.

However, other physicochemical parameters also change for these compounds with an increasing number of potential charge centres. For example, the $\log P$ value changes from 0.61 (pyridine) to -0.69 (2,6-diaminopyridine). The effect of $\log P$ can also be followed through the example of related compounds like pyridine, quinoline and acridine. The $\log P$ value increases from pyridine (0.61) to quinoline (1.74) and acridine (2.76). However only acridine (the most hydrophobic of these compounds) is in the pH-independent group in case of acetonitrile/buffer 80/20. For these two series of compounds, the $\log P$ effect on ionization efficiency is controversial. Therefore, it could be hypothesized that the analytes in the pH-independent group are either highly hydrophobic (tend to prefer droplet surface) or highly hydrophilic (tend to prefer droplets interior). This hypothesis was tested by using QDA with the octanol-water partition coefficients of the neutral forms of analytes ($\log P$) calculated with COSMO-RS method as an input parameter to explain the pH-dependent behaviour of compounds in acetonitrile/buffer 80/20.

$$F = \log^2 P - 2.4 \cdot \log P + 0.4 \quad \text{Eq. 17}$$

If $F > 0$, then the analyte was considered to be in a pH-dependent group; if $F < 0$, then the analyte was considered to be in the pH-independent group.

The QDA is able to predict the classification into pH dependent and independent compounds with the precision of 82.1%. This phenomenon is visualized in Figure 6 and could be related to the two possible mechanisms for the analyte to form gas phase ions (Figure 5). First, the analyte can partition to the droplet surface in a protonated form ($P_{is}(AH^+)$), this process is driven both by the charge-charge repulsion in the droplet but also by the hydrophobicity of the protonated analyte. Secondly, the analyte may partition to the droplet surface as a neutral ($P_{is}(A)$) and become protonated on the acidic surface of the droplet.¹⁰⁸ This process is driven solely by the hydrophobicity of the analyte (neutral form). However, the proportion of these effects is very complicated to estimate as the hydrophobicities of the protonated forms are not available. A similar effect has also been observed by Golubovic et al.,²¹ who observed a Gaussian shaped relation between the ESI/MS response and $\log P$ of the analytes. In case of acetonitrile/buffer 20/80, this phenomenon was not as evident.

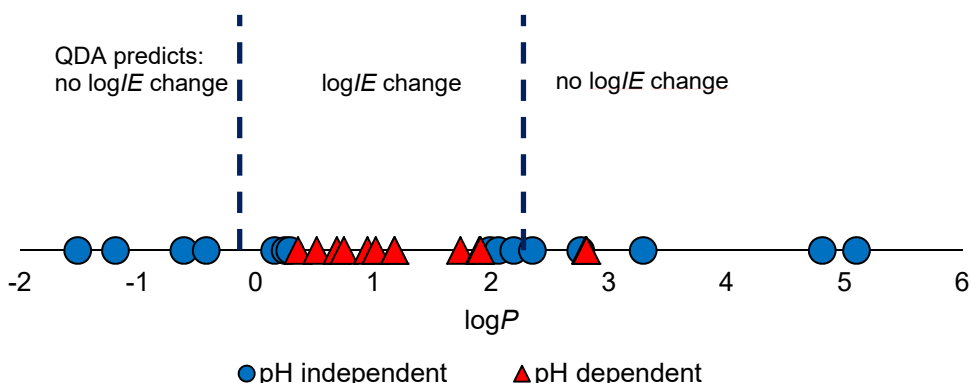


Figure 6 The relationship between pH-dependency and $\log P$ (calculated with COSMO-RS) of the neutral form of an analyte in case of acetonitrile/buffer 80/20. The dashed lines indicate the discriminating levels predicted with QDA.

Although the best discriminant function was obtained with two parameters the size of analyte plays a role in ESI source. The LDA functions of three parameters with the highest precision contained a parameter that describes size (area or molecular volume). Larger (by volume) analytes tend to be in the pH-independent group. 2,6-(NO₂)₂-C₆H₃-P(pyrr), *N,N*-diphenylbispidine, 4-dimethylamino-*N,N*-dimethylaniline, acridine, 2,4,6-trinitroaniline and 3-dimethylaminobenzoic acid are the six largest analytes among the studied compounds and all are in the pH-independent group. An explanation could be

that larger molecules tend to be more stable in the gas phase when protonated as they screen and stabilize the charge through the polar effect more efficiently if the nature of the protonation centre does not change dramatically (e.g. for alkylamine vs pyridine the change in the nature of the protonation centre is significant).¹⁰⁹ However, these compounds are among the most hydrophobic of those studied and, therefore, the molecular volume effect cannot be fully separated from the $\log P$ effect.

Comparing the results of measurements of α with results of ionization efficiency measurements (an example is given in Figure 4, similar graphs were observed for other analytes) for acetonitrile/buffer 80/20, we see that the ionization efficiency change occurs at 0.5 units higher pH (aqueous phase) than the α changes in the solution. This offset can be explained by the change of pH that occurs during the electrospray process. It has been shown in positive mode ESI that due to the electrochemical reaction occurring on the ESI needle tip, the pH of the eluent is lower in the plume compared to the original solution.⁶¹ During electrochemical reactions, additional hydrogen ions are generated in ESI positive mode.⁶¹ Additionally, the evaporation of solvent from the ESI droplets increases the concentration of protons; therefore pH decreases along the plume.⁶²⁻⁶⁴

One of the eluents used (pH = 2.1) contained TFA as a pH modifier. Previously, it has been observed in the literature^{50,110} that TFA may cause ionization suppression. In our case, several compounds showed lower $\log IE$ values in the eluent containing 0.1% TFA than in the eluent containing 0.1% formic acid, though the eluent with TFA had lower pH. The highest suppression was observed for 3-aminobenzoic acid (0.8 $\log IE$ units). However, the suppressive effect of TFA was rarely statistically significant. Interestingly, in both eluents $\log IE$ values have been anchored to tetraethylammonium, for which the $\log IE$ did not change remarkably with pH. This means that the suppressive effect of TFA is compound dependent.

Transferability between instruments

Until my studies, the majority of the ionization efficiency measurements in UT were conducted on one mass spectrometric setup. Although, that designs of ionization sources from different vendors vary it was hypothesized that the approach of ionization efficiency scales is a universal approach and the trends are applicable to different mass spectrometric setups. So next this hypothesis was tested.

The results of the $\log IE$ measurements conducted on different mass spectrometric setups are presented in Table 4, Table 5 and Table S 9 and graphically in Figure S 3 and Figure S 4. For each studied combination of MS setup and eluent, an ionization efficiency scale was compiled. The instrument comparison compounds set covers 4.1 orders of magnitude of $\log IE$ values.

Table 4 The positive mode ESI log I/E values in acetonitrile/0.1% formic acid(aq) 80/20 on four different mass spectrometers with four different ESI setups.

	Acetonitrile /0.1% formic acid(aq) 80/20 (v/v)				
	XCT ^a	Q ^b	3Q-Varian ^c	XCT-3R ^d	3Q-6495 ^e
Phe-Phe-Phe-Phe	5.05	NA ^g	3.64	5.04	2.87
2,6-(NO ₂) ₂ -C ₆ H ₃ -P(pyrr)	4.87	NA ^g	4.01	5.15	4.10
tetrapropylammonium	4.65	4.76	4.21	4.74	4.15
tetraethylammonium	3.95	3.95	3.95	3.95	3.95
triethylamine	3.80	3.32	3.36	3.35	3.25
1-naphthylamine	3.66	3.26	3.50	3.48	3.25
<i>N,N</i> -dimethylaniline	3.50	3.00	3.58	3.39	3.29
Ac-Gly-Lys-OMe	3.49	NA ^g	3.13	3.38	3.10
diphenyl phthalate	3.42	3.46	3.19	3.02	2.95
piperidine	3.20	3.19	3.28	2.80	NA ^f
dimethyl phthalate	2.98	3.19	3.14	2.97	2.34
pyrrolidine	2.90	3.30	3.11	2.60	NA ^f
pyridine	2.79	2.77	3.05	2.54	NA ^f
cysteine	1.70	NA ^g	1.68	1.05	0.98
glycine	1.18	NA ^g	2.12	1.13	NA ^f
<i>pooled standard deviation</i>	0.28	0.17	0.31	0.39	0.30
<i>Span</i>	3.87	1.98	2.53	4.10	3.18

^a Agilent XCT ion-trap with orthogonal ESI; ^b Agilent Single Quad 6100 with Agilent JetStream; ^c Varian J-320; ^d Agilent XCT ion-trap with in house developed 3R sprayer; ^e Agilent 3Q-6495; ^f It is not possible to measure because the lowest m/z value measurable with this MS system is 100. ^g not measured

Table 5 The positive mode ESI log I/E values in acetonitrile/0.1% formic acid(aq) 20/80 on three different mass spectrometers with three different ESI setups.

	Acetonitrile /0.1% formic acid(aq) 20/80 (v/v)		
	XCT ^a	Q ^b	3Q-Varian ^c
tetrapropylammonium	4.38	4.22	3.80
tetraethylammonium	3.74	3.46	3.62
triethylamine	3.39	3.14	3.56
1-naphthylamine	3.40	3.22	3.04
<i>N,N</i> -dimethylaniline	3.37	2.97	2.92
piperidine	2.91	3.00	3.15
pyrrolidine	2.33	3.01	2.97
dimethyl phthalate	3.30	3.50	NA ^d
pyridine	2.41	2.71	2.87
<i>pooled standard deviation</i>	0.02	0.03	0.03
<i>span</i>	2.05	1.51	0.93

^a Agilent XCT ion-trap with orthogonal ESI; ^b Agilent Single Quad 6100 with Agilent JetStream; ^c Varian J-320; ^d not measured

From the results in Table 4, Table 5, Table S 9, it can be concluded that $\log IE$ scales obtained in the same eluent on different instruments have in broad terms similar order of $\log IE$ values. On all instruments, high responders are 2,6-(NO₂)₂-C₆H₃-P(pyrr), tetrapropylammonium and tetraethylammonium and low responders glycine and cysteine. The Phe-Phe-Phe-Phe is quite a high responder for all mass spectrometric setups but especially in case of ion trap mass analyzer. One reason could be that the ion optics parameters applied are more suitable for compounds with higher m/z value and, therefore, generate an extra gain of response. For some analytes, the ionization efficiency values are statistically significantly different between different instruments. On the other hand, correlation coefficients obtained while comparing data from different instruments range from acceptable to very good (R^2 0.64–0.99) (Table S 10). Comparing the obtained R^2 with the pooled standard deviations (up to 0.39 $\log IE$ units) and spans (up to 4.1 $\log IE$ units) of the individual scales (Table S 10) the correlations are acceptable. Differences in the $\log IE$ scales for the different setups could be explained by the solution properties, the sprayer properties (i.e. source design) and the mass spectrometer properties (i.e. ion transport and detection).

Electrospray source design and solution properties

The scales could differ because of differences in electrospray sources. Indeed, the geometrical ESI source parameters that vary are the dimensions of the needle, the shape of the needle tip, the geometry of electrospray setup (e.g. angle between the needle and MS inlet capillary, on-axis or off-axis design) and the distance between needle tip and mass spectrometer inlet. Moreover, support gas parameters and voltages, such as the nebulizer gas pressure, drying gas temperature and flow rate, additional gas occurrence, the applied voltage between needle and mass spectrometer inlet and additional voltage occurrence, are different. These source properties are likely to cause differences in electrospray plume – e.g. in solvent evaporation rate or droplet size variations. This can lead to differences in droplet compositions from where on average the ion ejection occurs.

The results show that the ESI sprayer geometry is important. Comparing the spans with t -test there are statistically significant differences only between the scales obtained with the 3Q mass spectrometer and other instruments (Table S 10).

The scales obtained with the 3Q mass spectrometer are more than 21 times compressed compared to ones obtained with the other MS systems. One reason could be that, in this ESI source, the needle is at approximately 120 degrees with respect to the mass spectrometer inlet capillary as opposed to the orthogonal geometry of the remaining ion sources. Compared to the orthogonal geometry of the remaining ion sources the analytes have less time to evaporate from droplets and most of the droplets are blown to the counter electrode.²⁷

Voyksner and Lee¹¹¹ and Holčapek et al.¹¹² have shown that the orthogonal ESI source configuration gives better sensitivity than other source designs thanks to the prevention of clogging the MS orifice by non-volatile materials. Additionally, Tang and Smith¹¹³ and Gomez and Tang¹¹⁴ have shown that progeny droplets – sources for ions – are ejected in the sidewise direction toward the periphery region of the electrospray. Therefore, orthogonal source designs typically show better sensitivities.

Interestingly, we observed that standard deviation obtained with acetonitrile/0.1% formic acid(aq) 20/80 are significantly smaller than with acetonitrile/0.1% formic acid(aq) 80/20 in case of orthogonal pneumatically assisted ESI source and sheath gas assisted Jet Stream. In case of high acetonitrile percentage, the solvent fractionation and drying rate are more affected by the drying and nebulizing gas flow rate and temperature and the addition of a sheath gas due to the high volatility of acetonitrile. Electrospray plume obtained with a lower acetonitrile percentage (20%) is less affected by the gas parameters due to the high proportion of less volatile water. The solvent fractionation is less efficient whatever the gas parameters used which results in similar $\log IE$ values for the different systems.

Previous studies show that using different electrospray parameters (mainly sheath gas temperature and flow rate as well as capillary voltage) results in different droplet size, droplet composition and pH.^{62,85}

Comparing the ionization efficiencies obtained with the Jet Stream and with the orthogonal pneumatically assisted ESI source, the order of compounds in the scale changes. Additionally, regression analysis shows that the data points do not display a linear relationship. This could be explained by the fact that in the Jet Stream the optimum conditions are very analyte-dependent as shown by Stahnke et al.¹¹⁵ and Periat et al.³⁹

The study in publication IV extended the study with additional 5 mass spectrometric setups and the results confirm similar trends in ionization efficiencies measured and excellent correlation ($0.84 < R^2 < 0.96$) between the scales on different mass spectrometric setups.

Mass spectrometer properties

In addition to source design, the mass spectrometer may have an effect on ionization efficiency. In the previous part, the ionic optics parameters *target mass* of the XCT instrument was optimized and scales with optimized and default ionic optics parameters were compared.^{10,116} The optimized ion optics parameters improve the consistency in the scale and between the scales. In this study, we are unable to use the same ion source on different instruments and, therefore, it is not possible to statistically separate the effects of the ion source and mass spectrometer. As also mentioned in the previous paragraph, the source geometry and the addition of drying gas affect the desolvation process in ESI.

The early stages of ion train devices (i.e. transfer capillary, tube lens) may present different efficiencies with respect to partly desolvated ions.

The usefulness of ionization efficiency scales

The trends demonstrated by the IE scales obtained on different instruments are the same. Although the $\log IE$ values, as a rule, cannot be transferred from one MS setup to another, they correlate with each other. The order of compounds in the scale does not change remarkably and the ionization efficiencies are consistent, for the different setups, in the range of half logarithmic unit (equivalent to 3 times sensitivity difference). The good correlation between the different scales also assures that models built for predicting ionization efficiency are transferable between instruments and only the coefficients in the model may need some adjustment depending on the instrument.

It can be assumed that this type of adjustment can be easily carried out with measurements of three or more compounds from the scale on the new instrument. According to the obtained intensities, the adjustment of the predictive model can be made. Likely, three anchoring points will be sufficient to scale the ionization efficiencies and use them in the semi-quantitative analysis as seen below.

Independent validation

In order to demonstrate the inter-instrument transferability, the obtained $\log IE$ values from ref.¹⁰ (orthogonal ESI source geometry and ion trap mass analyzer) were applied to predict the concentrations of twelve analytes (7 of them were only used in the validation set) on a completely different mass spectrometric setup (approximately 120 degree ESI source geometry and hybrid mass analyzer that consist of triple quadrupole and FT-ICR). The used validation compounds set covers 3.5 $\log IE$ units. The data in Table 6 demonstrates that the concentrations of two compounds (pyridine and tetrapropylammonium) differ 2.0-2.5 times and for the remaining ten compounds the difference is less than 2 times. The average difference is 1.7 times. This validation gives additional support to the transferability of the $\log IE$ scale between different ESI-MS setups.

Table 6 The used concentrations (c_{sample}) and the predicted concentrations (c_{calc}) of independent validation.

	$\log IE^a$	c_{sample} (mol/L)	c_{calc} (mol/L)	$c_{\text{calc}}/c_{\text{sample}}$
tetramethylammonium	2.15	5.25E-06	NA ^b	
2-nitroaniline	2.44	2.36E-06	3.25E-06	1.38
benzamide	2.74	9.57E-07	1.42E-06	1.48
pyridine	2.94	4.89E-06	1.96E-06	0.40
piperidine	3.16	9.42E-07	4.92E-07	0.52
2,6-dimethylpyridine	3.41	3.50E-06	4.87E-06	1.39
triethylamine	3.53	6.66E-07	4.59E-07	0.69
<i>N,N</i> -dimethylaniline	3.72	1.02E-06	5.84E-07	0.57
tetraethylammonium	3.95	9.40E-07	NA ^b	
diazabicycloundecene	3.96	8.53E-07	1.57E-06	1.84
acridine	4.42	9.05E-07	7.95E-07	0.88
diphenylguanidine	4.61	4.08E-07	2.78E-07	0.68
tetrapropylammonium	4.97	3.82E-07	1.79E-07	0.47
tetrabutylammonium	5.13	2.83E-07	1.73E-07	0.61
tetrahexylammonium	5.65	7.96E-08	NA ^b	

^a values from ref.¹⁰

^b values used for calibration

The previous steps showed that we can measure accurately ionization efficiencies of compounds with various physicochemical properties and study the ionization efficiency for ion evaporation model quantitatively. In literature, there are some preliminary models that have tried to predict ionization efficiency for a specific set of compounds in specific eluents. My aim is to develop a universal model that is applicable to different mass spectrometric setups and eluents. The developments in machine learning algorithms make it possible to develop a universal model. Pooling the data from previous steps and incorporating the results from previous studies gave a reasonably large dataset. As more sophisticated supervised machine learning algorithms benefit from larger datasets, I measured another 200 compounds and a set of 40 compounds in an additional 21 eluent compositions to develop a universal model.

Standard substance free quantification

Predicting ionization efficiencies

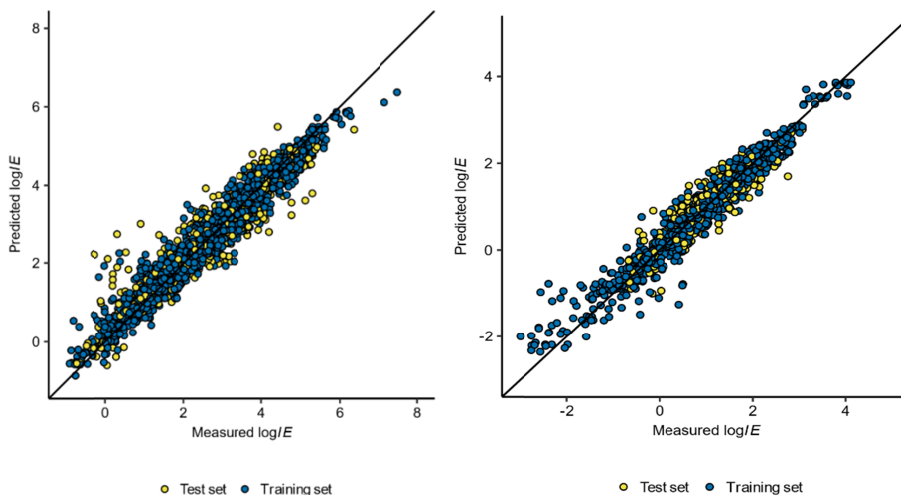
The developed model and approach presented graphically in Figure 1 is called Quantem. In order to develop the Quantem approach we (1) measured $\log IE$ values for a wide set of compounds, (2) used the measured $\log IE$ values as well as compound and eluent descriptors for developing the model that would allow predicting ionization efficiencies, and (3) validated the approach by using the

predicted $\log IE$ values to quantify a set of compounds in cereal and green tea samples. For ESI positive mode, a total of 3139 ionization efficiency values were measured and collected from our previous works.^{10,12,86,86,106,116} These data belong to 353 unique compounds (Table S 2) and 106 different eluent compositions (Table S 3). For ESI negative mode, an additional 1286 ionization efficiency values have been collected from our previous works,^{87,117} including 33 eluent compositions (Table S 11), and 101 unique compounds (Table S 2).

Based on these $\log IE$ values predictive models for positive and negative mode were developed. For positive mode, regularized random forest regression was used with 450 significant descriptors and 100 regression trees. The regression model explained 94 % of the variation in $\log IE$ values. The overall RMSE was 2.2 times (training set 1.9- and test set 3.0 times) (Figure 7a). This means that if the $\log IE$ of compound A is predicted to be 100 times higher than the $\log IE$ of the methyl benzoate the actual ionization efficiency would be 45 to 220 higher than that of methyl benzoate ($\log IE = 2.00 \pm 0.34$). The lowest possible prediction error is 1.0 and values close to 1.0 are desirable. In negative mode, the best performing model was obtained also with random forest regression with 145 significant descriptors and 100 regression trees. The regression model explained 93 % of the variation in ionization efficiency values. The overall RMSE was 2.0 times (training set 2.0- and test set 2.3 times, Figure 7b).

Upon closer examination of the ionization efficiency prediction model in ESI positive mode, it is observed that the model performs universally well for different organic modifier percentages (Figure S 5 and Figure S 6). The lowest prediction error, 1.4 times, was observed for eluents containing 20 % of organic modifier and the highest prediction error, 1.9 times, for eluent containing 90 % organic modifier. This is expected, as eluents containing 20 % of organic modifier have the highest number of data points, which improves prediction accuracy. Additionally, the model is well performing for both methanol as well as for acetonitrile containing eluent compositions (Figure S 5 and Figure S 6). Based on the pH of the eluent, basic conditions had the highest prediction error; 2.5 times and 3.7 times for the training and test set respectively.

Similar trends were observed for ESI negative mode; the prediction accuracy for the pure organic modifier is the lowest (prediction error of 4.1 times, Figure S 7 and Figure S 8). Regarding the pH, no significant differences in the prediction accuracy were observed (Figure S 7).



a: ESI positive mode with 3139 data points.

b: ESI negative mode with 1286 data points.

Figure 7 Performance of ionization efficiency prediction models. Black line denotes ideal fit.

Quantifying pesticides in cereals

The ionization efficiency predictions can be used to predict the concentrations of the compounds detected assuming that the structure is known. Firstly, we tested the Quantem approach on the analysis of pesticides from spiked cereal samples. We used the ionization efficiencies to predict the concentrations of 35 pesticides (Table S 4) in oat, barley, rye, wheat, rice, and maize. Each matrix was spiked with each pesticide at 10 concentration levels. The concentrations of the pesticides ranged over 5 orders of magnitude from 3.6 nM to 0.35 mM. Altogether 2233 data points (pesticide, matrix, and concentration combinations) were measured and corresponding concentrations were predicted.

For each pesticide, the ionization efficiency was predicted in ESI positive mode. However, it is known from previous studies that different instruments have somewhat different ionization sources and, therefore, compress and enhance the ionization efficiency scales differently.^{118,119} In order to transform the predicted $\log IE$ values to instrument-specific response factors a set of 31 compounds (Table S 12) was used. Thereafter, the instrument-specific response factors were used to convert LC/MS signals into concentration (Eq. 11).

Additionally, modelling of data using sets of 15, 10 and 6 compounds were performed and even with only 6 compounds the same accuracy of concentration prediction was achieved (Table S 13).

On average, the concentrations were predicted with the prediction error of 5.7 times. This means that if the pesticide concentration is estimated to be 1 ppm it would actually be between 0.2 and 6 ppm. Compared to the

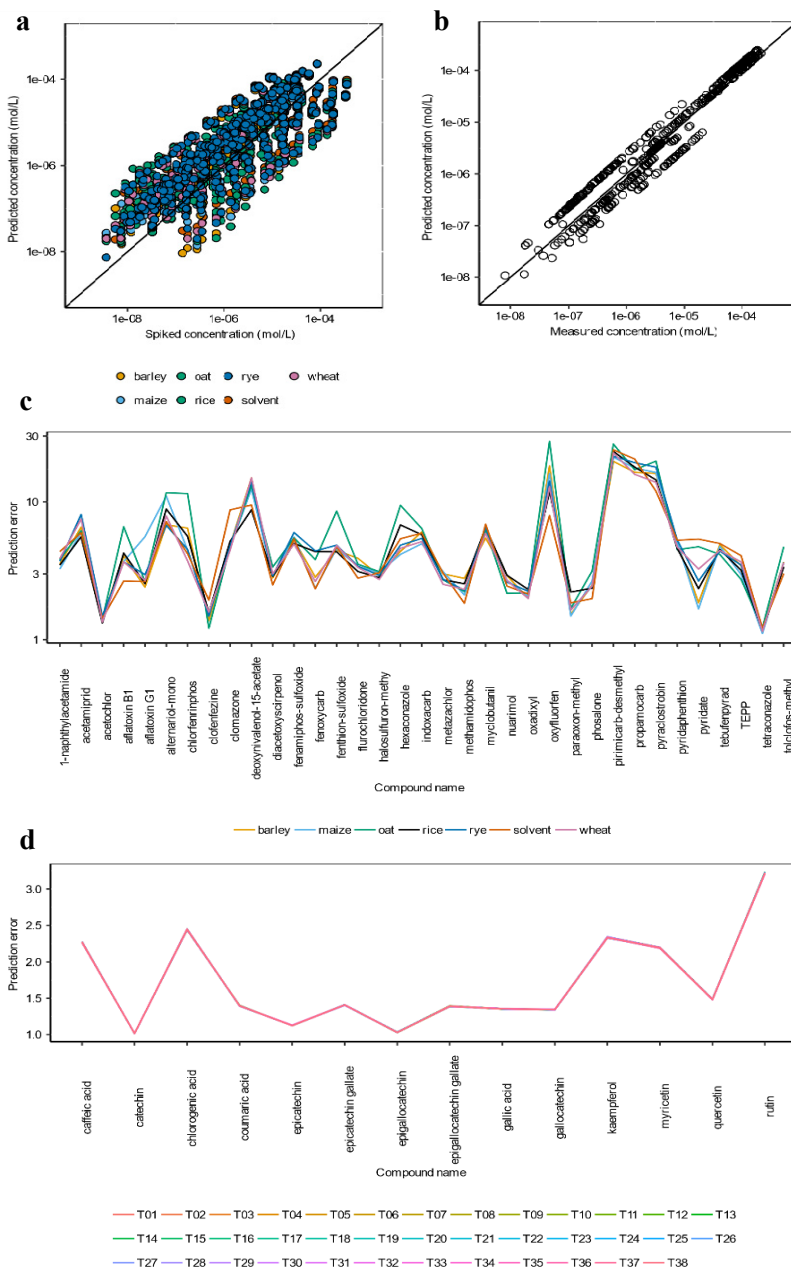
conventional approach of assuming the equal response to all compounds detected (average prediction error of 526 times, Table S 14), the Quantem approach improves prediction accuracy around 10 times and significantly reduces the width of the confidence interval. This, on the other hand, allows decision making based on the predicted concentrations.

The lowest error observed was 1.03 times for acetochlor in rice matrix, while the largest error, 65 times was observed for pyraclostrobin in oat matrix. For 86 % of the compounds the prediction error was lower than 10 times, for 65 % of the compounds it was lower than 5 times, and for 22 % of the compounds, it was lower than 2 times. The three compounds with the highest prediction error were pirimicarb-desmethyl (23 times), propamocarb (18 times), and pyraclostrobin (16 times). The three best-performing compounds are tetraconazole (1.2 times), acetochlor (1.4 times), and clonfezine (1.5 times).

Different matrices

Any model that aims at providing quantitative information needs to be applicable in a variety of matrices in order to be truly useful to researchers. The importance of matrices with LC/MS is even more relevant than for other analytical techniques, due to the possibility of significant matrix effects in the ESI source. A matrix effect is the suppression of ionization of a compound due to co-eluting compounds. Previously, it has been qualitatively observed that the matrix effect and ionization efficiencies are influenced by the physicochemical properties of the compound.¹⁹ Therefore, while applying the ionization efficiency predictions for concentration estimations it was assumed that a model that considers ionization efficiencies also helps to account for matrix effect. This assumption was based on the fact that a small set of compounds with known concentrations were spiked into every sample; this helped to account for the differences arising from the instrument and also for matrix effects (Eq. 10). Regarding different matrices, the prediction accuracy for all cereals was very similar. The lowest prediction error was observed for wheat and rice, 5.4 times, and highest for oat, 6.7 times. This is expected, as oat samples possess a high content of polar lipids and free fatty acids¹²⁰ which possess high surface affinity and are, therefore, expected to cause ionization suppression.¹²¹ Also, the mean prediction error for solvent (average 5.4 times) and all studied cereals (5.7 times) was close.

Moreover, the matrix effect is expected to vary strongly from sample to sample even for the same food commodity. In case matrix effect would play a major role in the accuracy of the concentration predictions the accuracy for one pesticide would also strongly vary from sample to sample. Here we observed a contradicting example; the compounds that performed worst in one matrix performed also poorly in other matrices and best performers were in the top for all matrices (Figure 8c and Figure S 9). This strongly indicates that the Quantem approach using ionization efficiency predictions together with the transformation, help sufficiently to account for matrix effects.



a: concentration prediction of pesticides in cereal samples. **b:** concentration prediction of metabolites in green tea samples. **c:** prediction error of pesticide concentration in cereal samples, y-axis in logarithmic scale. **d:** prediction error of metabolites in green tea samples.

Figure 8 Performance of ionization efficiency prediction in the example of pesticides in cereal and metabolites in green tea.

Quantifying metabolites in green tea

We studied the applicability of predicting ionization efficiency values on data collected completely independently in the past. In the metabolite analysis in green tea by Kellogg et al.¹⁰⁰ 19 metabolites (Table S 4) had been identified, of these, 14 were quantified with the aid of standard substances. The concentration of studied metabolites varied more than 3 orders of magnitude. The quantitative data available allowed the validation of Quantem approach. 5 metabolites were detected and identified in these samples but could not be previously quantified due to the lack of standard substances; these metabolites were quantified with the aid of Quantem approach.

First, the $\log IE$ values were predicted for all 19 identified metabolites. To transform the universal $\log IE$ values to instrumentation specific response factors 6 compounds quantified with the aid of standard substances were used (Eq. 10). For that, the relative response factors of chlorogenic acid, rutin, coumaric acid, epigallocatechin, gallic acid, and epigallocatechin gallate in one tea sample (NIST standard reference material green tea) were calculated and correlated with predicted ionization efficiencies. The instrument-specific ionization efficiency values were used to estimate the concentrations of remaining metabolites in 38 tea samples.

For the quantification of metabolites in green tea samples, high overall accuracy was observed; the average prediction error was 1.7 times and for all of the compounds the prediction error was less than 3.3 times. Comparing the different metabolites, the lowest error was achieved for catechin (1.0 times) and highest for rutin (3.3 times). It is important to note that the studied metabolites were structurally similar to one another, comprising flavonoids and catechin skeletons. Comparing the metabolite profiles obtained (i) with ionization efficiency prediction and (ii) with quantification with standard substances revealed high similarities (Figure S 10) suggests that ionization efficiency predictions allow retrieving reliable quantitative information of detected and identified compounds.

We also estimated the concentration for 5 metabolites that could not be quantified previously (Figure 9). The concentrations of the flavonoids quinic acid, apigenin glycoside, and caffeoylquinic acid were generally constant across the products, which was in line with the results of the previous study.¹²² However, a significant decrease in the concentration of the catechins 3-*O*-(3-*O*-methylgalloyl)epigallocatechin and epicatechin-3,5-digallate was observed in one of the samples, T23, which had been previously determined to be a non-green tea negative control (a turmeric-ginger tea). Thus, the concentrations derived from the ionization efficiency prediction are believed to be accurate representations of the concentrations of these metabolites in the tea samples.

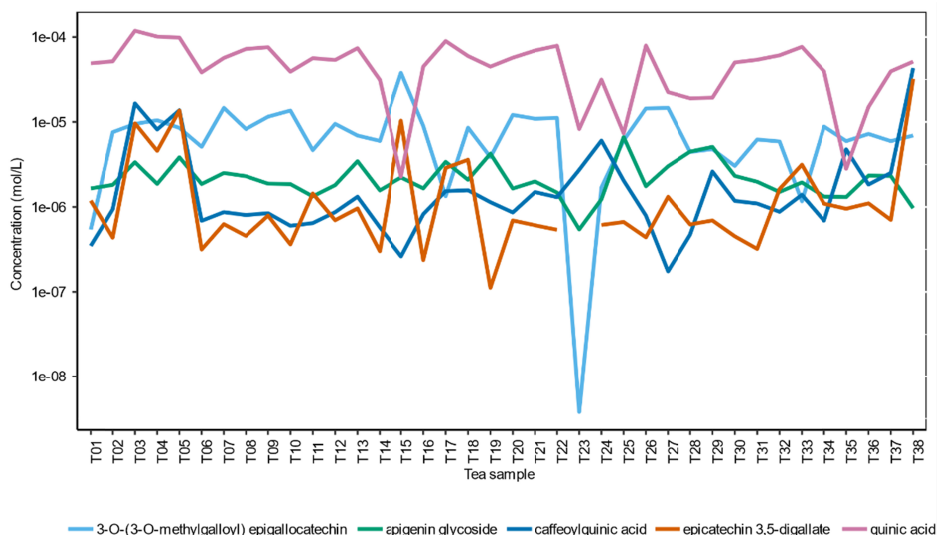


Figure 9 Estimated concentration of identified metabolites in green tea samples. T23 is a non-green tea negative control.

The concentration prediction accuracy for the green tea samples was significantly better than for the cereal samples; one of the reasons could be that the cereal samples were analysed in positive mode while green tea samples had been analysed in the negative mode. It is expected that the accuracy for negative mode is slightly higher, as understanding the ionization in the negative mode is significantly more straight forward than for the positive mode. In negative mode, only compounds with a significantly acidic moiety can be ionized, while in positive mode also very weak bases can be protonated and detected. The latter makes positive mode much more complicated to model.

Also, previous studies have shown that the ESI negative mode suffers much less from the matrix effect.¹²³ This is related to the fact that in ESI negative mode only a fraction of matrix compounds can be ionized and are, therefore, able to compete for the surface charge in ESI droplets. As a result, applying ionization efficiency predictions for predicting concentrations is expectedly showing higher accuracy in the negative mode.

Different instruments and labs

One of the biggest challenges for non-targeted analysis is to be universal over different instruments and different labs. This is essential for comparing the results from lab-to-lab and from day-to-day.

The ionization efficiency model was primarily developed on an ion trap instrument, but also data from seven other instruments from three other laboratories were incorporated, covering all major vendors. Additionally,

Quantem approach implements a transformation system that would allow transferring the ionization efficiency predictions to any instrument in any lab (Eq. 10).

Moreover, the validation of Quantem approach on cereal samples and green tea samples was also carried out on different instrument and/or labs. The cereal samples were analysed on a triple quadrupole instrument in Tartu (Estonia), while the tea samples were analysed on an Orbitrap instrument in University of North Carolina at Greensboro (USA). Both sample types showed low concentration prediction errors (5.9 times and 3.3 times). It is reasonable to conclude that instrument type and lab do not influence the prediction accuracy as long as all measurements are carried out in the linear response range.

Retrospective analysis

Applying Quantem approach retrospectively to already measured and/or published results would increase the scope of quantitative non-targeted analysis considerably. The retrospective analysis of the data originally published by Kellogg et al. in 2017¹⁰⁰ was made possible by the fact that some of the compounds in the tea samples were quantified with the authentic standards already during the time of the analysis. Interestingly, the prediction accuracy for the analysis done in retrospective was as good as for the cereal samples where compounds for transformation were intentionally chosen and analysed at the time of the sample analysis. It is apparent that any reasonably large set of compounds (at least 5) quantified from the sample can be used for transformation if the compounds are distributed around the chromatogram and have a reasonably different ionization efficiency (compared to the compounds discovered with non-targeted methods).

All in all, we have shown that ionization efficiencies can be predicted with sufficient accuracy to facilitate concentration predictions for compounds that lack standard substances. In general, the prerequisite is that at least some compounds have been analysed together with the sample and quantified. Such compounds could be any of the compounds confirmed with the aid of standard substances or compounds from the quality control samples used. This makes full scan LC/HRMS extremely appealing, as a combined targeted and non-targeted analysis method can be used.

The same strategy also allows analysing non-targeted data retrospectively. As a matter of fact, for all of the green tea samples described in this manuscript, the quantification was carried out a long time after the measurements were made and no additional measurements of any kind were conducted. This means that a very large portion of samples analysed with generic non-targeted or suspect screening methods can be now quantified retrospectively. We see a very high area of application in environmental as well as health-related LC/HRMS analysis where time-trends are of crucial importance.

Equally importantly, the quantification will also allow comparing data from different labs. Again, the only prerequisite being that some of the compounds have already been quantified within the lab. Of course, quantifying the data via ionization efficiencies inside one lab and exchanging the quantitative data directly would be convenient for regional monitoring programs. However, the ability to recalibrate the data from another lab and from previous timespans increases the transparency and validity of the results further. Additionally, for risk assessment of contaminants in food and environmental samples, even an estimated concentration of a compound is better than none to evaluate the exposure hence the risk. And in most cases, the error on the other parts of risk assessment (like intake and toxicology) is as large or even larger.¹²⁴

SUMMARY

Liquid chromatography electrospray ionization mass spectrometry (LC/ESI/MS) is a widely applied analytical technique. Furthermore, it is more and more applied in non-target analysis enabling to obtain a more complete picture of biological and chemical processes occurring in living organisms and environment. Standard substances are needed to obtain quantitative information from LC/ESI/MS analysis. This thesis proposed and developed an approach to predict ionization efficiencies to enable standard substance free quantification in LC/ESI/MS analysis.

During this study, the effect of compound structure to electrospray ionization efficiency was quantitatively investigated. For that ionization efficiencies for more than 350 compounds were collected and measured. In general, more basic and more hydrophobic compounds possess higher ionization efficiency in ESI positive mode.

Next, the effect of eluent on electrospray ionization efficiency was studied. As organic modifiers methanol, acetonitrile, isopropanol, and acetone were studied. The studied organic modifier percentages ranged from 0% to 100%. Furthermore, all mostly used water phase additives: formic acid, acetic acid, ammonium acetate, ammonia, ammonium formate, ammonium bicarbonate, TFA, and ammonium fluoride were studied. The studied water phase pH ranged from 2.1 to 10.7. Typically, in ESI positive mode higher ionization efficiencies are observed in high organic modifier eluents. The effect of eluent pH on electrospray ionization efficiency is more complex. For compounds with the pK_a close to the eluent pH, the ionization efficiency is strongly affected by the pH of eluent if the compounds have $\log P$ value close to 0. Highly hydrophobic as well as highly hydrophilic compounds are generally less affected by the pH of eluent.

Additionally, it was shown that the trends observed on one mass-spectrometric setup are universal among different instrumental setups from different vendors and can be applied to different mass-spectrometric setup. However, it was observed that electrospray ionization source design may strongly affect the ionization efficiency values and to use the values on different instrumental setups transformation with a small set of compounds is needed.

As a final step, a universal approach enabling standard substance free quantification in LC/ESI/MS analysis was developed. For ionization efficiency prediction random forest regression algorithm was used. This approach takes into account both the structure of the compound as well as the eluent composition at the retention time of the compound. The average prediction error for ionization efficiency prediction was 2.2-times which increases the reliability of results of standard substance free quantification up to 10 000 000 times. The developed approach uses a small set of compounds to transform the predicted ionization efficiencies to method and instrument-specific response factors to enable standard substance free quantification in any LC/ESI/MS analysis with

the average prediction error better than 5 times. Moreover, this approach is not only applicable in the future but can be used to retrospectively quantify compounds detected with LC/ESI/MS in the full scan mode. This approach was made available to the mass spectrometric community as an online tool.

SUMMARY IN ESTONIAN

Standardainete vaba kvantiseerimine LC/ESI/MS analüüsil kasutades ionisatsiooni efektiivsuste ennustamist

Kõrgefektiivne vedelik kromatograafia elektropihustus massispektromeetria (LC/ESI/MS) on laialt kasutatud väga võimekas analüüsimeetod. Antud meetod on levinud orgaaniliste ühendite, eriti jälgede, määramise meetod. Kahjuks on sellel meetodil üks puudus. Kõrgefektiivse vedelikkromatograafi ja massispektromeetri ühendamiseks kasutatava elektropihustuse ionisatsiooniefektiivsus on ühendist sõltuv ja võib erineda üle 10 miljoni korra. Ionisatsiooniefektiivsus on defineeritud lahuses olevate analüüdi molekulidest või ioonidest genereeritud gaasifaasiliste ioonide määrana. Seepärast tuleb LC/ES/MS kvantitatiivseks kasutamiseks kasutada standardaineid. Kahjuks ei pruugi standardained kättesaadavad olla, kui tegemist on uudse avastusega, antud ühendeid on raske eraldada või nad on ebastabiilsed. Lisaks avardub meie teadmine võimalikest arvukatest saasteainetest keskkonnas ning tuhandetest elusorganismide talitlust juhtivatest metaboliitidest. Kõigi nende ainete sisalduste määramisel standardainete kasutamine ei ole majanduslikult võimalik.

Suunatud analüüs (ingl *targeted analysis*) vaatab uuritava objektile peale kui silmaklappidega hobune: meetodiga on võimalik määrata ainult varasemalt valitud ühendeid. Suunatud analüüsi meetodid võimaldavad analüüsida kuni 200 ühendit ühe analüüsiga. Õnneks on massispektromeetria riistvaraline ja tarkvaraline kiire areng loonud võimaluse kasutada suunamata analüüsi (ingl *non-targeted analysis*), et detekteerida kõik võimalikud ühendid, mis jäävad selle meetodi rakendusallasse. Selliste meetoditega oleme võimelised määrama tuhandeid ühendeid ühe analüüsiga. Suunamata analüüsi tulemuste kvantitatiivseks muutmiseks vajame praeguseni ikka standardaineid. Minu doktoritöö eesmärgiks on arendada arvutuslik meetod elektropihustuse ionisatsiooni efektiivsuste ennustamiseks, et võimaldada standardainete vaba kvantitatiivset suunamata LC/ESI/MS analüüsi.

Elektropihustuse ionisatsiooni mehhanismi mudeldamiseks on vajalik teada, millised parameetrid seda mõjutavad. Varasematest uuringutest on teada, et ühendi struktuur mõjutab tema ionisatsiooniefektiivsust. Oma uuringu raames mõõtsin ja kogusin ühtekokku 353 erineva ühendi ionisatsiooniefektiivsused ESI positiivses režiimis ühes solvendis. Üldiselt saab järeldada, et mida hüdrofoobsem ja tugevam alus ühend on, seda kõrgem on tema ionisatsiooniefektiivsus ESI positiivses režiimis.

Järgmiseks on teada, et analüüsiks kasutatav eluent mõjutab ionisatsiooniefektiivsust. Selle mõju kvantitatiivseks uurimiseks mõõtsin ja kogusin varasematest uuringutest ionisatsiooniefektiivsused ühtekokku 106 erineva eluendi koostises. Minu uuring katab kõik enim kasutatavad orgaanilise faasina kasutatavad solvendid ning veefaasis kasutatavad lisandid. Uuritavate eluentide veefaasi pH katab vahemiku 2.1 kuni 10.7. Suures pildis saab järeldada, et mida kõrgem on orgaanilise faasi sisaldus eluendis, seda kõrgemad on ionisatsiooni

efektiivsused. Samas on veefaasi pH mõju mõistmine keerulisem. Väga hüdrofiilsete ja väga hüdrofoobsete ühendite ionisatsiooniefektiivsus ei ole mõjutatud veefaasi pHst. Samas keskmise hüdrofiilsuse/hüdrofoobsusega ühendite, mille pK_a on ligilähedane veefaasi pHga, ionisatsiooniefektiivsus on tugevalt mõjutatud veefaasi pH poolt.

Järgmise etapina uurisin, kas minu uuritud efektid on kasutatud instrumendi spetsiifilised või on need järeldused rakenduvad universaalselt. Minu uuringu tulemused näitavad, et ühel instrumendil mõõdetud ionisatsiooniefektiivsuseid ei saa numbriliselt üle viia teisele instrumendile, aga korrelatsioon erinevatel instrumentidel mõõdetud ionisatsiooniefektiivsuste vahel on kõrge. See näitab, et varasemalt uuritud efektid on erinevate instrumentide üleselt universaalsed ning ionisatsiooniefektiivsuste väärtuseid on võimalik ühelt instrumendilt teisele üle kanda, kasutades väikest kalibreerimisühendite valimit.

Eelnevate tulemuste põhjal töötasin välja meetodi, mis on võimeline ennustama ionisatsiooniefektiivsuseid, arvestades nii ühendi struktuuri kui ka eluendi koostisega analüüsil. Arendatud mudeli keskmine viga on 2,2 korda, mis suurendab ionisatsiooni efektiivsuse hindamise usaldusväärsust kuni 10 miljonit korda. Arendatud meetod kasutab väikest valimit ühendeid (6), et arvestada ka kasutatava instrumendi, meetodi ja proovimaatriksi efektidega ning võimaldab standardaine vaba kvantiseerimist keskmise veaga 5 korda. Näiteks kui laialt levinud pestitsiidi glüfosaat sisalduseks hindab minu meetod 1 ppm, siis tõeline väärtus jääb 0.2 ja 5 ppm vahemikku. Antud usaldusväärsus on piisav, eriti arvestades toksikoloogiliste mõõtmiste dispersiooni, mis on sama suur või isegi suurem. Minu doktoritöös arendatud meetod standardaine vabaks kvantiseerimiseks on saadaval LC/ES/MS auditooriumile *online*-tööriistana ning seda meetodit on võimalik rakendada ka varasemalt kogutud LC/ESI/MS andmetele.

REFERENCES

1. Cajka, T. & Fiehn, O. Toward Merging Untargeted and Targeted Methods in Mass Spectrometry-Based Metabolomics and Lipidomics. *Anal. Chem.* **88**, 524–545 (2016).
2. Xu, R. N., Fan, L., Rieser, M. J. & El-Shourbagy, T. A. Recent advances in high-throughput quantitative bioanalysis by LC–MS/MS. *J. Pharm. Biomed. Anal.* **44**, 342–355 (2007).
3. Alder, L., Greulich, K., Kempe, G. & Vieth, B. Residue analysis of 500 high priority pesticides: Better by GC–MS or LC–MS/MS? *Mass Spectrom. Rev.* **25**, 838–865 (2006).
4. Malik, A. K., Blasco, C. & Picó, Y. Liquid chromatography–mass spectrometry in food safety. *J. Chromatogr. A* **1217**, 4018–4040 (2010).
5. Iribarne, J. V. On the evaporation of small ions from charged droplets. *J. Chem. Phys.* **64**, 2287 (1976).
6. Thomson, B. A. & Iribarne, J. V. Field induced ion evaporation from liquid surfaces at atmospheric pressure. *J. Chem. Phys.* **71**, 4451–4463 (1979).
7. Winger, B. E., Light-Wahl, K. J., Ogorzalek Loo, R. R., Udseth, H. R. & Smith, R. D. Observation and implications of high mass-to-charge ratio ions from electrospray ionization mass spectrometry. *J. Am. Soc. Mass Spectrom.* **4**, 536–545 (1993).
8. Metwally, H., Duez, Q. & Konermann, L. Chain Ejection Model for Electrospray Ionization of Unfolded Proteins: Evidence from Atomistic Simulations and Ion Mobility Spectrometry. *Anal. Chem.* **90**, 10069–10077 (2018).
9. Constantopoulos, T. L., Jackson, G. S. & Enke, C. G. Effects of salt concentration on analyte response using electrospray ionization mass spectrometry. *J. Am. Soc. Mass Spectrom.* **10**, 625–634 (1999).
10. Oss, M., Kruve, A., Herodes, K. & Leito, I. Electrospray Ionization Efficiency Scale of Organic Compounds. *Anal. Chem.* **82**, 2865–2872 (2010).
11. Chalcraft, K. R., Lee, R., Mills, C. & Britz-McKibbin, P. Virtual Quantification of Metabolites by Capillary Electrophoresis-Electrospray Ionization-Mass Spectrometry: Predicting Ionization Efficiency Without Chemical Standards. *Anal. Chem.* **81**, 2506–2515 (2009).
12. Kruve, A. & Kaupmees, K. Adduct Formation in ESI/MS by Mobile Phase Additives. *J. Am. Soc. Mass Spectrom.* **28**, 887–894 (2017).
13. Kruve, A., Kaupmees, K., Liigand, J., Oss, M. & Leito, I. Sodium adduct formation efficiency in ESI source: *J. Mass Spectrom.* **48**, 695–702 (2013).
14. Mortier, K. A., Zhang, G.-F., Peteghem, C. H. & Lambert, W. E. Adduct formation in quantitative bioanalysis: Effect of ionization conditions on paclitaxel. *J. Am. Soc. Mass Spectrom.* **15**, 585–592 (2004).
15. Dole, M. *et al.* Molecular Beams of Macroions. *J. Chem. Phys.* **49**, 2240–2249 (1968).
16. Van Berkel, G. J., McLuckey, S. A. & Glish, G. L. Electrochemical origin of radical cations observed in electrospray ionization mass spectra. *Anal. Chem.* **64**, 1586–1593 (1992).
17. Cox, J. T., Marginean, I., Smith, R. D. & Tang, K. On the Ionization and Ion Transmission Efficiencies of Different ESI-MS Interfaces. *J. Am. Soc. Mass Spectrom.* **26**, 55–62 (2015).

18. Page, J. S., Kelly, R. T., Tang, K. & Smith, R. D. Ionization and transmission efficiency in an electrospray ionization—mass spectrometry interface. *J. Am. Soc. Mass Spectrom.* **18**, 1582–1590 (2007).
19. Truffelli, H., Palma, P., Famigliani, G. & Cappiello, A. An overview of matrix effects in liquid chromatography–mass spectrometry. *Mass Spectrom. Rev.* **30**, 491–509 (2011).
20. Furey, A., Moriarty, M., Bane, V., Kinsella, B. & Lehane, M. Ion suppression; A critical review on causes, evaluation, prevention and applications. *Talanta* **115**, 104–122 (2013).
21. Golubović, J., Birkemeyer, C., Protić, A., Otašević, B. & Zečević, M. Structure–response relationship in electrospray ionization-mass spectrometry of sartans by artificial neural networks. *J. Chromatogr. A* **1438**, 123–132 (2016).
22. Amad, M. H., Cech, N. B., Jackson, G. S. & Enke, C. G. Importance of gas-phase proton affinities in determining the electrospray ionization response for analytes and solvents. *J. Mass Spectrom.* **35**, 784–789 (2000).
23. Ehrmann, B. M., Henriksen, T. & Cech, N. B. Relative importance of basicity in the gas phase and in solution for determining selectivity in electrospray ionization mass spectrometry. *J. Am. Soc. Mass Spectrom.* **19**, 719–728 (2008).
24. Wu, L. *et al.* Quantitative structure–ion intensity relationship strategy to the prediction of absolute levels without authentic standards. *Anal. Chim. Acta* **794**, 67–75 (2013).
25. Henriksen, T., Juhler, R. K., Svensmark, B. & Cech, N. B. The relative influences of acidity and polarity on responsiveness of small organic molecules to analysis with negative ion electrospray ionization mass spectrometry (ESI-MS). *J. Am. Soc. Mass Spectrom.* **16**, 446–455 (2005).
26. Huffman, B. A., Poltash, M. L. & Hughey, C. A. Effect of Polar Protic and Polar Aprotic Solvents on Negative-Ion Electrospray Ionization and Chromatographic Separation of Small Acidic Molecules. *Anal. Chem.* **84**, 9942–9950 (2012).
27. Nguyen, T. B., Nizkorodov, S. A., Laskin, A. & Laskin, J. An approach toward quantification of organic compounds in complex environmental samples using high-resolution electrospray ionization mass spectrometry. *Anal. Methods* **5**, 72–80 (2013).
28. Cech, N. B. & Enke, C. G. Practical implications of some recent studies in electrospray ionization fundamentals. *Mass Spectrom. Rev.* **20**, 362–387 (2001).
29. Cech, N. B. & Enke, C. G. Relating Electrospray Ionization Response to Nonpolar Character of Small Peptides. *Anal. Chem.* **72**, 2717–2723 (2000).
30. Kostianen, R. & Kauppila, T. J. Effect of eluent on the ionization process in liquid chromatography–mass spectrometry. *J. Chromatogr. A* **1216**, 685–699 (2009).
31. Gao, S., Zhang, Z. & Karnes, H. Sensitivity enhancement in liquid chromatography/atmospheric pressure ionization mass spectrometry using derivatization and mobile phase additives. *J. Chromatogr. B* **825**, 98–110 (2005).
32. Charles, L., Laure, F., Raharivelomanana, P. & Bianchini, J.-P. Sheath liquid interface for the coupling of normal-phase liquid chromatography with electrospray mass spectrometry and its application to the analysis of neoflavonoids. *J. Mass Spectrom.* **40**, 75–82 (2005).
33. Kostianen, R. & Bruins, A. P. Effect of Solvent on Dynamic Range and Sensitivity in Pneumatically-assisted Electrospray (Ion Spray) Mass Spectrometry. *Rapid Commun. Mass Spectrom.* **10**, 1393–1399 (1996).

34. Smith, D. P. H. The Electrohydrodynamic Atomization of Liquids. *IEEE Trans. Ind. Appl.* **IA-22**, 527–535 (1986).
35. Kebarle, P. & Tang, L. From ions in solution to ions in the gas phase - the mechanism of electrospray mass spectrometry. *Anal. Chem.* **65**, 972A-986A (1993).
36. Straub, R. F. & Voyksner, R. D. Negative ion formation in electrospray mass spectrometry. *J. Am. Soc. Mass Spectrom.* **4**, 578–587 (1993).
37. Zhou, S. & Hamburger, M. Effects of solvent composition on molecular ion response in electrospray mass spectrometry: Investigation of the ionization processes. *Rapid Commun. Mass Spectrom.* **9**, 1516–1521 (1995).
38. Krueve, A. Influence of mobile phase, source parameters and source type on electrospray ionization efficiency in negative ion mode: Influence of mobile phase in ESI/MS. *J. Mass Spectrom.* **51**, 596–601 (2016).
39. Periat, A. *et al.* Hydrophilic interaction chromatography versus reversed phase liquid chromatography coupled to mass spectrometry: Effect of electrospray ionization source geometry on sensitivity. *J. Chromatogr. A* **1356**, 211–220 (2014).
40. Silvester, S. Mobile phase pH and organic modifier in reversed-phase LC–ESI-MS bioanalytical methods: assessment of sensitivity, chromatography and correlation of retention time with *in silico* logD predictions. *Bioanalysis* **5**, 2753–2770 (2013).
41. Thacker, J. B. & Schug, K. A. Effects of solvent parameters on the electrospray ionization tandem mass spectrometry response of glucose. *Rapid Commun. Mass Spectrom.* **32**, 1191–1198 (2018).
42. Periat, A., Boccard, J., Veuthey, J.-L., Rudaz, S. & Guillaume, D. Systematic comparison of sensitivity between hydrophilic interaction liquid chromatography and reversed phase liquid chromatography coupled with mass spectrometry. *J. Chromatogr. A* **1312**, 49–57 (2013).
43. Gao, H., Williams, J., Carrier, S. & Brummel, C. L. Bioanalytical solutions to acetonitrile shortages. *Bioanalysis* **2**, 1627–1640 (2010).
44. Steiner, F. & Hassel, M. Influence of solvent properties on separation and detection performance in non-aqueous capillary electrophoresis–mass spectrometry of basic analytes. *J. Chromatogr. A* **1068**, 131–142 (2005).
45. Monnin, C., Ramrup, P., Daigle-Young, C. & Vuckovic, D. Improving negative liquid chromatography/electrospray ionization mass spectrometry lipidomic analysis of human plasma using acetic acid as a mobile-phase additive. *Rapid Commun. Mass Spectrom.* **32**, 201–211 (2018).
46. Maragou, N. C., Thomaidis, N. S. & Koupparis, M. A. Optimization and Comparison of ESI and APCI LC-MS/MS Methods: A Case Study of Irgarol 1051, Diuron, and their Degradation Products in Environmental Samples. *J. Am. Soc. Mass Spectrom.* **22**, 1826–1838 (2011).
47. Campbell, J. L., Le Blanc, J. C. Y. & Schneider, B. B. Probing Electrospray Ionization Dynamics Using Differential Mobility Spectrometry: The Curious Case of 4-Aminobenzoic Acid. *Anal. Chem.* **84**, 7857–7864 (2012).
48. Kamel, A. M., Brown, P. R. & Munson, B. Effects of Mobile-Phase Additives, Solution pH, Ionization Constant, and Analyte Concentration on the Sensitivities and Electrospray Ionization Mass Spectra of Nucleoside Antiviral Agents. *Anal. Chem.* **71**, 5481–5492 (1999).
49. Cuyckens, F. & Claeys, M. Optimization of a liquid chromatography method based on simultaneous electrospray ionization mass spectrometric and ultraviolet photodiode array detection for analysis of flavonoid glycosides. *Rapid Commun. Mass Spectrom.* **16**, 2341–2348 (2002).

50. Mallet, C. R., Lu, Z. & Mazzeo, J. R. A study of ion suppression effects in electrospray ionization from mobile phase additives and solid-phase extracts. *Rapid Commun. Mass Spectrom.* **18**, 49–58 (2004).
51. Dams, R., Benijts, T., Günther, W., Lambert, W. & Leenheer, A. D. Influence of the eluent composition on the ionization efficiency for morphine of pneumatically assisted electrospray, atmospheric-pressure chemical ionization and sonic spray: Eluent composition effects on ionization efficiency for IS, SS and APCI. *Rapid Commun. Mass Spectrom.* **16**, 1072–1077 (2002).
52. Eshraghi, Jamshid. & Chowdhury, S. K. Factors affecting electrospray ionization of effluents containing trifluoroacetic acid for high-performance liquid chromatography/mass spectrometry. *Anal. Chem.* **65**, 3528–3533 (1993).
53. Chowdhury, S. K. & Chait, B. T. Method for the electrospray ionization of highly conductive aqueous solutions. *Anal. Chem.* **63**, 1660–1664 (1991).
54. Kuhlmann, F. E., Apffel, A., Fischer, S. M., Goldberg, G. & Goodley, P. C. Signal enhancement for gradient reverse-phase high-performance liquid chromatography-electrospray ionization mass spectrometry analysis with trifluoroacetic and other strong acid modifiers by postcolumn addition of propionic acid and isopropanol. *J. Am. Soc. Mass Spectrom.* **6**, 1221–1225 (1995).
55. Storm, T., Reemtsma, T. & Jekel, M. Use of volatile amines as ion-pairing agents for the high-performance liquid chromatographic–tandem mass spectrometric determination of aromatic sulfonates in industrial wastewater. *J. Chromatogr. A* **854**, 175–185 (1999).
56. Rainville, P. D., Smith, N. W., Cowan, D. & Plumb, R. S. Comprehensive investigation of the influence of acidic, basic, and organic mobile phase compositions on bioanalytical assay sensitivity in positive ESI mode LC/MS/MS. *J. Pharm. Biomed. Anal.* **59**, 138–150 (2012).
57. Mansoori, B. A., Volmer, D. A. & Boyd, R. K. ‘Wrong-way-round’ Electrospray Ionization of Amino Acids. *Rapid Commun. Mass Spectrom.* **11**, 1120–1130 (1997).
58. Zhou, S. & Cook, K. D. Protonation in electrospray mass spectrometry: Wrong-way-round or right-way-round? *J. Am. Soc. Mass Spectrom.* **11**, 961–966 (2000).
59. Hua, Y. & Jenke, D. Increasing the Sensitivity of an LC-MS Method for Screening Material Extracts for Organic Extractables via Mobile Phase Optimization. *J. Chromatogr. Sci.* **50**, 213–227 (2012).
60. Peng, L. & Farkas, T. Analysis of basic compounds by reversed-phase liquid chromatography–electrospray mass spectrometry in high-pH mobile phases. *J. Chromatogr. A* **1179**, 131–144 (2008).
61. Van Berkel, G. J., Zhou, F. & Aronson, J. T. Changes in bulk solution pH caused by the inherent controlled-current electrolytic process of an electrospray ion source. *Int. J. Mass Spectrom. Ion Process.* **162**, 55–67 (1997).
62. Girod, M., Dagany, X., Antoine, R. & Dugourd, P. Relation between charge state distributions of peptide anions and pH changes in the electrospray plume. A mass spectrometry and optical spectroscopy investigation. *Int. J. Mass Spectrom.* **308**, 41–48 (2011).
63. Zhou, S., Prebyl, B. S. & Cook, K. D. Profiling pH Changes in the Electrospray Plume. *Anal. Chem.* **74**, 4885–4888 (2002).
64. Liigand, P. *et al.* The Evolution of Electrospray Generated Droplets is Not Affected by Ionization Mode. *J. Am. Soc. Mass Spectrom.* **28**, 2124–2131 (2017).

65. Park, S. Y. & Jung, M. Y. UHPLC-ESI-MS/MS for the Quantification of Eight Major Gingerols and Shogaols in Ginger Products: Effects of Ionization Polarity and Mobile Phase Modifier on the Sensitivity. *J. Food Sci.* **81**, C2457–C2465 (2016).
66. Yuan, M., Namikoshi, M., Otsuki, A., Watanabe, M. F. & Rinehart, K. L. Electrospray Ionization Mass Spectrometric Analysis of Microcystins, Cyclic Heptapeptide Hepatotoxins: Modulation of Charge States and $[M + H]^+$ to $[M + Na]^+$ Ratio. *J. Am. Soc. Mass Spectrom.* **10**, 1138–1151 (1999).
67. Kostianen, R. & Bruins, A. P. Effect of multiple sprayers on dynamic range and flow rate limitations in electrospray and ionspray mass spectrometry. *Rapid Commun. Mass Spectrom.* **8**, 549–558 (1994).
68. Fenn, J. B. Ion formation from charged droplets: Roles of geometry, energy, and time. *J. Am. Soc. Mass Spectrom.* **4**, 524–535 (1993).
69. Tang, Liang. & Kebarle, Paul. Dependence of ion intensity in electrospray mass spectrometry on the concentration of the analytes in the electrosprayed solution. *Anal. Chem.* **65**, 3654–3668 (1993).
70. Bruins, A. P. Mechanistic aspects of electrospray ionization. *J. Chromatogr. A* **794**, 345–357 (1998).
71. Alymatiri, C. M., Kouskoura, M. G. & Markopoulou, C. K. Decoding the signal response of steroids in electrospray ionization mode (ESI-MS). *Anal Methods* **7**, 10433–10444 (2015).
72. Caetano, S. *et al.* Exploring and modelling the responses of electrospray and atmospheric pressure chemical ionization techniques based on molecular descriptors. *Anal. Chim. Acta* **550**, 92–106 (2005).
73. Cramer, C. J., Johnson, J. L. & Kamel, A. M. Prediction of Mass Spectral Response Factors from Predicted Chemometric Data for Druglike Molecules. *J. Am. Soc. Mass Spectrom.* **28**, 278–285 (2017).
74. Gioumouxouzis, C. I., Kouskoura, M. G. & Markopoulou, C. K. Negative electrospray ionization mode in mass spectrometry: A new perspective via modeling. *J. Chromatogr. B* **998–999**, 97–105 (2015).
75. Hermans, J., Ongay, S., Markov, V. & Bischoff, R. Physicochemical Parameters Affecting the Electrospray Ionization Efficiency of Amino Acids after Acylation. *Anal. Chem.* **89**, 9159–9166 (2017).
76. Basak, S. C., Harriss, D. K. & Magnuson, V. R. Comparative Study of Lipophilicity versus Topological Molecular Descriptors in Biological Correlations. *J. Pharm. Sci.* **73**, 429–437 (1984).
77. Volkenstein, M. V. Chapter 4. in *Configurational Statistics of Polymeric Chains* (Interscience, 1963).
78. Chalcraft, K. R., Lee, R., Mills, C. & Britz-McKibbin, P. Virtual Quantification of Metabolites by Capillary Electrophoresis-Electrospray Ionization-Mass Spectrometry: Predicting Ionization Efficiency Without Chemical Standards. *Anal. Chem.* **81**, 2506–2515 (2009).
79. Schymanski, E. L. *et al.* Non-target screening with high-resolution mass spectrometry: critical review using a collaborative trial on water analysis. *Anal. Bioanal. Chem.* **407**, 6237–6255 (2015).
80. Allen, F., Pon, A., Wilson, M., Greiner, R. & Wishart, D. CFM-ID: a web server for annotation, spectrum prediction and metabolite identification from tandem mass spectra. *Nucleic Acids Res.* **42**, W94–W99 (2014).

81. Ruttkies, C., Schymanski, E. L., Wolf, S., Hollender, J. & Neumann, S. MetFrag relaunched: incorporating strategies beyond in silico fragmentation. *J. Cheminformatics* **8**, 3 (2016).
82. Djoumbou-Feunang, Y. *et al.* BioTransformer: a comprehensive computational tool for small molecule metabolism prediction and metabolite identification. *J. Cheminformatics* **11**, 2 (2019).
83. Wishart, D. S. *et al.* HMDB 4.0: the human metabolome database for 2018. *Nucleic Acids Res.* **46**, D608–D617 (2018).
84. Krueve, A., Leito, I., Herodes, K., Laaniste, A. & Löhmus, R. Enhanced Nebulization Efficiency of Electrospray Mass Spectrometry: Improved Sensitivity and Detection Limit. *J. Am. Soc. Mass Spectrom.* **23**, 2051–2054 (2012).
85. Girod, M. *et al.* Profiling an electrospray plume by laser-induced fluorescence and Fraunhofer diffraction combined to mass spectrometry: influence of size and composition of droplets on charge-state distributions of electrosprayed proteins. *Phys. Chem. Chem. Phys.* **14**, 9389 (2012).
86. Liigand, J., Laaniste, A. & Krueve, A. pH Effects on Electrospray Ionization Efficiency. *J. Am. Soc. Mass Spectrom.* **28**, 461–469 (2017).
87. Krueve, A., Kaupmees, K., Liigand, J. & Leito, I. Negative Electrospray Ionization via Deprotonation: Predicting the Ionization Efficiency. *Anal. Chem.* **86**, 4822–4830 (2014).
88. Klamt, A. & Eckert, F. COSMO-RS: a novel and efficient method for the a priori prediction of thermophysical data of liquids. *Fluid Phase Equilibria* **172**, 43–72 (2000).
89. Eckert, F. & Klamt, A. Fast solvent screening via quantum chemistry: COSMO-RS approach. *AIChE J.* **48**, 369–385 (2002).
90. Eckert, F. & Klamt, A. *COSMOtherm*. (COSMOlogic GmbH & Co. KG, 2013).
91. Yap, C. W. PaDEL-descriptor: An open source software to calculate molecular descriptors and fingerprints. *J. Comput. Chem.* **32**, 1466–1474 (2011).
92. Dong, J. *et al.* ChemDes: an integrated web-based platform for molecular descriptor and fingerprint computation. *J. Cheminformatics* **7**, (2015).
93. Snyder, L. R., Kirkland, J. J. & Dolan, J. W. *Introduction to Modern Liquid Chromatography*. (John Wiley & Sons, Inc., 2009).
94. Rudakov, O. B., Belyaev, D. S., Khorokhordina, E. A. & Podolina, E. A. Surface tension of binary mobile phases for liquid chromatography. *Russ. J. Phys. Chem. A* **81**, 366–369 (2007).
95. Katz, E., Eksteen, R., Schoenmakers, P. & Miller, N. *Handbook of HPLC*. (M. Dekker, 1998).
96. Mikhail, S. Z. & Kimel, W. R. Densities and Viscosities of 1-Propanol-Water Mixtures. *J. Chem. Eng. Data* **8**, 323–328 (1963).
97. Noda, K., Ohashi, M. & Ishida, K. Viscosities and Densities at 298.15 K for Mixtures of Methanol, Acetone, and Water. *J Chem Eng Data* **27**, 326–328 (1982).
98. Howard, K. S. & McAllister, R. A. Surface tension of acetone-water solutions up to their normal boiling points. *AIChE J.* **3**, 325–329 (1957).
99. Deng, H. & Runger, G. Feature Selection via Regularized Trees. *ArXiv12011587 Cs Stat* (2012).

100. Kellogg, J. J. *et al.* Comparison of Metabolomics Approaches for Evaluating the Variability of Complex Botanical Preparations: Green Tea (*Camellia sinensis*) as a Case Study. *J. Nat. Prod.* **80**, 1457–1466 (2017).
101. Dzuman, Z., Zachariasova, M., Veprikova, Z., Godula, M. & Hajslova, J. Multi-analyte high performance liquid chromatography coupled to high resolution tandem mass spectrometry method for control of pesticide residues, mycotoxins, and pyrrolizidine alkaloids. *Anal. Chim. Acta* **863**, 29–40 (2015).
102. Gagliardi, L. G., Tascon, M. & Castells, C. B. Effect of temperature on acid–base equilibria in separation techniques. A review. *Anal. Chim. Acta* **889**, 35–57 (2015).
103. Ahadi, E. & Konermann, L. Ejection of Solvated Ions from Electrosprayed Methanol/Water Nanodroplets Studied by Molecular Dynamics Simulations. *J. Am. Chem. Soc.* **133**, 9354–9363 (2011).
104. Greenspan, P. & Fowler, S. D. Spectrofluorometric studies of the lipid probe, Nile red. *J. Lipid Res.* **26**, 781–789 (1985).
105. Subirats, X., Rosés, M. & Bosch, E. On the Effect of Organic Solvent Composition on the pH of Buffered HPLC Mobile Phases and the pK_a of Analytes—A Review. *Sep. Purif. Rev.* **36**, 231–255 (2007).
106. Ojakivi, M., Liigand, J. & Kruve, A. Modifying the Acidity of Charged Droplets. *ChemistrySelect* **3**, 335–338 (2018).
107. Wang, J. *et al.* Effect of mobile phase pH, aqueous-organic ratio, and buffer concentration on electrospray ionization tandem mass spectrometric fragmentation patterns: implications in liquid chromatography/tandem mass spectrometric bioanalysis. *Rapid Commun. Mass Spectrom.* **24**, 3221–3229 (2010).
108. Enami, S., Stewart, L. A., Hoffmann, M. R. & Colussi, A. J. Superacid Chemistry on Mildly Acidic Water. *J. Phys. Chem. Lett.* **1**, 3488–3493 (2010).
109. Santos, L. S. *Reactive Intermediates. MS Investigations in Solution.* (WILEY-VCH Verlag GmbH & Co. KGaA, 2010).
110. Kamel, A. M., Brown, P. R. & Munson, B. Effects of Mobile-Phase Additives, Solution pH, Ionization Constant, and Analyte Concentration on the Sensitivities and Electrospray Ionization Mass Spectra of Nucleoside Antiviral Agents. *Anal. Chem.* **71**, 5481–5492 (1999).
111. Voyksner, R. D. & Lee, H. Improvements in LC/Electrospray Ion Trap Mass Spectrometry Performance Using an Off-Axis Nebulizer. *Anal. Chem.* **71**, 1441–1447 (1999).
112. Holčapek, M. *et al.* Effects of ion-pairing reagents on the electrospray signal suppression of sulphonated dyes and intermediates. *J. Mass Spectrom.* **39**, 43–50 (2004).
113. Tang, K. & Smith, R. D. Theoretical prediction of charged droplet evaporation and fission in electrospray ionization. *Int. J. Mass Spectrom.* **185–187**, 97–105 (1999).
114. Gomez, A. & Tang, K. Charge and fission of droplets in electrostatic sprays. *Phys. Fluids* **6**, 404–414 (1994).
115. Stahnke, H., Kittlaus, S., Kempe, G., Hemmerling, C. & Alder, L. The influence of electrospray ion source design on matrix effects: Influence of ESI source design on matrix effects. *J. Mass Spectrom.* **47**, 875–884 (2012).
116. Liigand, J., Kruve, A., Leito, I., Girod, M. & Antoine, R. Effect of Mobile Phase on Electrospray Ionization Efficiency. *J. Am. Soc. Mass Spectrom.* **25**, 1853–1861 (2014).
117. Kruve, A. & Kaupmees, K. Predicting ESI/MS Signal Change for Anions in Different Solvents. *Anal. Chem.* **89**, 5079–5086 (2017).

118. Liigand, J. *et al.* Transferability of the Electrospray Ionization Efficiency Scale between Different Instruments. *J. Am. Soc. Mass Spectrom.* **26**, 1923–1930 (2015).
119. Liigand, J., Vries, R. de & Cuyckens, F. Optimization of flow splitting and make-up flow conditions in liquid chromatography/electrospray ionization mass spectrometry. *Rapid Commun. Mass Spectrom.* **33**, 314–322 (2019).
120. Krasilnikov, V. N., Batalova, G. A., Popov, V. S. & Sergejeva, S. S. Fatty Acid Composition of Lipids in Naked Oat Grain of Domestic Varieties. *Russ. Agric. Sci.* **44**, 406–408 (2018).
121. Ismaiel, O. A., Halquist, M. S., Elmamly, M. Y., Shalaby, A. & Thomas Karnes, H. Monitoring phospholipids for assessment of ion enhancement and ion suppression in ESI and APCI LC/MS/MS for chlorpheniramine in human plasma and the importance of multiple source matrix effect evaluations. *J. Chromatogr. B* **875**, 333–343 (2008).
122. Rusak, G., Komes, D., Likić, S., Horžić, D. & Kovač, M. Phenolic content and antioxidative capacity of green and white tea extracts depending on extraction conditions and the solvent used. *Food Chem.* **110**, 852–858 (2008).
123. Kloefer, A., Quintana, J. B. & Reemtsma, T. Operational options to reduce matrix effects in liquid chromatography-electrospray ionization-mass spectrometry analysis of aqueous environmental samples. *J. Chromatogr. A* **1067**, 153–160 (2005).
124. Blacquièrè, T., Smagghe, G., van Gestel, C. A. M. & Mommaerts, V. Neonicotinoids in bees: a review on concentrations, side-effects and risk assessment. *Ecotoxicology* **21**, 973–992 (2012).
125. Alfaro, C. M., Uwakweh, A.-O., Todd, D. A., Ehrmann, B. M. & Cech, N. B. Investigations of Analyte-Specific Linear Dynamic Range Limitations in Atmospheric Pressure Ionization Mass Spectrometry. 8
126. Basiri, B., Murph, M. M. & Bartlett, M. G. Assessing the Interplay between the Physicochemical Parameters of Ion-Pairing Reagents and the Analyte Sequence on the Electrospray Desorption Process for Oligonucleotides. *J. Am. Soc. Mass Spectrom.* **28**, 1647–1656 (2017).
127. Beach, D. G. & Gabryelski, W. Linear and Nonlinear Regimes of Electrospray Signal Response in Analysis of Urine by Electrospray Ionization-High Field Asymmetric Waveform Ion Mobility Spectrometry-MS and Implications for Nontarget Quantification. *Anal. Chem.* **85**, 2127–2134 (2013).
128. Bedner, M. & Duewer, D. L. Dynamic Calibration Approach for Determining Catechins and Gallic Acid in Green Tea Using LC–ESI/MS. *Anal. Chem.* **83**, 6169–6176 (2011).
129. Byrdwell, W. C. Quadruple parallel mass spectrometry for analysis of vitamin D and triacylglycerols in a dietary supplement. *J. Chromatogr. A* **1320**, 48–65 (2013).
130. Cífková, E. *et al.* Nontargeted Quantitation of Lipid Classes Using Hydrophilic Interaction Liquid Chromatography–Electrospray Ionization Mass Spectrometry with Single Internal Standard and Response Factor Approach. *Anal. Chem.* **84**, 10064–10070 (2012).
131. Dahal, U. P., Jones, J. P., Davis, J. A. & Rock, D. A. Small Molecule Quantification by Liquid Chromatography–Mass Spectrometry for Metabolites of Drugs and Drug Candidates. *Drug Metab. Dispos.* **39**, 2355–2360 (2011).
132. Espinosa, S., Bosch, E. & Rosés, M. Acid–base constants of neutral bases in acetonitrile–water mixtures. *Anal. Chim. Acta* **454**, 157–166 (2002).

133. Gao, F. *et al.* A Refined Model for Ionization of Small Molecules in Electrospray Mass Spectrometry. *Chem. Lett.* **45**, 955–957 (2016).
134. Ghosh, B. & Jones, A. D. Dependence of negative-mode electrospray ionization response factors on mobile phase composition and molecular structure for newly-authenticated neutral acylsucrose metabolites. *The Analyst* **140**, 6522–6531 (2015).
135. Hatsis, P., Waters, N. J. & Argikar, U. A. Implications for Metabolite Quantification by Mass Spectrometry in the Absence of Authentic Standards. *Drug Metab. Dispos.* **45**, 492–496 (2017).
136. Kalogiouri, N. P., Aalizadeh, R. & Thomaidis, N. S. Investigating the organic and conventional production type of olive oil with target and suspect screening by LC-QTOF-MS, a novel semi-quantification method using chemical similarity and advanced chemometrics. *Anal. Bioanal. Chem.* **409**, 5413–5426 (2017).
137. Kanga, A. W., Behar, F. & Hatcher, P. G. Quantitative Analysis of Long Chain Fatty Acids Present in a Type I Kerogen Using Electrospray Ionization Fourier Transform Ion Cyclotron Resonance Mass Spectrometry: Compared with BF₃/MeOH Methylation/GC-FID. *J. Am. Soc. Mass Spectrom.* **25**, 880–890 (2014).
138. Kiontke, A., Oliveira-Birkmeier, A., Opitz, A. & Birkemeyer, C. Electrospray Ionization Efficiency Is Dependent on Different Molecular Descriptors with Respect to Solvent pH and Instrumental Configuration. *PLOS ONE* **11**, e0167502 (2016).
139. Koivusalo, M., Haimi, P., Heikinheimo, L., Kostianen, R. & Somerharju, P. Quantitative determination of phospholipid compositions by ESI-MS: effects of acyl chain length, unsaturation, and lipid concentration on instrument response. *J. Lipid Res.* **42**, 663–672 (2001).
140. Leitner, A., Emmert, J., Boerner, K. & Lindner, W. Influence of Solvent Additive Composition on Chromatographic Separation and Sodium Adduct Formation of Peptides in HPLC–ESI MS. *Chromatographia* **65**, 649–653 (2007).
141. Mandra, V. J., Kouskoura, M. G. & Markopoulou, C. K. Using the partial least squares method to model the electrospray ionization response produced by small pharmaceutical molecules in positive mode: Modelling positive electrospray ionization response. *Rapid Commun. Mass Spectrom.* **29**, 1661–1675 (2015).
142. Mehta, N. *et al.* Mass Spectrometric Quantification of N-Linked Glycans by Reference to Exogenous Standards. *J. Proteome Res.* **15**, 2969–2980 (2016).
143. Monnin, C., Ramrup, P., Daigle-Young, C. & Vuckovic, D. Improving negative liquid chromatography/electrospray ionization mass spectrometry lipidomic analysis of human plasma using acetic acid as a mobile-phase additive. *Rapid Commun. Mass Spectrom.* **32**, 201–211 (2018).
144. Pieke, E. N., Granby, K., Trier, X. & Smedsgaard, J. A framework to estimate concentrations of potentially unknown substances by semi-quantification in liquid chromatography electrospray ionization mass spectrometry. *Anal. Chim. Acta* **975**, 30–41 (2017).
145. Raji, M. A. *et al.* Using multivariate statistical methods to model the electrospray ionization response of GXG tripeptides based on multiple physicochemical parameters. *Rapid Commun. Mass Spectrom.* **23**, 2221–2232 (2009).
146. Stavenhagen, K. *et al.* Quantitative mapping of glycoprotein micro-heterogeneity and macro-heterogeneity: an evaluation of mass spectrometry signal strengths using synthetic peptides and glycopeptides: Glycopeptide ionisation strength. *J. Mass Spectrom.* **48**, 627–639 (2013).

147. Zendong, Z., Sibat, M., Herrenknecht, C., Hess, P. & McCarron, P. Relative molar response of lipophilic marine algal toxins in liquid chromatography/electrospray ionization mass spectrometry. *Rapid Commun. Mass Spectrom.* **31**, 1453–1461 (2017).
148. Tang, W.-T., Fang, M.-F., Liu, X. & Yue, M. Simultaneous Quantitative and Qualitative Analysis of Flavonoids from Ultraviolet-B Radiation in Leaves and Roots of *Scutellaria baicalensis* Georgi Using LC-UV-ESI-Q/TOF/MS. *J. Anal. Methods Chem.* **2014**, 1–9 (2014).
149. Tu, J., Yin, Y., Xu, M., Wang, R. & Zhu, Z.-J. Absolute quantitative lipidomics reveals lipidome-wide alterations in aging brain. *Metabolomics* **14**, (2018).
150. Yang, W.-C., Mirzaei, H., Liu, X. & Regnier, F. E. Enhancement of Amino Acid Detection and Quantification by Electrospray Ionization Mass Spectrometry. *Anal. Chem.* **78**, 4702–4708 (2006).
151. Yang, J. *et al.* A chemical profiling strategy for semi-quantitative analysis of flavonoids in Ginkgo extracts. *J. Pharm. Biomed. Anal.* **123**, 147–154 (2016).
152. Ghose, A. K., Viswanadhan, V. N. & Wendoloski, J. J. Prediction of Hydrophobic (Lipophilic) Properties of Small Organic Molecules Using Fragmental Methods: An Analysis of ALOGP and CLOGP Methods. *J. Phys. Chem. A* **102**, 3762–3772 (1998).
153. Liigand, P. *et al.* Think Negative: Finding the Best Electrospray Ionization/MS Mode for Your Analyte. *Anal. Chem.* **89**, 5665–5668 (2017).
154. Liigand, P., Kaupmees, K. & Kruve, A. Influence of the amino acid composition on the ionization efficiencies of small peptides. *J. Mass Spectrom.* **54**, 481–487 (2019).
155. Liigand, P., Liigand, J., Cuyckens, F., Vreeken, R. J. & Kruve, A. Ionisation efficiencies can be predicted in complicated biological matrices: A proof of concept. *Anal. Chim. Acta* **1032**, 68–74 (2018).

ACKNOWLEDGMENTS

I thank the University of Tartu, Institute of Chemistry and Chair of Analytical Chemistry for a wide base good education and knowledge obtained during my studies from 2009 to 2019. I would like to express my very great appreciation to my supervisor Assoc. Prof. Anneli Kruve for guidance, support and encouragement.

I am particularly thankful to my family, my in-laws and especially my dear wife Piia for the support, for pushing the limits and for establishing the opportunities to fulfil my dreams.

I thank my course mates and fellow chemists Karl, Mihkel, Anni, Siiri, Liisa, Karl, Erki, Peeter, Asko, Maarja-Liisa, Mari and Hanno for support in discovering the wonders of chemistry and for lunches full of laughter and discussions on the topics from science to politics via fashion.

I am also grateful to my class fellows Gretlin, Kairi, Susanna and Märten for accompanying me through my 22 years of studies.

I thank University of Claude Bernard Lyon 1 and Dr Marion Girod and Dr Rodolphe Antoine for the possibility to learn about studying the aerosols with fluorescence spectroscopy.

I am grateful to the University of Konstanz for the possibility of exchange year and Prof. Helmut Cölfen and Dr Marius Schmidt for the possibility to discover the world of nanoparticles.

A very special gratitude goes out to Janssen Pharmaceutica and especially to Dr Filip Cuyckens and his team for the opportunity to learn and apply my knowledge in an industrial setting and to understand the needs of the industry.

I thank the University of Liege and Prof. Edwin De Pauw, Dr Johann Far and Andrea McCann for the possibility to learn about ion mobility and about glycan analysis.

A very special gratitude goes out to korp! Sakala and Corps Saxonia Konstanz and especially vil!! Paal, Stamm and b!vil! Järvan, AHAAH Jäger, Walter, Mette 2 and Eichstädt for a joyful time during my studies, encouragement, lifelong friends and examples in life.

I thank Dataminer fellows for introducing me to the world of data science.

For financial support, I thank Estonian Ministry of Education and Research (institutional funding IUT20-14 (TLOKT14014I)) and Estonian Research Council (personal research funding PUT34 and PRG300). Also, the smart specialization doctoral stipend and the Graduate School of Functional materials and technologies receiving funding from the European Regional Development Fund in the University of Tartu (project 2014-2020.4.01.16-0027) and Archimedes Foundation for support through Kristjan Jaak and Dora Plus scholarship.

APPENDIX

Table S 1 In literature available studies focusing on ionization efficiency investigation and modelling.

Ref.	Compound type	Number of unique compounds	Eluent	Mode	Model	Matrix
125	drug like	10	0.1% formic acid/acetonitrile 60/40	+	no	solvent
71	steroids	30	100% methanol; ammonia (pH = 10)/methanol 50/50	+/-	PLS	solvent
126	oligonucleotide	11	water/methanol 50/50 with ion-pairing reagents	-	PLS	solvent
127	metabolites	9	0.5 mM ammonium acetate/methanol 1/9	+	no	urine
128	natural products	8	0.1% formic acid/acetonitrile	+	no	solvent
129	lipids	15	100% methanol	+	no	solvent
72	drugs	170	1 mM ammonium acetate/acetonitrile 50/50	+	PCA, Projection Pursuit, Classification and Regression Trees, PLS and Stepwise MLR	solvent
29	oligopeptide	23	0.5% acetic acid/methanol 50/50	+	No	solvent
11	metabolites	58	0.1% formic acid/methanol 50/50	+	MLR	solvent; RBC lysates
130	lipids	8	5 mM ammonium acetate/acetonitrile	+	no	NIST human plasma; egg yolk; porcine liver
73	drugs	77	0.1% formic acid /acetonitrile	+	MLR	solvent
131	drugs	40	0.1% acetic/acetonitrile (0.1% acetic)	+	no	solvent
23	druglike	19	0.5% acetic acid in methanol	+	MLR	solvent
132	druglike	20	7 mM acetic acid /methanol 20/80; 7 mM ammonia/methanol 20/80	+/-	ANN	solvent
133	amino acids	4		+	no	no

Ref.	Compound type	Number of unique compounds	Eluent	Mode	Model	Matrix
134	natural products	25	10 mM ammonium formate/acetonitrile 60/40; 50/50; 40/60; 30/70; 20/80	- (formate adduct)	no	solvent
74	drugs	110	water/acetonitrile 20/80	-	PLS	solvent
21	sartans	7	pH = 5.5/methanol 40/60	+	ANN	solvent
135	drugs	71	water/acetonitrile 50/50	+	no	solvent
25	phenols	35	100% methanol; 100% acetonitrile; methanol/water 50/50; acetonitrile/water 50/50	-	no	solvent
75	amino acids, derivatives	127	acetonitrile (0.1% formic acid)/0.1% formic acid 100% acetonitrile; 100% acetone; 100% methanol; 100% water	+	MLR	solvent
26	druglike	49		-	no	solvent
136	natural products	13	5 mM ammonium acetate/ methanol (5 mM ammonium acetate)	-	no	olive oil
137	lipids	5	tetrahydrofuran	-	MLR	kerogen extract
138	small bases	56	pH = 3/acetonitrile 50/50; 20/80; pH = 7/acetonitrile 50/50; 20/80	+	no	solvent
139	lipids	15	chloroform/methanol 1:2 1% ammonia	-	no	solvent
140	peptide	4	0.1% ammonium acetate/acetonitrile	+	no	solvent
141	drug	99	ammonia (pH = 10)/methanol 50/50	+	PLS	solvent
142	glycans	8	1 mM NaOH/methanol 50/50	+	no	<i>Drosophila melanogaster</i> . solvent
143	steroid	7	10 mM ammonium acetate/acetonitrile/isopropanol (9/1); 0.02% acetic acid/ acetonitrile/isopropanol 9/1	-	no	solvent; human plasma
27	natural products	4	water	+	MLR	secondary organic aerosol in water
144	small molecules	17	pH = 3.1 /acetonitrile	-/+	no	solvent

Ref.	Compound type	Number of unique compounds	Eluent	Mode	Model	Matrix
145	oligopeptide	12	1 mM ammonium acetate (pH = 6)/methanol 90/10; 1 mM ammonium acetate (pH = 10)/methanol 90/10	+	MLR, regression tree, SVR	solvent
146	glycans	13	0.1% formic acid/acetonitrile 65/35	+	no	tryptic BSA peptides
147	lipophilic marine algal toxins	10	2 mM ammonium formate and 50 mM formic acid/acetonitrile (with additive) 40/60	+/-	no	solvent; mussel
148	flavonoids	6	formic acid acid (pH = 3)/acetonitrile	-	no	solvent
149	lipids	34	10 mM ammonium formate in water/acetonitrile (6/4) and 10 mM ammonium formate isopropanol/acetonitrile (9/1)	+/-	no	human plasma; mouse brain tissue; Jurkat cell pellet
24	small acids	25	0.025% acetic acid/methanol	-	MLR	solvent
150	amino acids	17	2% acetic acid/methanol 50/50	+	no	solvent
151	flavonoids	19	0.1% formic acid/acetonitrile	-	no	extract of <i>G. biloba</i>

Table S 2 Compounds used to develop ionization efficiency model.

#	CAS	Name	$\log P^{152}$	molar mass	ESI mode	SMILES
1	75-04-7	ethylamine	-0.40	45.06	ESI+	CCN
2	113-00-8	guanidine	-0.47	59.05	ESI+	NC(N)=N
3	75-50-3	trimethylamine	0.32	59.07	ESI+	CN(C)C
4	123-75-1	pyrrolidine	-0.97	71.07	ESI+	C1CCNC1
5	109-73-9	butylamine	-1.26	73.09	ESI+	CCCCN
6	109-89-7	diethylamine	0.29	73.09	ESI+	CCNCC
7	12545-87-8	tetramethylammonium	-1.03	74.10	ESI+	C[N+](C)(C)C
8	56-40-6	glycine	-1.19	75.03	ESI+	NCC(O)=O
9	594-09-2	trimethylphosphine	1.91	76.04	ESI+	CP(C)C
10	110-86-1	pyridine	0.68	79.04	ESI+	c1ccncc1
11	290-37-9	pyrazine	-0.47	80.04	ESI+	c1cncnc1
12	289-80-5	pyridazine	0.21	80.04	ESI+	c1ccmnc1
13	110-89-4	piperidine	-1.26	85.09	ESI+	C1CCNCC1
14	110-58-7	pentylamine	-1.55	87.10	ESI+	CCCCCN
15	56-41-7	alpha-alanine	-1.10	89.05	ESI+	CC(N)C(=O)O
16	107-95-9	beta-alanine	-0.94	89.05	ESI+/ESI-	NCCC(O)=O
17	109-06-8	2-methylpyridine	1.31	93.06	ESI+	Cc1ccccc1
18	62-53-3	aniline	1.21	93.06	ESI+	Nc1ccccc1
19	504-29-0	2-aminopyridine	0.24	94.05	ESI+	Nc1ccccc1
20	462-08-8	3-aminopyridine	0.06	94.05	ESI+	Nc1ccccc1
21	504-24-5	4-aminopyridine	0.06	94.05	ESI+	Nc1ccccc1
22	109-00-2	3-hydroxypyridine	0.54	95.04	ESI+	Oc1ccccc1
23	139252-84-9	N-methylpiperidine	-0.73	99.10	ESI+	CN1CCCCC1
24	111-26-2	hexylamine	-1.84	101.12	ESI+	CCCCCCN
25	121-44-8	triethylamine	1.07	101.12	ESI+	CCN(CC)CC
26	56-12-2	4-aminobutanoic acid	-1.23	103.06	ESI-	NCCC(O)=O
27	6898-95-9	serine	-1.60	105.04	ESI+/ESI-	N[C@@H](CO)C(O)=O
28	108-48-5	2,6-dimethylpyridine	1.51	107.07	ESI+	Cc1ccccc1N
29	95-53-4	2-methylaniline	1.57	107.07	ESI+	Cc1ccccc1N
30	106-49-0	4-methylaniline	1.70	107.07	ESI+	Cc1ccc(N)cc1
31	100-46-9	benzylamine	0.94	107.07	ESI+	NCc1ccccc1

#	CAS	Name	$\log P^{152}$	molar mass	ESI mode	SMILES
32	95-55-6	2-aminophenol	0.94	109.05	ESI+/ESI-	<chem>Nc1ccccc1O</chem>
33	591-27-5	3-aminophenol	1.07	109.05	ESI+	<chem>Nc1ccc(O)c1</chem>
34	123-30-8	4-aminophenol	1.07	109.05	ESI+/ESI-	<chem>Nc1ccc(O)cc1</chem>
35	1628-89-3	2-methoxypyridine	0.97	109.05	ESI+	<chem>COc1cccn1</chem>
36	620-08-6	4-methoxypyridine	0.79	109.05	ESI+	<chem>COc1ccncc1</chem>
37	141-86-6	2,6-diaminopyridine	-0.20	109.06	ESI+	<chem>Nc1ccc(N)n1</chem>
38	120-80-9	2-hydroxyphenol	1.42	110.04	ESI-	<chem>Oc1ccccc1O</chem>
39	123-31-9	4-hydroxyphenol	1.55	110.04	ESI-	<chem>Oc1ccc(O)cc1</chem>
40	1066-51-9	AMPA	-1.26	111.01	ESI+	<chem>NC[P](O)(O)=O</chem>
41	71-30-7	cytosine	-1.40	111.04	ESI+	<chem>NC1=NC(=O)NC=C1</chem>
42	65039-03-4	ethyl-methylimidazolium	-1.23	111.09	ESI+	<chem>CC[n+1]ccn(C)c1</chem>
43	66-22-8	uracil	-0.91	112.03	ESI+	<chem>O=C1NC=CC(=O)N1</chem>
44	110-44-1	sorbic acid	1.03	112.05	ESI-	<chem>C/C=C/C=C/C(O)=O</chem>
45	109-09-1	2-chloropyridine	1.32	113.00	ESI+	<chem>C1c1cccn1</chem>
46	626-60-8	3-chloropyridine	1.47	113.00	ESI+	<chem>C1c1ccncc1</chem>
47	527-73-1	2-nitroimidazole	0.77	113.02	ESI+	<chem>[O-][N+](=O)c1[nH]c[n1]</chem>
48	3034-38-6	4-nitroimidazole	0.77	113.02	ESI+	<chem>[O-][N+](=O)c1c[nH]c[n1]</chem>
49	24807-55-4	3-nitro-1 <i>H</i> -1,2,4-triazole	0.62	114.02	ESI+	<chem>[O-][N+](=O)c1n[nH]c[n1]</chem>
50	4305-67-3	proline	-1.38	115.06	ESI+	<chem>OC(=O)C@H(N)CCCCN1</chem>
51	31081-16-0	tetramethylguanidine	-0.40	115.11	ESI+	<chem>CNC(=NC)N(C)C</chem>
52	111-68-2	heptylamine	-2.13	115.14	ESI+	<chem>CCCCCCC</chem>
53	110-16-7	fumaric acid	-0.23	116.01	ESI-	<chem>OC(=O)/C=C/C(O)=O</chem>
54	10593-85-8	D-homocysteine-thiolactone	-0.72	117.02	ESI+	<chem>O=C1SCC[C@H]1N</chem>
55	2338-04-7	L-homocysteine-thiolactone	-0.72	117.02	ESI+	<chem>C1CSC(=O)[C@H]1N</chem>
56	7004-03-7	valine	-0.57	117.08	ESI+/ESI-	<chem>CC(C)[C@H](N)C(O)=O</chem>
57	51-17-2	benzimidazole	1.35	118.05	ESI+	<chem>[nH]1nc2ccccc12</chem>
58	271-44-3	indazole	1.47	118.05	ESI+	<chem>[nH]1ncc2ccccc12</chem>
59	611-20-1	2-cyanophenol	1.57	119.04	ESI+/ESI-	<chem>Oc1ccc1C#N</chem>
60	7013-32-3	threonine	-1.61	119.06	ESI+/ESI-	<chem>C[C@H](O)[C@H](N)C(O)=O</chem>
61	618-39-3	benzamide	1.21	120.07	ESI+	<chem>NC(=N)c1ccccc1</chem>
62	62488-11-3	cysteine	-0.62	121.02	ESI+	<chem>N[C@H](CS)C(O)=O</chem>
63	55-21-0	benzamide	1.05	121.05	ESI+	<chem>NC(=O)c1ccccc1</chem>

#	CAS	Name	$\log P^{152}$	molar mass	ESI mode	SMILES
64	77-86-1	trizma base	-2.38	121.07	ESI+	NC(CO)(CO)CO
65	108-75-8	2,4,6-trimethylpyridine	2.12	121.09	ESI+	Cc1cc(C)nc(C)c1
66	121-69-7	<i>N,N</i> -dimethylaniline	2.12	121.09	ESI+	CN(C)c1ccccc1
67	90-02-8	2-hydroxybenzaldehyde	1.45	122.04	ESI-	Oc1ccccc1C=O
68	123-08-0	4-hydroxybenzaldehyde	1.45	122.04	ESI+/ESI-	Oc1ccc(C=O)cc1
69	65-85-0	benzoic acid	1.44	122.04	ESI+/ESI-	OC(=O)c1ccccc1
70	98-92-0	nicotinamide	-0.10	122.05	ESI+	NC(=O)c1cccnc1
71	7003-89-6	chlormequat	-0.37	122.07	ESI+	C[N+](C)(C)CCC1
72	104-94-9	4-methoxyaniline	1.32	123.07	ESI+	COc1ccc(N)cc1
73	90-05-1	2-methoxyphenol	1.67	124.05	ESI-	COc1ccccc1O
74	150-76-5	4-methoxyphenol	1.80	124.05	ESI-	COc1ccc(O)cc1
75	452-86-8	4-methylcatechol	2.04	124.05	ESI+	Cc1ccc(O)c(O)c1
76	65-71-4	thymine	-0.36	126.04	ESI+	CC1=CNC(=O)NC1=O
77	95-51-2	2-chloroaniline	1.88	127.02	ESI+	Nc1ccccc1Cl
78	106-47-8	4-chloroaniline	2.00	127.02	ESI+	Nc1ccc(Cl)cc1
79	108-43-0	3-chlorophenol	2.48	128.00	ESI-	Oc1ccc(Cl)c1
80	106-48-9	4-chlorophenol	2.48	128.00	ESI-	Oc1ccc(Cl)cc1
81	91-22-5	quinoline	2.02	129.06	ESI+	c1ccc2ncccc2c1
82	253-52-1	phthalazine	1.12	130.05	ESI+	c1ccc2cnncc2c1
83	253-82-7	quinazoline	1.39	130.05	ESI+	c1ccc2ncnc2c1
84	91-19-0	quinoxaline	1.29	130.05	ESI+	c1ccc2ncnc2c1
85	66-40-0	tetraethylammonium	-0.03	130.16	ESI+	CC[N+](CC)(CC)CC
86	56-84-8	aspartic acid	-2.71	131.02	ESI-	O=C(O)C[C@H](N)C(=O)O
87	60-32-2	6-aminocaproic acid	-1.81	131.09	ESI+	NCCCCC(O)=O
88	73-32-5	isoleucine	-1.25	131.09	ESI+/ESI-	CC[C@H](C)[C@H](N)C(O)=O
89	61-90-5	leucine	-0.32	131.09	ESI+/ESI-	CC(C)[C@H](N)C(O)=O
90	108-59-8	dimethyl malonate	0.06	132.04	ESI+	COC(=O)CC(=O)OC
91	328-41-6	asparagine	-1.75	132.05	ESI+/ESI-	N[C@@H](C)[C@H](N)C(O)=O
92	6899-03-2	aspartic acid	-1.35	133.04	ESI+	N[C@@H](C)[C@H](N)C(O)=O
93	934-32-7	2-aminobenzimidazole	1.06	133.06	ESI+	Nc1[nH]c2ccccc2n1
94	73-24-5	adenine	-0.80	135.05	ESI+	Nc1ncnc2[nH]c1c2
95	68-94-0	hypoxanthine	-0.68	136.04	ESI+	O=C1NC=NC2nc[nH]c1c2

#	CAS	Name	$\log P^{152}$	molar mass	ESI mode	SMILES
96	135-02-4	2-methoxybenzaldehyde	1.70	136.05	ESI+	COc1ccccc1C=O
97	93-58-3	methyl benzoate	1.69	136.05	ESI+	COC(=O)c1ccccc1
98	123-11-5	<i>p</i> -anisaldehyde	1.70	136.05	ESI+	COc1ccc(C=O)cc1
99	88-69-7	2-isopropylphenol	1.98	136.09	ESI-	CC(C)c1ccccc1O
100	99-98-9	4-amino- <i>N,N</i> -dimethylamine	1.50	136.10	ESI+	CN(C)c1cccn1
101	118-92-3	2-aminobenzoic acid	0.82	137.05	ESI+/ESI-	Nc1ccccc1C(=O)O
102	99-05-8	3-aminobenzoic acid	0.82	137.05	ESI+/ESI-	Nc1ccc(c1)C(=O)O
103	150-13-0	4-aminobenzoic acid	0.82	137.05	ESI+/ESI-	Nc1ccc(cc1)C(=O)O
104	99-96-7	4-hydroxybenzoic acid	1.30	138.03	ESI+/ESI-	OC(=O)c1ccc(O)cc1
105	69-72-7	salicylic acid	1.18	138.03	ESI+/ESI-	OC(=O)c1ccccc1O
106	88-74-4	2-nitroaniline	1.72	138.04	ESI+	Nc1ccccc1[N+](=O)[O-]
107	99-09-2	3-nitroaniline	1.72	138.04	ESI+	Nc1ccc(c1)[N+](=O)[O-]
108	100-01-6	4-nitroaniline	1.72	138.04	ESI+	Nc1ccc(cc1)[N+](=O)[O-]
109	672-66-2	phenyldimethylphosphine	3.31	138.06	ESI+	CP(C)c1ccccc1
110	88-75-5	2-nitrophenol	2.20	139.03	ESI-	Oc1ccccc1[N+](=O)[O-]
111	554-84-7	3-nitrophenol	2.20	139.03	ESI-	Oc1ccc(c1)[N+](=O)[O-]
112	100-02-7	4-nitrophenol	2.20	139.03	ESI-	Oc1ccc(cc1)[N+](=O)[O-]
113	6231-18-1	2,6-dimethoxy pyridine	1.26	139.06	ESI+	COc1ccc(OC)cn1
114	934-00-9	3-methoxycatechol	1.53	140.05	ESI+	COc1ccc(O)c1O
115	10265-92-6	methamidophos	0.12	141.00	ESI+	CO[P](N)(=O)SC
116	488-21-1	dimethylmaleate	-0.47	142.03	ESI+	OC(=O)C(\C)=C(\C)C(=O)O
117	134-32-7	1-naphthylamine	2.12	143.07	ESI+	Nc1ccc2ccccc12
118	102-69-2	tripropylamine	-0.66	143.17	ESI+	CCCN(CCC)CC
119	106-65-0	dimethyl succinate	0.09	146.06	ESI+	COC(=O)CCC(=O)OC
120	56-85-9	glutamine	-2.03	146.07	ESI+/ESI-	N[C@@H](CCC(N)=O)C(=O)O
121	6899-06-5	lysine	-2.75	146.11	ESI+	NCCCC[C@H](N)C(=O)O
122	51-84-3	acetylcholine	-1.20	146.12	ESI+	CC(=O)OCC[N+](C)(C)C
123	85-41-6	phthalimide	0.78	147.03	ESI-	O=C1NC(=O)c2ccccc12
124	56-86-0	glutamic acid	-1.64	147.05	ESI+/ESI-	N[C@@H](CCC(O)=O)C(=O)O
125	140-10-3	cinnamic acid	1.80	148.05	ESI+	OC(=O)C=Cc1ccccc1
126	3654-96-4	methionine	-0.73	149.05	ESI+/ESI-	CSCC[C@H](N)C(=O)O
127	102-97-6	<i>N</i> -isopropylbenzylamine	1.32	149.12	ESI+	CC(C)NCc1ccccc1

#	CAS	Name	log ^p ¹⁵²	molar mass	ESI mode	SMILES
128	93-89-0	ethyl benzoate	1.95	150.07	ESI+	CCOC(=O)c1ccccc1
129	88-18-6	2- <i>tert</i> -butylphenol	2.96	150.10	ESI-	CC(C)(C)c1ccccc1O
130	552-89-6	2-nitrobenzaldehyde	2.18	151.03	ESI+	[O-][N+](=O)c1ccccc1C=O
131	99-61-6	3-nitrobenzaldehyde	2.18	151.03	ESI+	[O-][N+](=O)c1cccc(C=O)c1
132	555-16-8	4-nitrobenzaldehyde	2.18	151.03	ESI+	[O-][N+](=O)c1ccc(C=O)cc1
133	15197-75-8	2-pyrridinepropionic acid	0.92	151.06	ESI+/ESI-	OC(=O)CC1cccn1
134	6318-43-0	4-pyridinepropionic acid	0.38	151.06	ESI+/ESI-	OC(=O)CC1ccncc1
135	15799-79-8	3-methoxy- <i>N,N</i> -dimethylaniline	2.10	151.10	ESI+	COc1cccc(c1)N(C)C
136	701-56-4	4-methoxy- <i>N,N</i> -dimethylaniline	2.10	151.10	ESI+	COc1ccc(cc1)N(C)C
137	100-09-4	4-methoxybenzoic acid	1.55	152.05	ESI+	COc1ccc(cc1)C(=O)O
138	99-76-3	methyl paraben	1.55	152.05	ESI+	COC(=O)c1ccc(O)cc1
139	6674-22-2	1,8-diazabicyclo(5.4.0)undec-7-ene	-1.78	152.13	ESI+	C1CCN2CCCN=C2CC1
140	51-61-6	dopamine	0.91	153.08	ESI+	NCCc1ccc(O)c(O)c1
141	71-00-1	histidine	-0.98	155.07	ESI+/ESI-	N[C@@H](Cc1c[nH]cn1)C(O)=O
142	535-80-8	3-chlorobenzoic acid	2.24	156.00	ESI-	OC(=O)c1cccc(Cl)c1
143	364-76-1	4-fluoro-3-nitroaniline	2.05	156.03	ESI+	Nc1ccc(F)c(c1)[N+](=O)[O-]
144	366-18-7	2,2-bipyridine	1.82	156.07	ESI+	c1ccc(nc1)c2cccn2
145	18978-78-4	8-aminoquinoline	1.94	158.08	ESI+	Cc1ccc2cccc(N)c2n1
146	1119-40-0	dimethyl glutarate	-0.20	160.07	ESI+	COC(=O)CCCC(=O)OC
147	533-74-4	dazomet	1.60	162.03	ESI+	CN1CSC(=S)N(C)C1
148	98-17-9	3-(trifluoromethyl)phenol	2.63	162.03	ESI-	Oc1ccc(c1)C(F)(F)F
149	16752-77-5	methomyl	0.76	162.05	ESI+	CNC(=O)ON=C(C)SC
150	524-38-9	<i>N</i> -hydroxy-phthalimide	0.32	163.03	ESI-	ON1C(=O)c2ccccc2C1=O
151	94-52-0	5-nitrobenzimidazole	1.94	163.04	ESI+	[O-][N+](=O)c1cccc[nH]c2c1
152	7597-18-4	6-nitroindazole	2.07	163.04	ESI+	[O-][N+](=O)c1ccc2cn[nH]c2c1
153	536-66-3	4-isopropylbenzoic acid	1.86	164.08	ESI-	CC(C)c1ccc(cc1)C(=O)O
154	100-22-1	4-dimethylamino- <i>N,N</i> -dimethylaniline	2.28	164.13	ESI+	CN(C)c1ccc(cc1)N(C)C
155	99-64-9	3-dimethylaminobenzoic acid	1.73	165.08	ESI+/ESI-	CN(C)c1ccc(c1)C(=O)O
156	63-91-2	phenylalanine	0.59	165.08	ESI+/ESI-	N[C@@H](Cc1ccccc1)C(O)=O
157	769-39-1	2,3,5,6-tetrafluorophenol	2.89	166.00	ESI-	Oc1c(F)c(F)cc(F)c1F
158	88-99-3	phthalic acid	1.06	166.03	ESI+/ESI-	OC(=O)c1ccccc1C(=O)O
159	100-21-0	terephthalic acid	1.06	166.03	ESI+/ESI-	OC(=O)c1ccc(cc1)C(=O)O

#	CAS	Name	log ^p ¹⁵²	molar mass	ESI mode	SMILES
160	120-47-8	ethyl paraben	1.81	166.06	ESI+	CCOC(=O)c1ccc(O)cc1
161	66215-27-8	cyromazine	-2.03	166.10	ESI+	Nc1nc(N)nc(NC2CC2)n1
162	552-16-9	2-nitrobenzoic acid	1.95	167.02	ESI+/ESI-	OC(=O)c1ccc(O)cc1
163	62-23-7	4-nitrobenzoic acid	1.95	167.02	ESI+/ESI-	OC(=O)c1ccc(O)cc1
164	66-72-8	pyridoxal	-0.11	167.06	ESI+	Cc1nc(CO)c(C=O)c1O
165	171058-17-6	hexyl-methylimidazolium	-2.78	167.15	ESI+	C[n+](C)ccc(C)cc1
166	85-87-0	pyridoxamine	-0.76	168.09	ESI+	Cc1nc(CO)c(CN)c1O
167	1071-83-6	glyphosate	-1.37	169.01	ESI+	OC(=O)CNC[P](O)(O)=O
168	65-23-6	pyridoxine	-0.47	169.07	ESI+	Cc1nc(CO)c(CO)c1O
169	122-39-4	diphenylamine	3.63	169.09	ESI+	N(c1ccccc1)c2ccccc2
170	90-43-7	2-phenylphenol	3.21	170.07	ESI-	Oc1ccccc1c2ccccc2
171	92-69-3	4-phenylphenol	3.21	170.07	ESI-	Oc1ccc(O)cc1
172	535-89-7	crimidine	1.20	171.06	ESI+	CN(C)c1cc(C)nc(Cl)n1
173	95-56-7	2-bromophenol	2.44	171.95	ESI-	Oc1ccccc1Br
174	591-20-8	3-bromophenol	2.57	171.95	ESI-	Oc1ccccc1Br
175	89-63-4	4-chloro-2-nitroaniline	2.51	172.00	ESI+	Nc1ccc(Cl)cc1
176	63-74-1	sulphanilamide	0.12	172.03	ESI+	Nc1ccc(cc1)S(N)=O
177	74-79-3	arginine	-2.18	174.11	ESI+	N[C@@H](CCCC(N)N)C(O)=O
178	120-12-7	anthracene	3.65	178.08	ESI+	c1ccc2cc3ccccc3cc2c1
179	98-73-7	4- <i>tert</i> -butylbenzoic acid	2.84	178.10	ESI-	CC(C)(C)c1ccc(cc1)C(O)=O
180	59-26-7	<i>N,N</i> -diethylnicotinamide	0.60	178.11	ESI+	CCN(CC)C(=O)c1ccncc1
181	230-27-3	7,8-benzoquinoline	2.92	179.07	ESI+	c1ccc2c(c1)ccc3ccncc23
182	260-94-6	acridine	3.35	179.07	ESI+	c1ccc2nc3ccccc3cc2c1
183	66-71-7	1,10-phenanthroline	2.20	180.07	ESI+	c1ene2c(c1)ccc3ccncc23
184	94-13-3	propyl paraben	1.23	180.08	ESI+	CCCOC(=O)c1ccc(O)cc1
185	140-43-2	tyrosine	0.45	181.07	ESI+/ESI-	N[C@@H](Cc1ccc(O)cc1)C(O)=O
186	119-61-9	benzophenone	3.23	182.07	ESI+	O=C(c1ccccc1)c2ccccc2
187	111-55-7	ethylene glycol diacetate	-1.36	182.08	ESI+	CC(=O)OCCOC(=O)C
188	97-02-9	2,4-dinitroaniline	2.23	183.03	ESI+	Nc1ccc(cc1[N+](=O)[O-])C(O)=O
189	97-31-4	normetanephrine	0.27	183.09	ESI+	COc1cc(O)cc1
190	771-61-9	pentafluorophenol	3.23	183.99	ESI-	Oc1c(F)c(F)c(F)c(F)c1F
191	51-28-5	2,4-dinitrophenol	2.71	184.01	ESI-	Oc1ccc(cc1[N+](=O)[O-])C(O)=O

#	CAS	Name	log ^p ¹⁵²	molar mass	ESI mode	SMILES
192	329-71-5	2,5-dinitrophenol	2.71	184.01	ESI-	<chem>Oc1cc(ccc1[N+](=O)[O-])[N+](=O)[O-]</chem>
193	573-56-8	2,6-dinitrophenol	2.71	184.01	ESI-	<chem>Oc1c(ccc1[N+](=O)[O-])[N+](=O)[O-]</chem>
194	1020178-63-5	<i>N,N,N'</i> - tripropylguanidine	-1.37	185.19	ESI+	<chem>CCCN(CCCC)=NCC</chem>
195	102-82-9	tributylamine	-1.53	185.21	ESI+	<chem>CCCCN(CCCC)CCCC</chem>
196	13010-31-6	tetrapropylammonium	-2.34	186.22	ESI+	<chem>CCC[N+](CCC)CCC)CCC</chem>
197	140-40-9	2-acetamido-5-nitrothiazole	0.68	187.01	ESI+	<chem>CC(=O)Nc1sc(cn1)[N+](=O)[O-]</chem>
198	35790-47-7	Gly ₃ -NH ₂	-3.26	188.09	ESI+	<chem>NCC(=O)NCC(=O)NCC(N)=O</chem>
199	123-99-9	azelaic acid	-1.85	188.10	ESI+	<chem>OC(=O)CCCCCCCC(=O)O</chem>
200	24579-73-5	propamocarb	-0.03	188.15	ESI+	<chem>CCCOC(O)=NCCCN(C)C</chem>
201	454-92-2	3-trifluoromethylbenzoic acid	2.39	190.02	ESI-	<chem>OC(=O)c1cccc(c1)C(F)(F)F</chem>
202	116-06-3	aldicarb	1.27	190.08	ESI+	<chem>CNC(=O)O=N=C(C)C)SC</chem>
203	10605-21-7	carbendazim	1.67	191.07	ESI+	<chem>COC(=O)Nc1[nH]c2ccccc2n1</chem>
204	2556-43-6	phenyl tetramethylguanidine	1.41	191.14	ESI+	<chem>CN=C(N(C)C)N(C)C1c1ccccc1</chem>
205	131-11-3	dimethyl phthalate	1.56	194.06	ESI+	<chem>COC(=O)c1ccccc1C(=O)OC</chem>
206	58-08-2	caffeine	-0.96	194.08	ESI+	<chem>CN1C=NC2=C1C(=O)N(C(=O)N2C)C</chem>
207	578-95-0	9(10 <i>H</i>)acridanone	0.84	195.07	ESI+	<chem>C1=CC=C2C(=C1)C(=O)C3=CC=CC=C3N2</chem>
208	93-98-1	benzamide	2.86	197.08	ESI+	<chem>O=C(Nc1ccccc1)c2ccccc2</chem>
209	5001-33-2	metanephthrine	0.83	197.11	ESI+	<chem>CNCC(O)c1ccc(O)c(OC)c1</chem>
210	103-49-1	dibenzylamine	2.95	197.12	ESI+	<chem>C(NC1c1ccccc1)c2ccccc2</chem>
211	93-99-2	phenylbenzoate	3.40	198.07	ESI+	<chem>O=C(Oc1ccccc1)c2ccccc2</chem>
212	1689-82-3	4-phenylazophenol	0.68	198.08	ESI+	<chem>C1=CC=C(C=C1)NN=C2C=CC(=O)C=C2</chem>
213	53112-28-0	pyrimethamil	2.70	199.11	ESI+	<chem>Cc1cc(C)nc(Nc2ccccc2)n1</chem>
214	143-07-7	dodecanoic acid	-2.75	200.18	ESI-	<chem>CCCCCCCCCCCC(=O)O</chem>
215	122-34-9	simazine	0.84	201.08	ESI+	<chem>CCNc1nc(Cl)nc(NCC)n1</chem>
216	121-52-8	3-nitrobenzenesulphonamide	1.33	202.00	ESI-	<chem>N[S](=O)(=O)c1ccc(c1)[N+](=O)[O-]</chem>
217	129-00-0	pyrene	3.95	202.08	ESI+	<chem>c1ccc2ccc3ccc4ccc(c1)c2c34</chem>
218	41394-05-2	metamitron	0.53	202.09	ESI+	<chem>CC1=NN=C(c2ccccc2)C(=O)N1N</chem>
219	98-47-5	3-nitrobenzenesulfonic acid	1.73	202.99	ESI-	<chem>O[S](=O)(=O)c1ccc(c1)[N+](=O)[O-]</chem>
220	80206-30-0	tryptophan	0.88	204.09	ESI+/ESI-	<chem>N[C@@H](Cc1c[nH]c2ccccc12)C(O)=O</chem>
221	1646-87-3	aldicarb-sulfoxide	0.16	206.07	ESI+	<chem>CNC(=O)O=N=C(C)C)S(C)C(=O)O</chem>
222	34123-59-6	isoproturon	1.80	206.14	ESI+	<chem>CC(C)c1ccc(NC(=O)N(C)C)cc1</chem>
223	85-47-2	naphthalenesulfonic acid	2.13	208.02	ESI-	<chem>O[S](=O)(=O)c1ccc2ccccc12</chem>

#	CAS	Name	log ^p ¹⁵²	molar mass	ESI mode	SMILES
224	84-65-1	anthraquinone	2.81	208.05	ESI+	O=C1c2ccccc2C(=O)c3ccccc13
225	588-68-1	benzalazine	3.50	208.10	ESI+	N(N=C/c1ccccc1)=C/c1ccccc1
226	114-26-1	propoxur	1.76	209.11	ESI+	CNC(=O)Oc1ccccc1OC(C)C
227	20277-92-3	diphenylguanidine	3.14	211.11	ESI+	NC(=N)N(c1ccccc1)c2ccccc2
228	602-94-8	perfluorobenzoic acid	2.98	211.99	ESI-	OC(=O)c1c(F)c(F)c(F)c(F)c1F
229	610-30-0	2,4-dinitrobenzoic acid	2.46	212.01	ESI-	OC(=O)c1ccc(cc1)[N+](=[O-])=O)[N+](=[O-])=O
230	99-34-3	3,5-dinitrobenzoic acid	2.46	212.01	ESI-	OC(=O)c1cc(cc(c1)[N+](=[O-])=O)[N+](=[O-])=O
231	21087-64-9	metribuzin	1.47	214.09	ESI+	CSC1=NN=C(C(=O)N)N(C)C(C)C
232	1912-24-9	atrazine	0.53	215.09	ESI+	CCNc1nc(Cl)nc(NC(C)C)n1
233	87-13-8	diethyl ethoxymethylenemalonate	0.47	216.10	ESI+	CCOC=C(C(=O)OCC)C(=O)OCC
234	123312-89-0	pymetrozin	-0.33	217.10	ESI+	CC1=NNC(=O)N(C)N=C(C)C=Cc2ccccc2
235	78677-27-7	Gly-β-Ala-β-Ala	-2.37	217.11	ESI+	NCC(=O)NCCC(=O)NCCC(=O)O
236	91-53-2	ethoxyquin	3.38	217.15	ESI+	CCOc1ccc2NC(C)C(=C)C(C)c2c1
237	102-76-1	glyceryl triacetate	-0.27	218.08	ESI+	CC(=O)OCC(COC(=O)C)OC(=O)C
238	24469-50-9	(1 <i>Z</i>)-1-benzylidene-2-(1- <i>tert</i> -butoxyethenyl)hydrazine	2.92	218.14	ESI+	CC(C)C)OC(=C)N)N=C/c1ccccc1
239	23135-22-0	oxamyl	0.32	219.07	ESI+	CNC(=O)O)N=C(SC)C(=O)N(C)C
240	1698-60-8	chloridazon	0.78	221.04	ESI+	NC1=C(C)C(=O)N(N=C1)c2ccccc2
241	946-65-6	3-[(trifluoromethyl)sulphonyl]benzoic acid	3.35	222.00	ESI-	OC(C1=CC=CC(SC(F)(F)F)=C1)=O
242	135410-20-7	acetamiprid	-0.14	222.07	ESI+	CC(=NC#N)N(C)CC1=CN=C(C=C1)Cl
243	1646-88-4	aldicarb-sulfone	0.26	222.07	ESI+	CNC(=O)O)N=C(C)C)S]C(C)=O=O
244	20283-21-0	1-decanesulfonic acid	0.96	222.34	ESI-	CCCCCCCCCS(=O)(=O)O
245	110235-47-7	mepanipyrim	3.50	223.11	ESI+	CC#Cc1cc(C)nc(Nc2ccccc2)n1
246	716-16-5	methiocarb	3.47	225.08	ESI+	CNC(=O)O)c1cc(C)et(SC)c(C)c1
247	609-99-4	3,5-dinitrosalicylic acid	2.19	228.00	ESI-	OC(=O)c1cc(cc(c1O)[N+](=[O-])=O)[N+](=[O-])=O
248	489-98-5	2,4,6-trinitroaniline	2.74	228.01	ESI+	Nc1c(cc(cc1[N+](=[O-])=O)[N+](=[O-])=O)[N+](=[O-])=O
249	544-63-8	myristic acid	-3.32	228.21	ESI+/ESI-	CCCCCCCCCCCCCCC(O)=O
250	1020178-65-7	<i>N</i> -[[CH ₂] ₃ NMe ₂]- <i>N,N</i> -propylguanidine	-1.19	228.23	ESI+	CCCN=C(NCCC)NCCCN(C)C
251	7286-69-3	sebuthylazine	0.25	229.11	ESI+	CCNc1nc(Cl)nc(NC(C)C)n1

#	CAS	Name	log ^p ¹⁵²	molar mass	ESI mode	SMILES
252	195-41-5	quinoquinoline	3.54	230.08	ESI+	c1ccc2nc3ccc4ccene4c3cc2c1
253	22204-53-1	naproxen	2.75	230.09	ESI-	COc1ccc2cc(c1)C(C)C(O)=O
254	137-58-6	lidocaine	2.66	234.17	ESI+	CCN(CC)CC(=O)Nc1c(C)cccc1C
255	2378-02-1	perfluoro- <i>tert</i> -butanol	2.55	235.99	ESI-	OC(C(F)(F)C(F)(F)C(F)(F)F)
256	1085-12-7	heptyl paraben	0.08	236.14	ESI+	CCCCCCCOC(=O)c1ccc(O)cc1
257	5707-69-7	draxolon	2.04	237.03	ESI+	CC1=NOC(=O)C1=N1Nc2cccc2C1
258	137-26-8	thiram	3.16	239.99	ESI+	CN(C)C(=S)SSC(=S)N(C)C
259	2635-10-1	methiocarb-sulfoxide	2.53	241.08	ESI+	CN=C(O)c1cc(C)c(S(C)=O)c(C)c1
260	13194-48-4	ethoprophos	0.92	242.06	ESI+	CCCS[P](=O)(OC)SCCC
261	63314-37-4	tetrabutylammonium	-3.50	242.28	ESI+	CCCC[N+](CCCC)CCCC
262	82-71-3	2,4,6-trinitro-1,3-benzenediol	3.08	244.99	ESI-	Oc1cc(c(O)c1[N+](=O)[O-])=O
263	29110-47-2	guanifacine hydrochloride	0.74	245.01	ESI+	O[N+](=O)c1cc(O)c1
264	54132-81-9	GlyDEEMM	-0.59	245.09	ESI+	CCOC(=O)C(=CNCC(=O)O)C(=O)OCC
265	603-34-9	triphenylamine	5.42	245.12	ESI+	c1ccc(cc1)N(c2ccccc2)c3ccccc3
266	301-12-2	demeton- <i>S</i> -methyl sulfoxide	0.52	246.01	ESI+	CC[S](=O)CCS[P](=O)(OC)OC
267	89-02-1	2,4-dinitro-benzenesulfonic acid	2.24	247.97	ESI-	O[S](=O)(=O)c1ccc(cc1[N+](=O)[O-])[N+](=O)[O-]
268	330-55-2	linuron	2.81	248.01	ESI+	CON(C)C(=O)Nc1ccc(C)c(C)c1
269	842-07-9	sudan I	3.32	248.09	ESI+	O=C1C=Cc2cccc2C1=N/Ne3ccccc3
270	3157-03-7	diphenylhydantoin	2.66	252.09	ESI+	O=C1CN(C(=O)N1c2ccccc2)c3ccccc3
271	723-46-6	SMX	1.10	253.05	ESI+	Cc1onc(N[S](=O)(=O)c2ccc(N)cc2)c1
272	28159-98-0	cybutryn	-0.20	253.14	ESI+	CC(C)CNC1=NC(=NC(=N1)NC2CC2)SC
273	79676-59-8	2-(trifluoromethane)sulfonylbenzoic acid	3.11	253.99	ESI+	O=C(O)c1ccccc1S(=O)(=O)C(F)F
274	952-69-2	3-[(trifluoromethyl)sulphonyl]benzoic acid	2.33	253.99	ESI-	OC(C)=CC=CC(S(=O)(C(F)F)F)=O=C1=O
275	952-69-2	3-trifluoromethylsulfonylbenzoic acid	3.11	253.99	ESI-	OC(=O)c1ccccc1[S](=O)(=O)C(F)F
276	35589-04-9	((CH ₃) ₂ N) ₃ -P=N-C ₆ H ₅	1.09	254.17	ESI+	CN(C)P(=Nc1ccccc1)(N(C)C)N(C)C
277	105827-78-9	imidacloprid	1.17	255.05	ESI+	[O-][N+](=O)NC1=NCCN1C2ccc(C)nc2
278	119-91-5	biquinoline	4.41	256.10	ESI+	c1ccc2nc(ccc2c1)c3ccc4cccc4n3
279	2179-25-1	methiocarb-sulfone	2.62	257.07	ESI+	CN=C(O)c1cc(C)c(S(C)=O)c(C)c1

#	CAS	Name	log ^p ¹⁵²	molar mass	ESI mode	SMILES
280	10236-44-9	Ac-Gly-Lys-OMe	-3.21	259.15	ESI+	COC(=O)C(CCCCN)NC(=O)NC(C)=O
281	525-66-6	propanolol	0.49	259.16	ESI+	CC(C)NCC(COC1=CC=CC2=CC=CC=C2)O
282	298-02-2	phorate	3.01	260.01	ESI+	CCOP(=S)(OC)SCSCC
283	603-35-0	triphenylphosphine	5.96	262.09	ESI+	c1ccccc1P(c1ccccc1)c1ccccc1
284	732-26-3	2,4,6-tri- <i>tert</i> -butylphenol	5.89	262.23	ESI-	CC(C)(C)c1cc(c(O)c(c1)C(C)(C)C(C)C)C
285	87-86-5	pentachlorophenol	5.52	263.85	ESI-	Oc1c(Cl)c(Cl)c(Cl)c(Cl)c1Cl
286	74070-46-5	aclofenfen	4.33	264.03	ESI+	Nc1c(Cl)c(Oc2ccccc2)ccc1N+([O-])=O
287	78684-63-6	mianserin	3.83	264.16	ESI+	CN1CCN2C(C1)c3ccccc3c4cccc24
288	70-16-6	thiamine	-3.84	265.11	ESI+	CC1=C(SC=[N+][CC2=CN=C(N=C2N)C]C)C
289	29122-68-7	atenolol	-0.85	266.16	ESI+	CC(C)NCC(COC1=CC=C(C=C1)CC(=O)N)O
290	15972-60-8	alachlor	1.84	269.12	ESI+	CCc1ccccc1N(COC)C(=O)CC1
291	727-49-1	heptafluoromaph-2-ol	0.75	269.99	ESI-	FC1=C(O)C(F)=C(F)C2=C(F)C(F)=C(F)C(F)=C
292	1020178-64-6	<i>N,N</i> -[(CH ₂) ₃ NMe ₂] ₂ - <i>N</i> -propylguanidini	-1.01	271.27	ESI+	CCCN=C(NCCCN(C)C)NCCCN(C)C
293	41125-53-5	3-[tris(trifluoromethyl)methyl]benzoic acid	3.46	274.04	ESI-	FC(F)(F)C(c1ccccc1)C(=O)O)C(F)(F)C(F)(F)F
294	3118-97-6	sudan II	4.30	276.13	ESI+	Cc1ccc(NN=C2/C(C=O)C=Cc3ccccc23)c(C)c1
295	50-48-6	amitriptyline	2.36	277.18	ESI+	CN(C)CCC=C1C2=CC=CC=C2C1CC3=CC=CC=C3
296	1884453-39-7	benzyl ethylethoxymethylenemalonate	1.14	278.12	ESI+	CC/C(OCC)=C/C(=O)OCCc1ccccc1)C(=O)O
297	54171-89-0	<i>N,N</i> -diphenylbispidine	3.33	278.18	ESI+	c1ccc(N2CC3CC(C2)CN(c2ccccc2)C3)cc1
298	332855-88-6	(<i>S</i>)-3-Anilino-5-methyl-5-phenylimidazolidine-2,4-dione	1.15	281.12	ESI+	C1C@H(C(=O)N(C(=O)N1)NC2=CC=CC=C2)C3=CC=CC=C3
299	32809-16-8	procymidone	3.63	283.02	ESI+	CC12CC1(C)C(=O)N(C2=O)c3ccc(Cl)cc(Cl)c3
300	50471-44-8	vinclozolin	4.04	285.00	ESI+	CC1(OC(=O)N(C1=O)c2cc(Cl)cc(Cl)c2)C=C
301	26225-79-6	ethofumesate	2.61	286.09	ESI+	CCOC1Oc2ccc(O)S1(C)C(=O)O)cc2C1(C)C
302	13054-03-0	Gly-Pro-Gly-Gly	-4.22	286.13	ESI+	NCC(=O)N1CCCC[C@H]1C(=O)NCC(=O)NCC(=O)O
303	2275-23-2	vamidothion	0.64	287.04	ESI+	CNC(=O)C(C)SCCS[P](=O)(OC)OC
304	603-53-2	triphenylguanidine	4.90	287.14	ESI+	NC(=Nc1ccccc1)N(c2ccccc2)c3ccccc3
305	84-48-0	2-anthraquinonesulfonic acid	2.20	288.01	ESI-	O[S](=O)(=O)c1ccc2C(=O)c3ccccc3C(=O)c2c1

#	CAS	Name	log ^p ¹⁵²	molar mass	ESI mode	SMILES
306	88671-89-0	myclobutamil	1.37	288.11	ESI+	CCCC(Cn1cncn1)(C#N)c2ccc(Cl)cc2
307	571-41-5	testosterone	0.26	288.21	ESI+	CC12CCCC3C(C1CCC2O)CCC4=CC(=O)CCC34C
308	103972-83-4	4-phenylazophenol	5.39	290.11	ESI-	Oc1ccccc1N=Ne2cc(ccc2O)c3ccccc3
309	153719-23-4	thiamethoxam	0.09	291.02	ESI+	CN\1COCN/C1=N/[N+](=O)[O-]
310	56-38-2	parathion-ethyl	3.82	291.03	ESI+]CC2=CN=C(S2)Cl
311	82336-55-8	paclobutrazol	1.41	293.13	ESI+	CCO[P](=S)(OCC)Oc1ccc(cc1)[N+]([O-])=O
312	58479-52-0	<i>R</i> (-)-propylorapomorphine	0.77	295.16	ESI+	CC(C)C[C@H](C[C@@H](CC1=CC=C(C=C1)C1)N2C=NC=N2)O
313	35554-44-0	imazalil	3.60	296.05	ESI+	CCCN1CCC2=CC=CC3=C2C1CC4=C3C(=C(C=C4)O)
314	97-77-8	tetraethylthiuram disulfide	4.16	296.05	ESI+	Clc1ccc(C(Cn2scnc2)OCC=C)c(Cl)c1
315	29022-11-5	GlyFmoc	2.49	297.10	ESI+	CCN(CC)C(=S)SSC(=S)N(C)CC
316	5131-24-8	ditalimfos	2.25	299.04	ESI+	O=C(O)N(C(=O)O)CC1c2ccccc2-c2ccccc21
317	126833-17-8	fenhexamid	2.02	301.06	ESI+	CCO[P](=S)(OCC)N1C(=O)c2ccccc2C1=O
318	74115-24-5	clofentezine	4.60	302.01	ESI+	CC1(CCCC1)C(=O)Nc2ccc(O)c(Cl)c2Cl
319	60-01-5	glyceryl tributyrate	-0.91	302.17	ESI+	Clc1ccccc1c2nnc(nn2)c3ccccc3Cl
320	2303-17-5	tri-allate	2.41	303.00	ESI+	CCCC(=O)OCC(COC(=O)CCC)OC(=O)CCC
321	13067-93-1	cyanophenphos	4.26	303.05	ESI+	CC(C)N(C)C(C)C(=O)SCC(Cl)=C(Cl)Cl
322	51-34-3	scopolamine	0.12	303.15	ESI+	CCO[P](=S)(Oc1ccc(cc1)C#N)c2ccccc2
323	67564-91-4	fenpropimorph	2.92	303.26	ESI+	CN1[C@@H]2CC(C[C@H]1)[C@H]3[C@@H]2
324	69327-76-0	buprofezin	3.41	305.16	ESI+	O3)OC(=O)[C@H](CO)C4=CC=CC=C4
325	124495-18-7	quinoxifen	5.75	307.00	ESI+	C[C@@H]1CN[C@C@H](O1)CC(C)CC2=C
326	81-81-2	warfarin	3.06	308.10	ESI-	C=C(C=C2)C(C)C(C)
327	52341-67-0	fluoxetine	2.27	309.13	ESI+	CC(C)N1C(=O)N(CS1=NC(C)C)c2ccccc2
328	24017-47-8	triazophos	3.00	313.06	ESI+	Fc1ccc(Oc2ccnc3cc(Cl)cc(Cl)c23)cc1
329	57-83-0	progesterone	0.92	314.22	ESI+	CC(=O)CC(c1ccccc1)C2=C(O)Oc3ccccc3C2=O
						CNCCC(Cl)=CC=CC=C1)OC2=CC=C(C=C2)C(F)(F)F
						CCO[P](=S)(OCC)Oc1ncn(n1)c2ccccc2
						CC(=O)C1CCC2C1(CCC3C2CCC4=CC(=O)CC
						C34C)C

#	CAS	Name	log P^{152}	molar mass	ESI mode	SMILES
371	69257-04-1	(8 <i>S</i> ,9 <i>R</i>)-(-)- <i>N</i> -benzylcinchonidinium	1.63	385.23	ESI+	<chem>C=C[C@H]1CN+(C3CCCCC3)CC[C@H]1C[C@H]2C(O)c1ccnc2cccc12</chem>
372	36505-84-7	buspirone	-3.36	385.25	ESI+	<chem>C1CCC2(C)CC(=O)N(C(=O)C2)C(C)CCN3CCN(CC3)C4=NC=CC=N4</chem>
373	35661-40-6	PheFmoc	4.27	387.15	ESI+	<chem>O=C(O)C(Cc1cccc1)NC(=O)OCC1c2cccc2-c2cccc21</chem>
374	133-91-5	3,5-dihydroxybenzoic acid	2.59	389.82	ESI-	<chem>OC(=O)c1cc(O)ccc1c1O</chem>
375	-	In house synthesized phosphazene	5.38	391.19	ESI+	<chem>CN(C)P(=Nc1cccc(N=Nc2cccc2)cc1)(c1cccc1)N(C)C</chem>
376	300363-70-6	2,5-Cl ₂ -C ₆ H ₃ -P(pyrr)	0.40	400.14	ESI+	<chem>C1c1cccc(C1)c(N=P(N2CCCCC2)(N2CCCCC2)N2C(C)C)C1</chem>
377	417706-59-3	4-CF ₃ -C ₆ H ₄ -P(pyrr)	-0.24	400.20	ESI+	<chem>FC(F)(F)c1cccc(N=P(N2CCCCC2)(N2CCCCC2)N2CCCC2)cc1</chem>
378	82097-50-5	triasulfuron	-0.58	401.06	ESI+	<chem>CC1=NC(=NC(=N1)OC)NC(=O)NS(=O)(=O)C2=CC=CC=C2OCC1</chem>
379	131860-33-8	azoxystrobin	0.87	403.12	ESI+	<chem>CO/C=C(\C1=CC=CC=C1OC2=NC=NC(=C2)OC3=CC=CC=C3C#N)/C(=O)OC</chem>
380	88489-83-2	3-[tris(trifluoromethyl)methylsulphonyl]-benzoic acid	3.11	403.98	ESI-	<chem>OC(C1=CC=CC(S(=O)(C(C(F)(F)F)(C(F)(F)F)C(F)(F)F)=O)=C1)=O</chem>
381	154-21-2	lineomycin	-2.12	406.21	ESI+/ESI-	<chem>CCCC1CC(N(C)C1)C(=O)NC(C(O)C2OC(SC(C(O)C(O)C2O)C(O)C(O)C2O)C(O)C(O)C2O)c1cccc1CO\N=C(O)c2cccc(c2)C(F)F</chem>
382	141517-21-7	trifloxystrobin	4.05	408.13	ESI+	<chem>C1C@H](CCC(O)=O)[C@H]1CCC[C@H]2[C@@H]3[C@H](O)[C@C]([C@H]4[C@H](O)CC[C@]4(C)[C@H]3C[C@H](O)[C@]12C)O(CCN1CCN(CC1)CCCC1cccc1)C(c1cccc1)c1cccc1</chem>
383	81-25-4	choleic acid	-0.47	408.29	ESI+	<chem>CC(C)C(=O)OC(C#N)c1cccc(Oc2cccc2)c1c3ccc(C)cc3</chem>
384	76778-22-8	GBR-12935	4.70	414.27	ESI+	<chem>Cc1c(COC(=O)C2C(C=C(C1)C(F)F)C2(C)C)cccc1c3cccc3</chem>
385	51630-58-1	fenvalerate	6.17	419.13	ESI+	
386	82657-04-3	bifenthrin	6.17	422.13	ESI+	

#	CAS	Name	log P^{152}	molar mass	ESI mode	SMILES
401	2097489-41-1	4-[2-(4-nitrophenyl)diazeny]- <i>N</i> -(phenyl)-1-pyrrolidinylphosphoranylidene)benzenamine	4.46	488.21	ESI+	<chem>O=[N+]([O-])c1ccc(N=Nc2ccc(N=P(c3cccc3)(N3CCCC3)cc2)cc1</chem>
402	2097489-43-3	4-[2-[4-[(diphenyl)-1-pyrrolidinylphosphoranylidene]amino]phenyl]diazeny]- <i>N,N</i> -dimethylbenzenamine	7.46	493.24	ESI+	<chem>CN(C)c1ccc(N=Nc2ccc(N=P(c3cccc3)(c3cccc3)N3CCCC3)cc2)cc1</chem>
403	37248-47-8	validamycin A	-6.01	497.21	ESI+	<chem>OC[C@H]1C[C@H](N[C@H]2C=C(CO)[C@@H]1O)[C@H](O)[C@H]2O)[C@H](O)[C@@H](O)[C@@H]1O[C@H]3O[C@H](CO)[C@@H](O)[C@H](O)[C@H]3O</chem>
404	1763-23-1	perfluorooctanesulfonic acid	4.50	499.94	ESI-	<chem>O=S(O)(C(C)(C(C)(F)(F)(F)F)F)F</chem>
405	33354-65-3	<i>N,N</i> -dimethyl-4-[2-[4-[(triphenylphosphoranylidene)amino]phenyl]diazeny]-benzenamine	9.35	500.21	ESI+	<chem>CN(C)c1ccc(N=Nc2ccc(N=P(c3cccc3)(c3cccc3)cc2)cc1</chem>
406	33341-94-5	4-[2-(4-nitrophenyl)diazeny]- <i>N</i> -(triphenylphosphoranylidene)-benzenamine	9.65	502.16	ESI+	<chem>O=[N+]([O-])c1ccc(N=Nc2ccc(N=P(c3cccc3)(c3cccc3)cc2)cc1</chem>
407	81-24-3	taurocholic acid	-1.38	515.29	ESI+/ESI-	<chem>C[C@H](CCC(=O)NCC[S](O)(=O)O)[C@H]1CC[C@H]2[C@@H]3[C@H](O)[C@H]4[C@@H]1O)CC[C@]4(C)[C@H]3C[C@H](O)[C@]12C</chem>
408	173584-44-6	indoxacarb	6.21	527.07	ESI+	<chem>COC(=O)N(C(=O)N)CO[C@]2(Cc3cc(Cl)ccc3C2=N)C(=O)OC)s4ccc(OC(F)F)cc4</chem>
409	79156-75-5	ketoconazole	-0.24	530.15	ESI+	<chem>CC(=O)N1CCN(CC1)C2=CC=C(C=C2)OCC3COC(O3)CN4C=CN=C4)C5=C(C=C(C=C5)Cl)C1</chem>
410	91608-15-0	[2,4,6-(MeO) ₃ C ₆ H ₂] ₃ P	6.45	532.19	ESI+	<chem>COc1cc(OC)cc(OC)c1P(c1c(OC)cc(OC)cc1OC)c1c(ccc1OC)OC</chem>
411	417706-58-2	2-Cl-C ₆ H ₄ -P ₃ (pyrr)	-3.29	551.28	ESI+	<chem>Clc1cccc1N=P(N1CCCC1)(N1CCCC1)N1CCCC1)N1CCCC1)N1CCCC1</chem>

#	CAS	Name	log ^p ¹⁵²	molar mass	ESI mode	SMILES
412	1263293-53-3	2-hydroxy-1,3,5-tris(2,2,2-trifluoroethyl)-1,3,5-benzenetrisulfonic acid ester	1.65	579.92	ESI-	O=S(Cl=C(O)C(S(=O)(OCC(F)(F)F)=O)=CC(S(=O)(OCC(F)(F)F)=O)=Cl)(OCC(F)(F)F)=O
413	2667-02-9	Phe-Phe-Phe-Phe	3.42	606.28	ESI+	NC(Cc1cccc1)C(=O)NC(Cc1cccc1)C(=O)NC(Cc1cccc1)C(=O)NC(Cc1cccc1)C(=O)O
414	50-55-5	reserpine	3.99	608.27	ESI+	CO[C@H]1[C@@H](C[C@@H]2CN3CCc4c([nH]c5cc(OC)c6cc45)[C@H]3C[C@@H]2[C@@H]1C(=O)OC)C(=O)c6cc(OC)c(OC)c(OC)c6
415	1951-25-3	amidaron	1.81	645.02	ESI+	CCCCC1=C(C2=CC=CC=C2O1)C(=O)C3=CC(=C(C(=C3))OCCN(CC)CC)I
416	1263293-54-4	2-hydroxy-, 1,3,5-tris(2,2,3,3-tetrafluoro-propyl) 1,3,5-benzenetrisulfonic acid ester	1.64	675.94	ESI-	O=S(Cl=C(O)C(S(=O)(OCC(F)(C(F)F)F)=O)=C(C(S(=O)(OCC(F)(C(F)F)F)=O)=Cl)(OCC(F)(C(F)F)F)=O
417	176298-44-5	1,4-bis(dihydroquinidine)anthraquinone	3.48	858.44	ESI+	CCC1CN2CCC1CC2C(OC1C=CC(OC(c2ccnc3cc(OC)c32)C2CC3CCN2CC3CC)C2=C1C(=O)c1cccc1C2=O)c1ccnc2cccc(OC)cc21
418	874220-62-9	4-MeO-C ₆ H ₄ -P ₄ (pyrr)	-9.59	917.55	ESI+	COc1ccc(cc1)N=[P](N=[P](N2CCCC2)N3CCC(C3)N4CCCC4)(N=[P](N5CCCC5)(N6CCCCC6)N7CCCC7)N=[P](N8CCCC8)(N9CCCC9)N%10CCCC%10
419	874220-63-0	4-Br-C ₆ H ₄ -P ₄ (pyrr)	-8.83	965.45	ESI+	Brc1ccc(cc1)N=[P](N=[P](N2CCCC2)N3CCCC3)N4CCCC4)(N=[P](N5CCCC5)(N6CCCCC6)N7CCCC7)N=[P](N8CCCC8)(N9CCCC9)N%10CCCC%10
420	153136-13-1	<i>t</i> -Bu-P ₅ (pyrr)	-13.58	1052.68	ESI+	CC(C)C(N=[P](N=[P](N=[P](N1CCCC1)N2CCCC2)N3CCCC3)(N4CCCC4)N5CCCC5)(N=[P](N6CCCC6)(N7CCCC7)N8CCCC8)N=[P](N9CCCC9)(N%10CCCC%10)N%11CCCC%11

Table S 3 For model development studied eluent compositions in ESI positive mode (* -measurements carried out during this study).

Organic modifier percentage	Organic modifier	water phase percentage	Additive	additive concentration (mM)	pH(aq)	Number of unique compounds	Ref.
100	Methanol	0	formic acid	27.0	2.7	35	* ¹⁰⁶
100	Methanol	0	trifluoroacetic acid	5.0	3.6	11	¹⁰⁶
100	Methanol	0	oxalic acid	5.0	4.1	11	¹⁰⁶
100	Methanol	0	oxalic acid	1.0	5.4	11	¹⁰⁶
100	Methanol	0	formic acid	5.0	5.4	11	¹⁰⁶
100	Methanol	0	formic acid	1.0	5.9	11	¹⁰⁶
100	Methanol	0	formic acid	5.0	6.1	11	¹⁰⁶
			ammonium acetate				
100	Methanol	0	formic acid	5.0	6.3	11	¹⁰⁶
			ammonium acetate				
100	Methanol	0	acetic acid	5.0	6.5	11	¹⁰⁶
100	Methanol	0	formic acid	0.1	6.6	11	¹⁰⁶
100	Methanol	0	formic acid	5.0	7.6	11	¹⁰⁶
			ammonium acetate				
100	Methanol	0	formic acid	5.0	8.4	11	¹⁰⁶
			ammonium acetate				
100	Methanol	0	ammonium formate	5.0	9.4	11	¹⁰⁶
100	Methanol	0	ammonium acetate	5.0	10.1	11	¹⁰⁶
100	Methanol	0	ammonia	5.0	12.2	11	¹⁰⁶
90	Methanol	10	oxalic acid	1.0	2.1	20	¹¹⁹
90	Methanol	10	formic acid	3.0	2.7	20	¹¹⁹
90	Methanol	10	formic acid	1.0	2.9	20	¹¹⁹
90	Methanol	10	propionic acid	1.0	3.4	20	¹¹⁹
80	Methanol	20	formic acid	27.0	2.7	89	*
50	Methanol	50	trifluoroacetic acid	10.0	2.0	40	*
50	Methanol	50	formic acid	27.0	2.7	40	*
50	Methanol	50	ammonium fluoride	10.0	5.5	40	*

Organic modifier percentage	Organic modifier	water phase percentage	Additive	additive concentration (mM)	pH(aq)	Number of unique compounds	Ref.
50	Methanol	50	ammonium acetate	10.0	6.8	40	*
50	Methanol	50	ammonium formate	10.0	6.8	40	*
50	Methanol	50	ammonium bicarbonate	10.0	7.8	40	*
50	Methanol	50	ammonia	52.0	10.7	36	*
20	Methanol	80	formic acid	27.0	2.7	40	*
100	Acetonitrile	0	formic acid	27.0	2.7	35	*
90	Acetonitrile	10	oxalic acid	1.0	2.1	20	119
90	Acetonitrile	10	formic acid	1.0	2.9	20	119
90	Acetonitrile	10	propionic acid	1.0	3.4	20	119
80	Acetonitrile	20	trifluoroacetic acid	3.0	1.9	65	86
80	Acetonitrile	20	oxalic acid	1.0	2.1	17	12
80	Acetonitrile	20	formic acid	5.0	2.7	352	*10,116,118,119,133,134
80	Acetonitrile	20	ammonium acetate	1.0	3.0	20	86
80	Acetonitrile	20	acetic acid	3.0	3.2	17	12
80	Acetonitrile	20	ammonium acetate	1.0	3.5	20	86
80	Acetonitrile	20	ammonium acetate	1.0	4.0	20	86
80	Acetonitrile	20	ammonium acetate	1.0	4.5	19	86
80	Acetonitrile	20	ammonium acetate	1.0	5.0	26	86,116
80	Acetonitrile	20	ammonium acetate	1.0	5.5	20	86
80	Acetonitrile	20	—	—	—	16	117
80	Acetonitrile	20	ammonium acetate	1.0	6.0	20	86
80	Acetonitrile	20	ammonium acetate	1.0	6.5	20	86
80	Acetonitrile	20	ammonium acetate	1.0	6.7	15	86
80	Acetonitrile	20	ammonium acetate	1.0	7.0	46	86
80	Acetonitrile	20	methylamine	0.0	7.9	14	12
80	Acetonitrile	20	ammonia	0.2	9.8	10	116
80	Acetonitrile	20	ammonia	10.0	10.7	36	116

Organic modifier percentage	Organic modifier	water phase percentage	Additive	additive concentration (mM)	pH(aq)	Number of unique compounds	Ref.
50	Acetonitrile	50	trifluoroacetic acid	10.0	2.0	40	*
50	Acetonitrile	50	formic acid	27.0	2.7	45	* ¹¹⁶
50	Acetonitrile	50	ammonium acetate	2.5	5.0	10	¹¹⁶
50	Acetonitrile	50	ammonium fluoride	10.0	5.5	40	*
50	Acetonitrile	50	ammonium acetate	10.0	6.8	40	*
50	Acetonitrile	50	ammonium formate	10.0	6.8	40	*
50	Acetonitrile	50	ammonium bicarbonate	10.0	7.8	40	*
50	Acetonitrile	50	ammonia	0.5	9.8	10	¹¹⁶
50	Acetonitrile	50	ammonia	52.0	10.7	50	*
20	Acetonitrile	80	trifluoroacetic acid	10.0	1.9	28	⁸⁶
20	Acetonitrile	80	formic acid	27.0	2.7	60	* ¹¹⁶
20	Acetonitrile	80	ammonium acetate	4.0	3.0	17	⁸⁶
20	Acetonitrile	80	ammonium acetate	4.0	3.5	21	⁸⁶
20	Acetonitrile	80	ammonium acetate	4.0	4.0	20	⁸⁶
20	Acetonitrile	80	ammonium acetate	4.0	4.5	19	⁸⁶
20	Acetonitrile	80	ammonium acetate	4.0	5.0	20	⁸⁶
20	Acetonitrile	80	ammonium acetate	4.0	5.5	19	⁸⁶
20	Acetonitrile	80	ammonium acetate	4.0	6.0	20	⁸⁶
20	Acetonitrile	80	ammonium acetate	4.0	6.5	25	⁸⁶
20	Acetonitrile	80	ammonium acetate	4.0	7.0	19	⁸⁶
90	Isopropanol	10	oxalic acid	1.0	2.1	20	¹¹⁹
90	Isopropanol	10	formic acid	1.0	2.9	18	¹¹⁹
90	Isopropanol	10	propionic acid	1.0	3.4	14	¹¹⁹
90	Acetone	10	oxalic acid	1.0	2.1	19	¹¹⁹
90	Acetone	10	formic acid	1.0	2.9	19	¹¹⁹
90	Acetone	10	propionic acid	1.0	3.4	20	¹¹⁹
0	—	100	oxalic acid	50.0	1.4	11	¹⁰⁶

Organic modifier percentage	Organic modifier	water phase percentage	Additive	additive concentration (mM)	pH(aq)	Number of unique compounds	Ref.
0	-	100	oxalic acid	5.0	2.1	11	¹⁰⁶
0	-	100	trifluoroacetic acid	5.0	2.4	11	¹⁰⁶
0	-	100	citric acid	5.0	2.5	11	¹⁰⁶
0	-	100	formic acid	27.0	2.7	39	* ¹⁰⁶
0	-	100	oxalic acid	1.0	2.8	11	¹⁰⁶
0	-	100	formic acid	5.0	2.8	11	¹⁰⁶
0	-	100	formic acid ammonium acetate	5.0	3.0	11	¹⁰⁶
0	-	100	formic acid. ammonium formate	5.0	3.0	11	¹⁰⁶
0	-	100	formic acid	1.0	3.1	11	¹⁰⁶
0	-	100	acetic acid	5.0	3.2	11	¹⁰⁶
0	-	100	formic acid ammonium acetate	5.0	3.3	11	¹⁰⁶
0	-	100	formic acid ammonium acetate	5.0	3.5	11	¹⁰⁶
0	-	100	formic acid ammonium acetate	0.1	3.7	11	¹⁰⁶
0	-	100	formic acid ammonium acetate	5.0	4.0	11	¹⁰⁶
0	-	100	formic acid. ammonium formate	5.0	4.0	11	¹⁰⁶
0	-	100	formic acid ammonium acetate	5.0	5.0	11	¹⁰⁶
0	-	100	formic acid ammonium acetate	5.0	5.0	11	¹⁰⁶
0	-	100	formic acid ammonium formate	5.0	5.5	11	¹⁰⁶
0	-	100	formic acid ammonium acetate	5.0	5.9	11	¹⁰⁶

Organic modifier percentage	Organic modifier	water phase percentage	Additive	additive concentration (mM)	pH(aq)	Number of unique compounds	Ref.
0	-	100	formic acid ammonium formate	5.0	5.9	11	¹⁰⁶
0	-	100	ammonium acetate	1.0	6.1	11	¹⁰⁶
0	-	100	ammonium acetate	5.0	6.7	11	¹⁰⁶
0	-	100	ammonium acetate	10.0	6.8	11	¹⁰⁶
0	-	100	methylamine	1.0	7.9	9	¹⁰⁶
0	-	100	ammonia ammonium acetate	5.0	8.1	11	¹⁰⁶
0	-	100	ammonia ammonium acetate	5.0	9.0	11	¹⁰⁶
0	-	100	ammonia	1.0	9.4	11	¹⁰⁶
0	-	100	ammonia	5.0	10.1	11	¹⁰⁶
0	-	100	ammonia	10.0	10.3	11	¹⁰⁶

Table S 4 Compounds used in validation and application studies (* denotes calibrant in green tea study, † denotes previously detected and identified but not quantified metabolites in green tea samples, ‡ two possible isomers may correspond to this compound - quinic acid 4-O-caffeate and neochlorogenic acid).

#	CAS	Name	application	SMILES
P1	88337-96-6	deoxynivalenol-15-acetate	cereal	<chem>CC1=C[C@@H]2[C@]([C@@H]1(C1=O)O)[C@]3[C[C@H]1][C@H]([C@@H]([C@@]34CO4)O2)OC(=O)C</chem>
P2	30614-22-3	pyrimidin-2(1H)-one	cereal	<chem>CC1=C(N=C(N=C1O)N)C(=O)N</chem>
P3	100784-20-1	halosulfuron-methyl	cereal	<chem>CN1C(=C(C(=N1)Cl)C(=O)OC)S(=O)(=O)NC(=O)NC2=NC(=CC(=N2)OC)OC</chem>
P4	2310-17-0	phosalone	cereal	<chem>CCOP(=S)(OC)SCN1C2=C(C=C(C=C2)Cl)OC1=O</chem>
P5	950-35-6	paraoxon-methyl	cereal	<chem>COP(=O)(OC)OC1=CC=C(C=C1)[N+](=O)[O-]</chem>
P6	107-49-3	TEPP	cereal	<chem>CCOP(=O)(OC)OP(=O)(OC)OCC</chem>
P7	31972-43-7	fenamiphos-sulfoxide	cereal	<chem>CCOP(=O)(NC(C)OC)OC1=CC(=C(C=C1)S(=O)C)C</chem>
P8	3761-41-9	fenthion-sulfoxide	cereal	<chem>CC1=C(C=C(=C1)OP(=S)(OC)OC)S(=O)C</chem>
P9	72490-01-8	fenoxycarb	cereal	<chem>CCOC(=O)NCCOC1=CC=C(C=C1)OC2=CC=CC=C2</chem>
P10	57018-04-9	tololofos-methyl	cereal	<chem>CC1=CC(=C(C=C1)Cl)OP(=S)(OC)OC1</chem>
P11	88671-89-0	myclobutanil	cereal	<chem>CCCC(CN1C=NC=N1)(C#N)C2=CC=C(C=C2)Cl</chem>
P12	67129-08-2	metazachlor	cereal	<chem>CC1=C(C(=CC=C1)C)N(CN2C=CC=N2)C(=O)CC1</chem>
P13	61213-25-0	flurochloridone	cereal	<chem>C1C(C(C(=O)N1C2=CC=CC(=C2)C(F)F)Cl)CC1</chem>
P14	42874-03-3	oxyfluorfen	cereal	<chem>CCOC1=C(C=CC(=C1)OC2=C(C=C(C=C2)C(F)F)Cl)[N+](=O)[O-]</chem>
P15	34256-82-1	acetochlor	cereal	<chem>CCC1=CC=CC(=C1N(COCC)C(=O)CC)C</chem>
P16	63284-71-9	nuarimol	cereal	<chem>C1=CC=C(C=C1)C(C2=CC=C(C=C2)F)(C3=CN=CN=C3)O)Cl</chem>
P17	79983-71-4	hexaconazole	cereal	<chem>CCCC(CN1C=NC=N1)C2=C(C=C(C=C2)Cl)Cl)O</chem>
P18	23452-05-3	alternariol-monomethyl ether	cereal	<chem>CC1=CC(=CC2=C1C3=CC(=CC(=C3C(=O)O2)O)OC)O</chem>
P19	55512-33-9	pyridate	cereal	<chem>CCCCCCCSC(=O)O)Cl=CC(=NN=C1C2=CC=CC=C2)Cl</chem>
P20	86-86-2	1-naphthylacetamide	cereal	<chem>C1=CC=C2C(=C1)C=CC=C2CC(=O)N</chem>
P21	175013-18-0	pyraclastrobin	cereal	<chem>COC(=O)N(C1=CC=CC=C1)COC2=NN(C=C2)C3=CC=C(C=C3)Cl)O</chem>
P22	1165-39-5	aflatoxin G1	cereal	<chem>COC1=C2C3=C(C(=O)OCC3)C(=O)OC2=C4C5C=COC5OC4=C1</chem>

#	CAS	Name	application	SMILES
P23	74115-24-5	clofentazine	cereal	<chem>C1=CC=C(C(=C1)C2=NN=C(N=N2)C3=CC=CC=C3C1)Cl</chem>
P24	112281-77-3	tetraconazole	cereal	<chem>C1=CC(=C(C=C1Cl)Cl)C(CN2C=NC=N2)COC(C(F)F)(F)F</chem>
P25	81777-89-1	clomazone	cereal	<chem>CC1(CON(C1=O)CC2=CC=CC=C2Cl)C</chem>
P26	24579-73-5	propamocarb	cereal	<chem>CCOC(=O)NCCCN(C)C</chem>
P27	119168-77-3	tebufenpyrad	cereal	<chem>CCCl=NN(C(=Cl)C(=O)NCC2=CC=C(C(=C2)C(C)C)C</chem>
P28	135410-20-7	acetamiprid	cereal	<chem>CC(=NC#N)N(C)CC1=CN=C(C(=C1)Cl)</chem>
P29	10265-92-6	methamidophos	cereal	<chem>COP(=O)(N)SC</chem>
P30	173584-44-6	indoxacarb	cereal	<chem>COC(=O)[C@]12CC3=C(C1=NN(CO2)C(=O)N(C4=CC=C(C(=C4)O</chem> <chem>C(F)F)C(=O)OC)C=CC(=C3)Cl</chem>
P31	77732-09-3	oxadixyl	cereal	<chem>CC1=C(C(=CC=C1)C)N(C(=O)COC)N2CCOC2=O</chem>
P32	119-12-0	pyridaphenthion	cereal	<chem>CCOP(=S)(OC)OC1=NN(C(=O)C=C1)C2=CC=CC=C2</chem>
P33	470-90-6	chlorfenvinphos	cereal	<chem>CCOP(=O)(OCC)O(C(=Cl)Cl)C1=C(C(=C1)Cl)Cl</chem>
P34	2270-40-8	diacetoxyscirpenol	cereal	<chem>CC1=C[C@@H]2[C@](CC1)(C@)3[C@@H]([C@@H]([C@@H]([C@@</chem> <chem>]34C04)O2)OC(=O)C)COC(=O)C</chem>
P35	1162-65-8	aflatoxin B1	cereal	<chem>COC1=C2C3=C(C(=O)CC3)C(=O)OC2=C4[C@@H]5C=CO[C@@@</chem> <chem>H]5OC4=C1</chem>
M1	331-39-5	caffeic acid	green tea	<chem>OC(=O)C=C/c1ccc(O)c(O)c1</chem>
M2	154-23-4	catechin	green tea	<chem>O[C@@H]1Cc2c(O)cc(O)cc2O[C@@H]1c3ccc(O)c(O)c3</chem>
M3	327-97-9	chlorogenic acid*	green tea	<chem>O[C@@H]1[C@@](O)(C[C@@H](OC(=O)C=C)c2ccc(O)c(O)c2)[C</chem> <chem>@H]1O)C(O)=O</chem>
M4	501-98-4	coumaric acid*	green tea	<chem>C1=CC(=CC=C1/C=C/C(=O)O)O</chem>
M5	17334-50-8	epicatechin	green tea	<chem>O[C@@H]1Cc2c(O)cc(O)cc2O[C@@H]1c3ccc(O)c(O)c3</chem>
M6	863-03-6	epicatechin gallate	green tea	<chem>Oc1cc(O)c2[C@@H](OC(=O)c3cc(O)c(O)c(O)c3)[C@@H](O)c2c1)c4</chem> <chem>ccc(O)c(O)c4</chem>
M7	970-74-1	epigallocatechin*	green tea	<chem>O[C@@H]1Cc2c(O)cc(O)cc2O[C@@H]1c3cc(O)c(O)c(O)c3</chem>
M8	989-51-5	epigallocatechin gallate*	green tea	<chem>C1[C@@H]([C@@H](OC2=CC(=CC(=C21)O)O)C3=CC(=C(C(=C3)O)</chem> <chem>O)OC(=O)C4=CC(=C(C(=C4)O)O)O</chem>
M9	149-91-7	gallic acid	green tea	<chem>OC(=O)c1cc(O)c(O)c(O)c1</chem>
M10	970-73-0	gallocatechin*	green tea	<chem>C1[C@@H]([C@@H](OC2=CC(=CC(=C21)O)O)C3=CC(=C(C(=C3)O)</chem> <chem>O)O)O</chem>

#	CAS	Name	application	SMILES
M11	520-18-3	kaempferol	green tea	<chem>Oc1ccc(cc1)C2=C(O)C(=O)c3c(O)cc(O)cc3O2</chem>
M12	529-44-2	myricetin	green tea	<chem>Oc1cc(O)c2C(=O)C(=C(Oc2c1)c3cc(O)c(O)c3)O</chem>
M13	117-39-5	quercetin	green tea	<chem>Oc1cc(O)c2C(=O)C(=C(Oc2c1)c3ccc(O)c(O)c3)O</chem>
M14	153-18-4	rutin*	green tea	<chem>C[C@@H]1O[C@@H](OC[C@H]2O[C@@H](OC3=C(O)c4cc(O)cc(O)c4C3=O)c5ccc(O)c(O)c5)[C@H](O)[C@@H](O)[C@@H]2O)[C@@H]1O)[C@H](O)[C@H]1O</chem>
M15	77-95-2	quinic acid [†]	green tea	<chem>OC1CC(O)(CC(O)C1O)C(O)=O</chem>
M16	NA [†]	caffeoylquinic acid [†]	green tea	<chem>C1[C@@H](C([C@H](CC1(C(=O)O)O)OC(=O)/C=C/C2=CC(=C(C=C2)O)O)</chem>
M17	83104-87-4	3-O-(3-O-methylgalloyl)epigallocatechin [†]	green tea	<chem>COC1=CC(=CC(=C1O)O)C(=O)O[C@@H]2CC3=C(C=C(C=C3O)[C@@H]2C4=CC(=C(C(=C4)O)O)O)O</chem>
M18	37484-74-5	epicatechin 3,5-digallate [†]	green tea	<chem>C1[C@H]([C@H](OC2=CC(=CC(=C21)OC(=O)C3=CC(=C(C(=C3)O)O)O)C4=CC(=C(C(=C4)O)O)OC(=O)C5=CC(=C(C(=C5)O)O)O)</chem>
M19	520-36-5	apigenin glycoside [†]	green tea	<chem>C1=CC(=CC=C1C2=CC(=O)C3=C(C=C(C=C3O2)O)[C@H]4C([C@@H]([C@@H](C(O4)CO)O)O)O)O</chem>

Table S 5 The positive mode ESI ionization efficiency (\log/E) values and the approximate ionization degrees (α) in solution at different eluents.

	acetoneitrile/ 0.1% formic acid(aq)			acetoneitrile/ (0.1% formic acid(aq))						acetoneitrile/ 5 mM ammonium acetate(aq)			acetoneitrile/1 mM ammonia(aq)				
	80/20 ^c		\log/E	80/20		50/50		20/80		80/20		50/50		80/20		50/50	
	\log/E	α^b		\log/E	α	\log/E	α	\log/E	α	\log/E	α	\log/E	α	\log/E	α	\log/E	α
tetrapropylammonium	4.97	1.00	4.76	1.00	4.62	1.00	4.17	1.00	4.74	1.00	4.56	1.00	4.43	1.00	4.71	1.00	
tetraethylammonium	3.95	1.00	3.95	1.00	3.91	1.00	3.53	1.00	3.95	1.00	3.80	1.00	3.95	1.00	4.01	1.00	
triethylamine	3.53	1.00	3.87	1.00	3.85	1.00	3.18	1.00	3.68	1.00	3.74	1.00	3.29	0.90	3.88	0.90	
1-naphthylamine	4.04	0.95	3.71	0.95	3.61	0.95	3.19	0.95	3.23	0.08	2.30	0.08	2.60	0.00	3.33	0.00	
<i>N,N</i> -dimethylamine	3.72	1.00	3.54	1.00	3.50	1.00	3.16	1.00	2.14	0.56	2.15	0.56	0.31	0.00	1.73	0.00	
diphenyl phthalate	4.10	0.00	3.45	0.00	3.97	0.00	NA ^e	0.00	4.30	0.00	3.97	0.00	3.33	0.00	4.56	0.00	
piperidine	3.16	1.00	3.26	1.00	3.19	1.00	2.70	1.00	3.09	1.00	2.69	1.00	2.63	0.96	3.11	0.96	
pyrrolidine	2.70	1.00	2.99	1.00	2.32	1.00	2.12	1.00	2.30	1.00	2.17	1.00	1.71	0.97	2.72	0.97	
dimethyl phthalate	3.54	0.00	2.95	0.00	3.20	0.00	3.09	0.00	3.39	0.00	2.92	0.00	2.74	0.00	3.90	0.00	
pyridine	2.94	1.00	2.92	1.00	2.23	1.00	2.20	1.00	1.53	0.67	1.22	0.67	-0.82	0.00	0.94	0.00	
<i>pooled standard deviation</i>	<i>0.30</i>		<i>0.32</i>		<i>0.39</i>		<i>0.06</i>		<i>0.28</i>		<i>0.34</i>		<i>0.45</i>		<i>0.39</i>		
pH ^d					2.7					5.0				9.8			

^a \log/E values vs tetraethylammonium; ^b The α is calculated using the aqueous phase pH obtained by glass electrode and aqueous pK_a values; ^c \log/E values in ref¹⁰; ^d aqueous phase pH obtained with glass electrode; ^e Diphenyl phthalate could not be measured in this eluent due to poor solubility.

Table S 6 log/*E* values of studied eluents.

10%	0.1% formic acid(aq)		10 mM formic acid(aq)				10 mM oxalic acid(aq)				10 mM propionic acid(aq)			
	MeCN ^a	MeOH	MeOH	MeCN	acetone	iPrOH	MeOH	MeCN	acetone	iPrOH	MeOH	MeCN	acetone	iPrOH
terfenadine	4.51	4.27	4.45	4.28	3.87	3.60	4.06	4.01	4.06	3.01	4.10	4.12	3.79	3.41
loperamide	4.59	4.40	4.43	4.48	4.26	4.34	4.34	4.29	4.29	4.14	4.26	4.37	4.07	4.13
amitriptyline	3.88	4.15	4.30	4.07	3.87	3.52	3.89	3.99	3.91	3.60	3.88	4.11	3.88	3.33
bupirone	3.78	3.91	4.23	3.95	3.58	3.28	3.58	3.71	3.17	2.72	3.86	4.06	3.73	3.12
propranolol	3.79	3.85	4.21	3.85	3.53	3.04	3.48	3.55	3.39	3.12	3.63	3.62	3.34	2.68
aripiprazole	3.83	3.75	4.12	3.81	3.67	2.65	3.34	3.48	2.80	3.21	3.78	3.61	2.96	1.87
amiodarone	4.10	4.15	4.11	4.10	3.76	3.13	3.76	3.93	3.74	3.27	3.85	4.00	3.45	2.55
haloperidol	3.72	4.01	4.02	3.93	3.52	3.22	3.88	4.01	3.54	3.38	3.77	3.83	3.50	2.71
ketoconazole	3.47	3.88	4.02	3.50	3.63	3.11	3.40	3.70	2.83	2.14	3.80	3.56	3.59	NA
trazodone	3.97	4.00	3.95	3.63	3.45	3.23	3.59	3.68	3.39	2.91	3.67	3.79	3.45	2.71
tetraethylammonium	3.95	3.99	3.88	3.96	3.87	3.85	3.84	3.83	3.58	3.67	3.88	3.91	3.82	3.71
fluoxetine	3.42	3.56	3.72	3.62	3.33	2.62	3.12	3.28	3.30	2.74	3.37	3.48	3.24	2.24
quinidine	3.50	3.62	3.52	3.22	3.14	2.88	2.78	2.44	2.12	2.96	3.47	3.26	3.07	2.73
atenolol	3.30	3.41	3.29	3.17	2.97	2.22	2.54	2.78	2.59	2.10	3.10	2.99	2.78	1.96
lincomycin	3.43	3.45	3.22	2.80	3.15	1.94	2.83	2.68	2.38	1.72	2.89	3.00	2.49	NA
pyridine	2.56	2.33	2.50	2.43	2.32	1.14	2.30	2.80	2.63	1.76	2.25	2.33	2.10	NA
progesterone	2.55	2.67	2.17	1.58	1.91	0.79	2.75	2.70	2.56	2.07	1.81	1.82	1.56	NA
testosterone	2.40	2.66	2.11	1.86	1.87	0.84	2.94	2.81	2.66	1.99	1.93	1.99	1.63	NA
norfloxacin	3.24	3.00	1.87	2.80	2.66	1.45	2.49	2.35	NA	1.65	2.60	2.55	1.96	0.90
caffeine	2.38	2.22	1.85	1.51	1.78	0.43	2.33	2.37	2.27	1.70	1.60	1.76	1.32	NA
<i>pooled standard deviation</i>	0.12	0.10	0.15	0.10	0.11	0.29	0.09	0.11	0.19	0.18	0.09	0.11	0.23	0.15

^a acetonitrile/ 0.1% formic acid(aq) 80/20

Table S 7 The results of *t*-tests on the obtained ionization efficiency scales in different eluents.

	Compared eluents		A statistically significant difference in log/E values
pH change	acetone/nitrile/0.1% formic acid(aq) 80/20	acetone/nitrile/5 mM ammonium acetate (aq) 80/20	1-naphthylamine, <i>N,N</i> -dimethylaniline, pyrrolidine, pyridine, diphenyl phthalate, dimethyl phthalate
	acetone/nitrile/0.1% formic acid(aq) 80/20	acetone/nitrile/1 mM ammonium(aq) 80/20	tetraethylammonium, 1-naphthylamine, <i>N,N</i> -dimethylaniline, pyrrolidine, pyridine
	acetone/nitrile/0.1% formic acid(aq) 50/50	acetone/nitrile/5 mM ammonium acetate (aq) 50/50	1-naphthylamine, <i>N,N</i> -dimethylaniline, piperidine, pyridine
	acetone/nitrile/0.1% formic acid(aq) 50/50	acetone/nitrile/1 mM ammonium(aq) 50/50	<i>N,N</i> -dimethylaniline, pyridine, pyrrolidine, dimethyl phthalate, diphenyl phthalate
	acetone/nitrile/5 mM ammonium acetate (aq) 80/20	acetone/nitrile/1 mM ammonium(aq) 80/20	Diphenyl phthalate, <i>N,N</i> -dimethylaniline, pyridine
	acetone/nitrile/5 mM ammonium acetate (aq) 50/50	acetone/nitrile/1 mM ammonium(aq) 50/50	<i>N,N</i> -dimethylaniline, diphenyl phthalate, 1-naphthylamine, dimethyl phthalate, piperidine, pyrrolidine
	acetone/nitrile/0.1% formic acid(aq) 80/20	acetone/nitrile/0.1% formic acid(aq) 50/50	Diphenyl phthalate, pyrrolidine, pyridine
	acetone/nitrile/0.1% formic acid(aq) 80/20	acetone/nitrile/0.1% formic acid(aq) 20/80	tetrapropylammonium, tetraethylammonium, triethylamine, 1-naphthylamine, <i>N,N</i> -dimethylaniline, pyridine, pyrrolidine, piperidine
Change of organic modifier percentage	acetone/nitrile/0.1% formic acid(aq) 50/50	acetone/nitrile/0.1% formic acid(aq) 20/80	tetrapropylammonium, tetraethylammonium, triethylamine, 1-naphthylamine, piperidine
	acetone/nitrile/5 mM ammonium acetate (aq) 80/20	acetone/nitrile/5 mM ammonium acetate (aq) 50/50	Diphenyl phthalate, 1-naphthylamine, dimethyl phthalate, piperidine, pyridine
	acetone/nitrile/1 mM ammonium(aq) 80/20	acetone/nitrile/1 mM ammonium(aq) 50/50	Diphenyl phthalate, dimethyl phthalate, pyrrolidine, pyridine, <i>N,N</i> -dimethylaniline

Table S 8 The ionization efficiency values of analytes in both eluent composition with two different water phases: pH = 2.1 and pH = 7.0. Grey background indicates analyte's water phase pH dependence.

pH	Acetonitrile/buffer 80/20													Acetonitrile/buffer 20/80												
	log I/E													log I/E												
	2.1	2.7	3.0	3.5	4.0	4.5	5.0	5.5	6.0	6.5	7	2.1	2.7	3.0	3.5	4.0	4.5	5.0	5.5	6.0	6.5	7.0				
2,6-(NO ₂) ₂ -C ₆ H ₃ -P(pyrr)	5.07	4.90	4.81	5.00	4.91	4.79	4.66	4.83	4.70	5.38	5.01	4.29	NA ^a	NA ^a	4.39	4.29	4.44	4.42	NA ^a	4.64	NA ^a	4.45				
<i>N,N</i> -diphenylbispidine	4.42	4.59	4.41	4.59	4.50	4.49	4.39	4.47	4.36	4.95	4.63	3.80	NA ^a	NA ^a	4.01	3.97	NA ^a	4.11	NA ^a	4.11	NA ^a	3.89				
acridine	3.99	3.91	3.76	3.84	3.96	3.56	3.66	3.77	3.71	4.16	3.96	3.57	3.92	3.07	3.26	2.98	2.75	2.77	2.93	2.86	3.11	2.49				
3-methoxy- <i>N,N</i> -dimethylamine	3.72	3.83	2.97	2.90	2.99	2.67	2.42	2.43	2.47	2.47	2.49	3.29	3.66	1.96	1.90	1.95	1.97	1.88	2.11	1.94	2.03	1.67				
4-dimethylamino- <i>N,N</i> -dimethylamine	3.61	NA ^a	3.47	3.24	NA ^a	NA ^a	NA ^a	NA ^a	NA ^a	NA ^a	NA ^a	NA ^a	2.99	2.97												
<i>N,N</i> -dimethylamine	3.53	3.43	1.94	1.64	1.61	1.54	1.51	1.61	1.61	1.43	1.60	3.22	3.15	1.23	1.20	1.46	1.50	1.28	1.54	1.58	1.69	1.13				
8-aminoquinoline	3.53	3.42	2.96	3.24	3.20	3.12	3.09	3.25	3.10	2.62	3.25	2.98	3.47	2.09	2.31	2.23	2.14	2.36	2.22	2.33	2.07					
quinoline	3.44	3.59	2.75	2.75	2.81	2.66	2.40	2.41	2.44	2.39	2.40	2.96	3.47	1.73	1.76	1.74	1.78	1.75	2.02	1.85	1.89	1.59				
2,6-dimethylpyridine	3.39	3.31	2.62	2.62	2.67	2.42	2.32	2.25	2.26	2.03	2.13	2.86	3.17	1.72	1.71	1.68	1.62	1.48	1.78	1.61	1.78	1.45				
2-aminoimidazole	3.39	3.55	3.24	3.40	3.47	3.16	3.37	3.33	3.23	3.05	3.21	2.81	NA ^a	NA ^a	3.01	2.82	3.02	2.95	3.18	3.08	NA ^a	2.91				
1-naphthylamine	3.28	3.60	2.74	2.65	2.67	2.55	2.43	2.54	2.56	2.45	2.64	2.68	3.44	1.35	1.46	1.34	1.61	1.58	1.81	1.62	1.88	1.56				
4-amino- <i>N,N</i> -dimethylamine	3.24	NA ^a	2.96	2.41	NA ^a	NA ^a	NA ^a	NA ^a	NA ^a	NA ^a	NA ^a	NA ^a	2.77	2.53												
2,6-diaminopyridine	3.05	NA ^a	2.85	2.77	2.71	NA ^a	NA ^a	NA ^a	NA ^a	NA ^a	NA ^a	NA ^a	2.53	2.41												
2-aminopyridine	2.99	NA ^a	2.64	2.62	NA ^a	NA ^a	NA ^a	NA ^a	NA ^a	NA ^a	NA ^a	NA ^a	2.35	2.14												
aniline	2.91	3.20	2.07	1.81	1.52	0.90	0.59	0.48	0.69	0.54	0.71	2.59	3.09	0.97	0.73	0.48	0.44	0.49	0.73	0.61	0.85	0.39				
2-aminophenol	2.71	3.13	2.22	2.30	2.37	2.13	2.09	2.13	2.24	2.44	2.11	1.94	2.83	1.50	1.73	1.80	1.90	1.75	1.89	1.70	1.63	1.28				
3-hydroxypyridine	2.72	NA ^a	2.43	2.50	NA ^a	NA ^a	NA ^a	NA ^a	NA ^a	NA ^a	NA ^a	NA ^a	2.19	1.96												
3-nitroaniline	2.66	2.75	1.03	0.62	0.58	0.31	0.06	0.15	0.32	0.71	0.36	1.90	2.37	-0.31	-0.46	-0.49	-0.24	-0.25	-0.10	-0.30	0.07	-0.70				
pyridine	2.55	2.61	1.60	1.38	1.03	0.75	0.80	0.84	0.93	0.72	0.82	2.16	2.55	0.74	0.74	0.78	0.92	0.64	1.07	0.82	1.09	0.61				
3-aminobenzoic acid	2.49	3.19	1.82	1.60	1.66	0.89	1.42	1.32	1.48	1.20	1.53	1.75	2.57	0.77	1.05	1.09	1.41	0.85	1.11	1.16	1.25	0.84				
4-aminobenzoic acid	2.47	2.73	1.62	1.83	1.93	1.41	1.44	1.54	1.55	1.50	1.52	1.61	2.40	1.13	1.41	1.38	1.75	1.10	1.28	1.34	1.23	0.90				
<i>n</i> -aminophenol	2.45	NA ^a	2.13	1.99	NA ^a	NA ^a	NA ^a	NA ^a	NA ^a	NA ^a	NA ^a	NA ^a	1.64	2.34												
3-dimethylaminobenzoic acid	2.43	NA ^a	2.46	2.84	NA ^a	NA ^a	NA ^a	NA ^a	NA ^a	NA ^a	NA ^a	NA ^a	2.46	2.19												
4-nitroaniline	2.38	2.20	NA ^a	2.35	1.93	1.93	NA ^a	NA ^a	NA ^a	NA ^a	NA ^a	NA ^a	NA ^a	NA ^a	1.86											
trizma base	2.32	2.35	NA ^a	1.95	2.33	2.16	NA ^a	1.36	1.49	NA ^a	1.43	NA ^a	NA ^a	1.78	0.00											
2-nitroaniline	2.28	1.79	1.33	1.56	1.86	1.28	1.48	1.69	1.73	1.64	1.71	1.57	1.85	0.48	0.61	0.65	0.97	0.72	1.11	0.94	0.90	0.47				
2,4-dinitroaniline	1.18	0.47	-0.62	-0.03	-0.65	-1.22	-1.30	-0.79	-0.46	0.08	0.00	-1.15	-1.20	-1.01	-0.77	NA ^b										
2,4,6-trinitroaniline	1.06	NA ^a	0.75	NA ^b	NA ^b	NA ^b	NA ^b	NA ^b	NA ^b	NA ^b	NA ^b	NA ^b	NA ^b	NA ^b												

^a not measured, because measurements in pH 2.1 and 7.0 did not reveal any change in log I/E .

^b not possible to measure

Table S 10 The results of bilateral comparison *t*-tests on the ionization efficiency scales obtained on different mass spectrometers with different ESI setups and linear analysis results from scales comparison. Slope and intercept are obtained so that \log/E values from 1. ESI setup is on the x-axis and \log/E values from the 2. setup are on the y-axis.

1.	2.	Statistical differences	average difference	residuals standard deviation	Slope	Intercept	R^2
XCT	Q	-	0.27	0.30	0.98 ± 0.03	0	0.99
XCT	3Q-Varian	Phe-Phe-Phe-Phe, 2,6-(NO ₂) ₂ -C ₆ H ₃ -P(pyrr), tetrapropylammonium, glycine	0.38	0.29	$0.57 \pm 0.07^*$	$1.33 \pm 0.26^*$	0.82
XCT	XCT-3R	-	0.27	0.21	$1.12 \pm 0.05^*$	$-0.58 \pm 0.19^*$	0.97
XCT	3Q-6495	Phe-Phe-Phe-Phe, 2,6-(NO ₂) ₂ -C ₆ H ₃ -P(pyrr), tetrapropylammonium	0.33	0.55	$0.83 \pm 0.04^*$	0.00	0.98
Q	3Q-Varian	tetrapropylammonium, <i>N,N</i> -dimethylalanine	0.23	0.22	$0.58 \pm 0.13^*$	$1.46 \pm 0.45^*$	0.71
Q	XCT-3R	-	0.39	0.49	0.96 ± 0.03	0.00	0.99
Q	3Q-6495	tetrapropylammonium, dimethyl phthalate	0.38	0.40	$1.67 \pm 0.2^*$	$-2.21 \pm 0.65^*$	0.99
3Q-Varian	3Q-6495	Phe-Phe-Phe-Phe, dimethyl phthalate	0.34	0.35	0.93 ± 0.04	0.00	0.99
3Q-Varian	XCT-3R	Phe-Phe-Phe-Phe, 2,6-(NO ₂) ₂ -C ₆ H ₃ -P(pyrr)	0.57	0.49	$0.93 \pm 0.03^*$	0.00	0.85
XCT-3R	3Q-6495	Phe-Phe-Phe-Phe, 2,6-(NO ₂) ₂ -C ₆ H ₃ -P(pyrr), dimethyl phthalate	0.55	0.55	$0.85 \pm 0.04^*$	0.00	0.97
XCT	Q	all except piperidine	0.29	0.24	$0.59 \pm 0.14^*$	$1.32 \pm 0.44^*$	0.73
XCT	3Q	all except tetraethylammonium and triethylamine	0.38	0.24	$0.43 \pm 0.13^*$	$1.85 \pm 0.43^*$	0.64
Q	3Q	tetrapropylammonium, triethylamine	0.20	0.22	0.66 ± 0.18	1.13 ± 0.58	0.69

Table S 11 The eluent compositions used for model development in ESI negative mode.

Organic modifier percentage	Organic modifier	water phase percentage	Additive	additive concentration (mM)	pH(aq)	Number of unique compounds	Ref.
100	Methanol	0	ammonia	52.0	10.5	17	*
100	Methanol	0	-	-	7.0	17	*
80	Methanol	20	ammonia	10.0	10.5	17	*
80	Methanol	20	-	-	7.0	16	*
60	Methanol	40	ammonia	21.0	10.5	17	*
60	Methanol	40	-	-	7.0	17	*
40	Methanol	60	ammonia	31.0	10.5	17	*
40	Methanol	60	-	-	7.0	17	*
20	Methanol	80	ammonia	41.0	10.5	17	*
20	Methanol	80	-	-	7.0	17	*
0	Methanol	100	-	-	7.0	17	*
100	Acetonitrile	0	ammonia	52.0	10.5	60	38
100	Acetonitrile	0	-	-	7.0	17	38
80	Acetonitrile	20	ammonia	10.0	10.5	101	* 38,87,117,133,135
80	Acetonitrile	20	ammonium acetate	1.0	7.8	59	117
80	Acetonitrile	20	ammonium acetate	1.0	7.0	22	*
80	Acetonitrile	20	-	-	7.0	16	38
80	Acetonitrile	20	ammonium acetate	0.2	5.0	60	117
80	Acetonitrile	20	ammonium acetate	1.0	5.0	62	117
80	Acetonitrile	20	ammonium acetate	1.0	3.5	56	117
80	Acetonitrile	20	formic acid	5.0	2.8	61	117
60	Acetonitrile	40	ammonia	21.0	10.5	17	38
60	Acetonitrile	40	-	-	7.0	17	38
50	Acetonitrile	50	ammonia	26.0	10.5	59	117
40	Acetonitrile	60	ammonia	31.0	10.5	17	38
40	Acetonitrile	60	-	-	7.0	17	38

Organic modifier percentage	Organic modifier	water phase percentage	Additive	additive concentration (mM)	pH(aq)	Number of unique compounds	Ref.
20	Acetonitrile	80	ammonia	41.0	10.5	62	117
20	Acetonitrile	80	–	–	7.0	17	38
20	Acetonitrile	80	ammonium acetate	4.0	5.0	57	117
20	Acetonitrile	80	formic acid	21.0	2.8	49	117
0	–	100	ammonia	52.0	10.5	17	38
0	–	100	ammonia	52.0	10.5	17	38
0	–	100	–	–	7.0	17	38

Table S 12 Compounds to transfer the predicted ionization efficiencies to instrument-specific response factors in the cereals application example.

#	Name
36	4-methoxypyridine
58	indazole
68	4-hydroxybenzaldehyde
85	tetraethylammonium
98	<i>p</i> -anisaldehyde
114	3-methoxycatechol
118	tripropylamine
120	glutamine
125	cinnamic acid
135	3-methoxy- <i>N,N</i> -dimethylaniline
154	4-dimethylamino- <i>N,N</i> -dimethylaniline
158	phthalic acid
183	1,10-phenanthroline
196	tetrapropylammonium
197	2-acetamido-5-nitrothiazole
218	metamitrone
222	isoproturon
243	aldicarb-sulfone
290	alachlor
321	cyanophenphos
322	scopolamine
335	phenthoate
352	thiophanate-methyl
364	tetraconazole
377	4-CF ₃ -C ₆ H ₄ -P(pyrr)
401	4-[2-(4-nitrophenyl)diazenyl]- <i>N</i> -(phenyldi-1-pyrrolidinylphosphoranylidene)benzenamine
402	4-[2-[4-[(diphenyl-1-pyrrolidinylphosphoranylidene)amino]phenyl]diazenyl]- <i>N,N</i> -dimethyl-benzenamine
405	<i>N,N</i> -dimethyl-4-[2-[4-[(triphenylphosphoranylidene)amino]phenyl]diazenyl]-benzenamine
411	2-Cl-C ₆ H ₄ -P ₂ (pyrr)
413	Phe-Phe-Phe-Phe
414	reserpine

Table S 13 Average concentration prediction error in case of different sizes of transformation sets. The difference in performance is not statistically significant.

# of transforming compounds	mean error
6	5.01
10	5.01
15	5.02
31	5.68

Table S 14 Comparison of errors in concentration prediction by the compound in case of pesticides in cereal matrices using three different approaches.

compound	retention time	mean error¹	mean error²	mean error³
methamidophos	0.85	2.30	12.60	8.33
propamocarb	1.23	17.81	2.80	4.34
pirimicarb-desmethyl	1.71	22.63	1142.42	5.37
deoxynivalenol-15-acetate	2.48	12.53	29.69	71.88
acetamiprid	2.79	6.57	2.15	1.51
TEPP	3.10	3.37	1.56	1.71
1-naphthylacetamide	3.14	3.72	1.51	2.86
fenamiphos-sulfoxide	3.15	5.38	2.23	1.28
aflatoxin G1	3.37	3.07	1.48	2.43
diacetoxyscirpenol	3.37	2.92	5.01	11.72
oxadixyl	3.39	2.13	1.35	2.54
paraoxon-methyl	3.43	1.72	1.50	3.33
aflatoxin B1	3.58	4.08	232.94	1.73
fenthion-sulfoxide	3.84	5.19	168.63	1.38
metazachlor	4.34	2.84	320.97	2.10
clomazone	4.45	5.36	169.02	1.53
nuarimol	4.51	2.64	309.76	2.04
alternariol-mono	4.74	8.28	7916.96	51.36
myclobutanil	4.88	6.25	160.12	1.23
halosulfuron-methy	4.93	2.95	283.66	1.85
tetraconazole	5.02	1.17	177.02	1.27
pyridaphenthion	5.03	4.93	135.82	1.26
hexaconazole	5.21	5.67	246.25	1.74
acetochlor	5.28	1.41	897.34	5.86
fenoxycarb	5.28	3.29	437.50	3.00
flurochloridone	5.30	3.36	3718.81	24.48
chlorfenrinphos	5.45	5.81	30.49	2.06
pyraclostrobin	5.84	15.77	5.32	3.66
clofenfezine	5.95	1.52	74.42	4.74
tolclofos-methyl	5.96	3.67	323.54	20.53
phosalone	5.98	2.50	212.02	13.45
indoxacarb	6.05	5.67	14.29	1.24
tebufenpyrad	6.22	4.59	18.62	1.26
oxyfluorfen	6.42	15.30	1285.53	82.52
pyridate	7.49	3.13	49.44	3.33

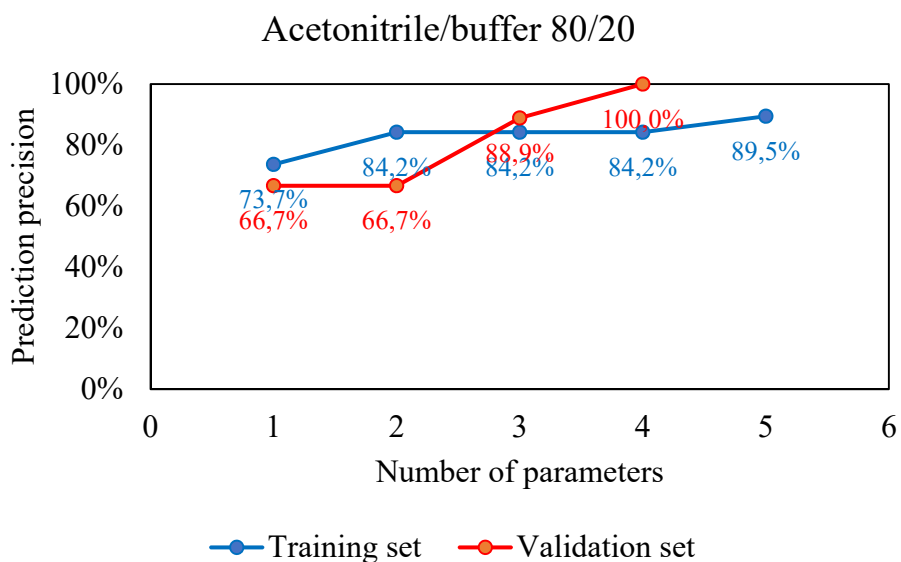


Figure S 1 The prediction precision dependence on a number of used parameters in LDA in case of acetonitrile/buffer 80/20.

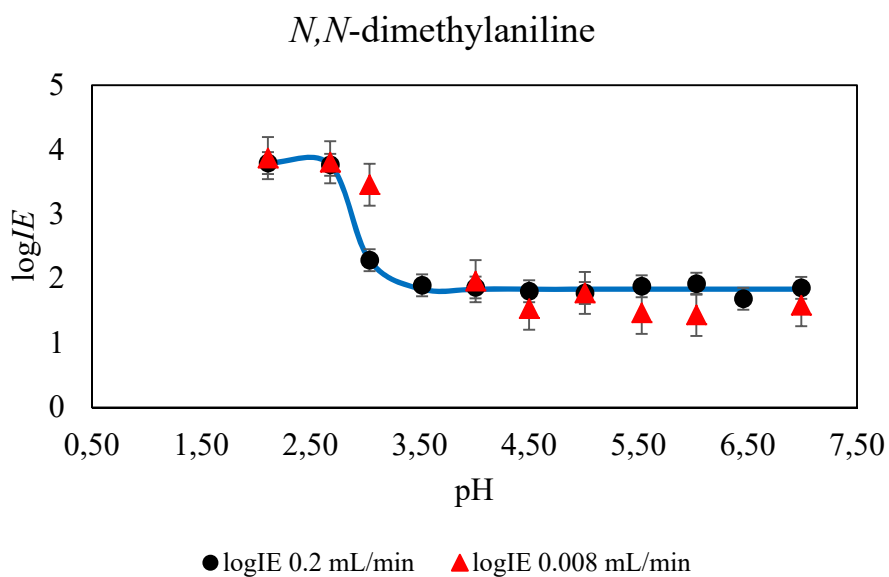


Figure S 2 The $\log I/E$ dependencies on aqueous pH with different flow rates.

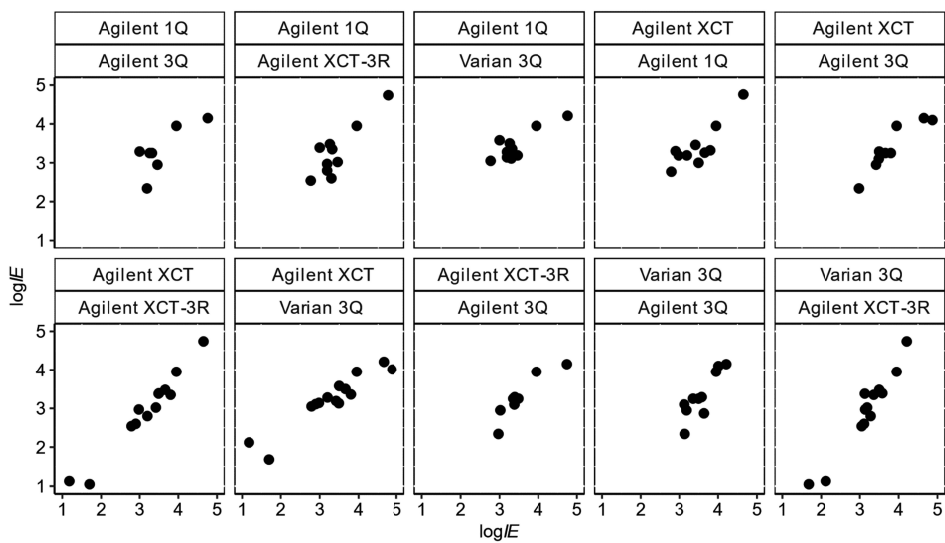


Figure S 3 Comparison of ionization efficiencies measured on different instruments studied in publication II acetonitrile/0.1% formic acid(aq) 80/20.

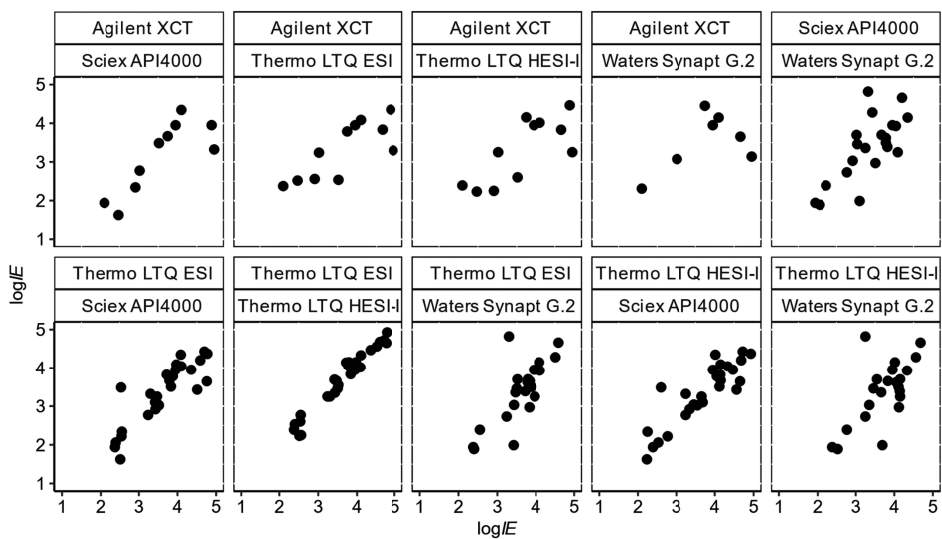
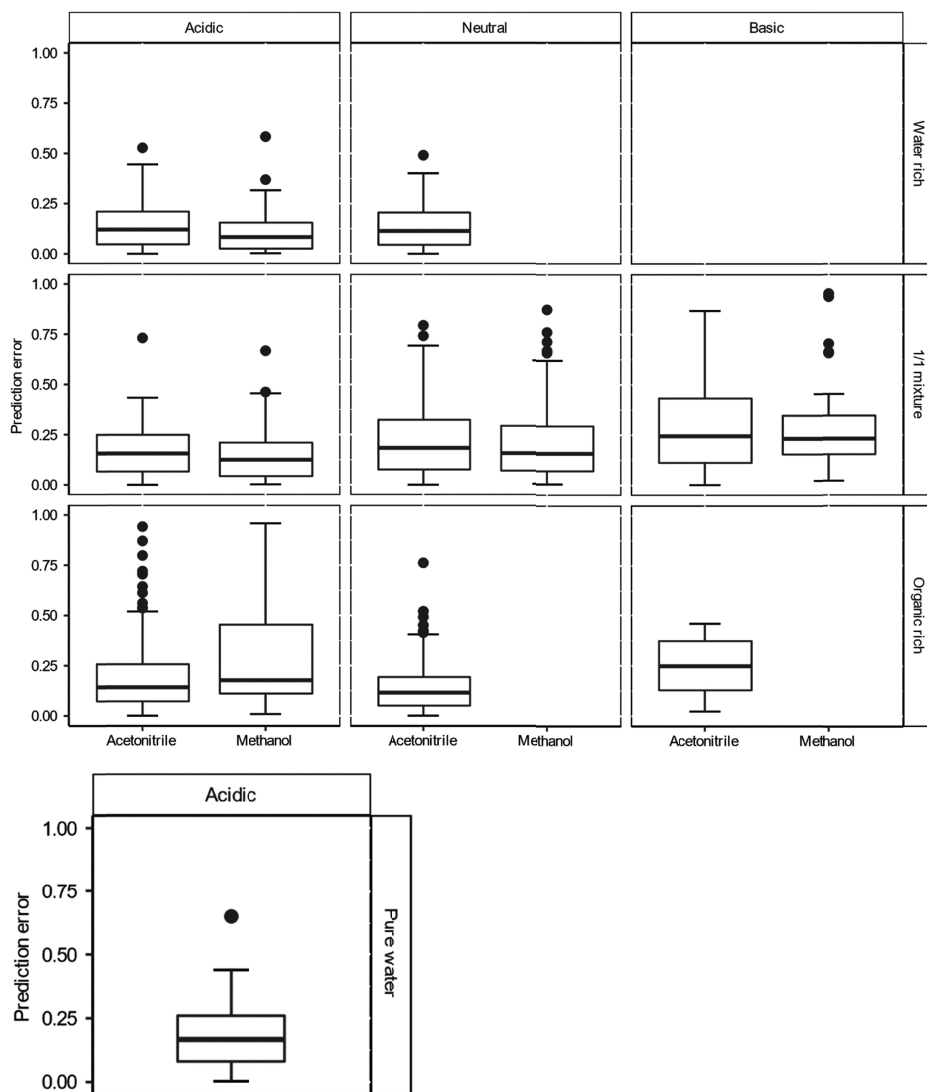
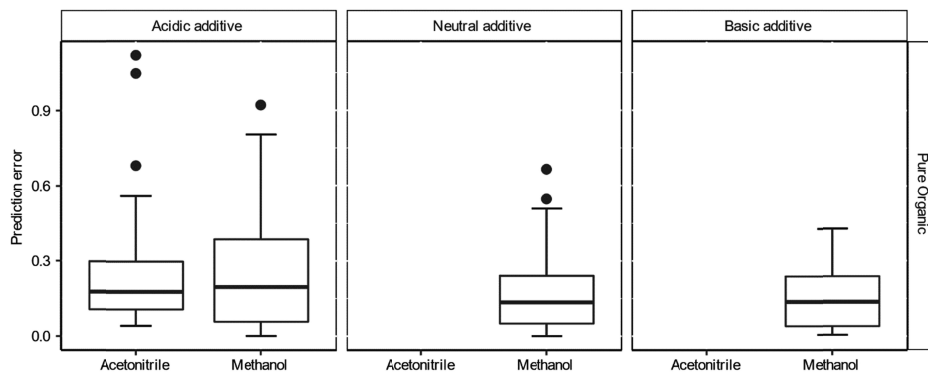


Figure S 4 Comparison of ionization efficiencies measured on different instruments studied in publication IV acetonitrile/0.1% formic acid(aq) 80/20.



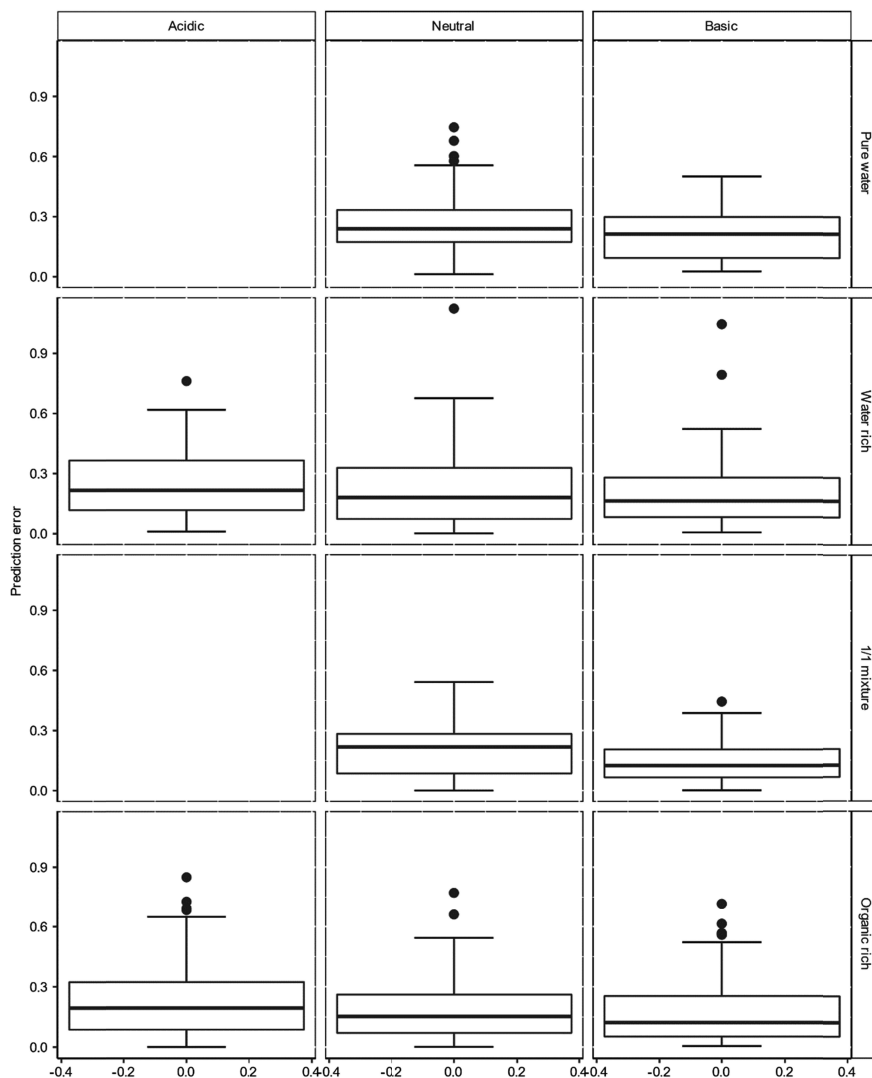
Acidic: $\text{pH} < 5$. **Neutral:** $5 \leq \text{pH} < 8$. **Basic:** $\text{pH} \geq 8$. **Pure water:** organic modifier percentage = 0%. **Water rich:** $0\% < \text{organic modifier percentage} < 40\%$. **1/1 mixture:** $40\% \leq \text{organic modifier percentage} < 60\%$. **Organic rich:** $60\% \leq \text{organic modifier percentage} < 100\%$.

Figure S 5 Comparison of prediction errors ionization efficiencies between acetonitrile and methanol containing eluents in ESI positive mode. Results are divided into groups by water phase pH and organic modifier content. Comparison based on the intersection of compounds measured in methanol as well as in acetonitrile. The compared results are measured on one instrument.



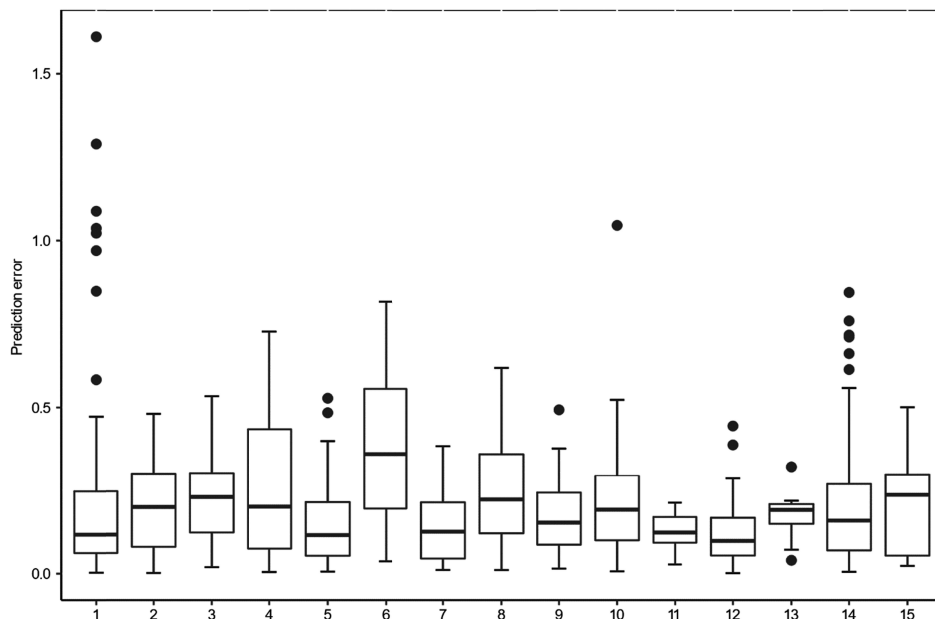
Acidic additive: formic acid, trifluoroacetic acid, oxalic acid, **Neutral additive:** ammonium acetate, ammonium formate, **Basic additive:** ammonia.

Figure S 6 Comparison of the prediction error of ionization efficiencies between neat acetonitrile and methanol in ESI positive mode. Divided into groups by pH adjusting additive type. Comparison is based on the intersection of compounds measured in methanol as well as in acetonitrile. The compared results are measured on one instrument.



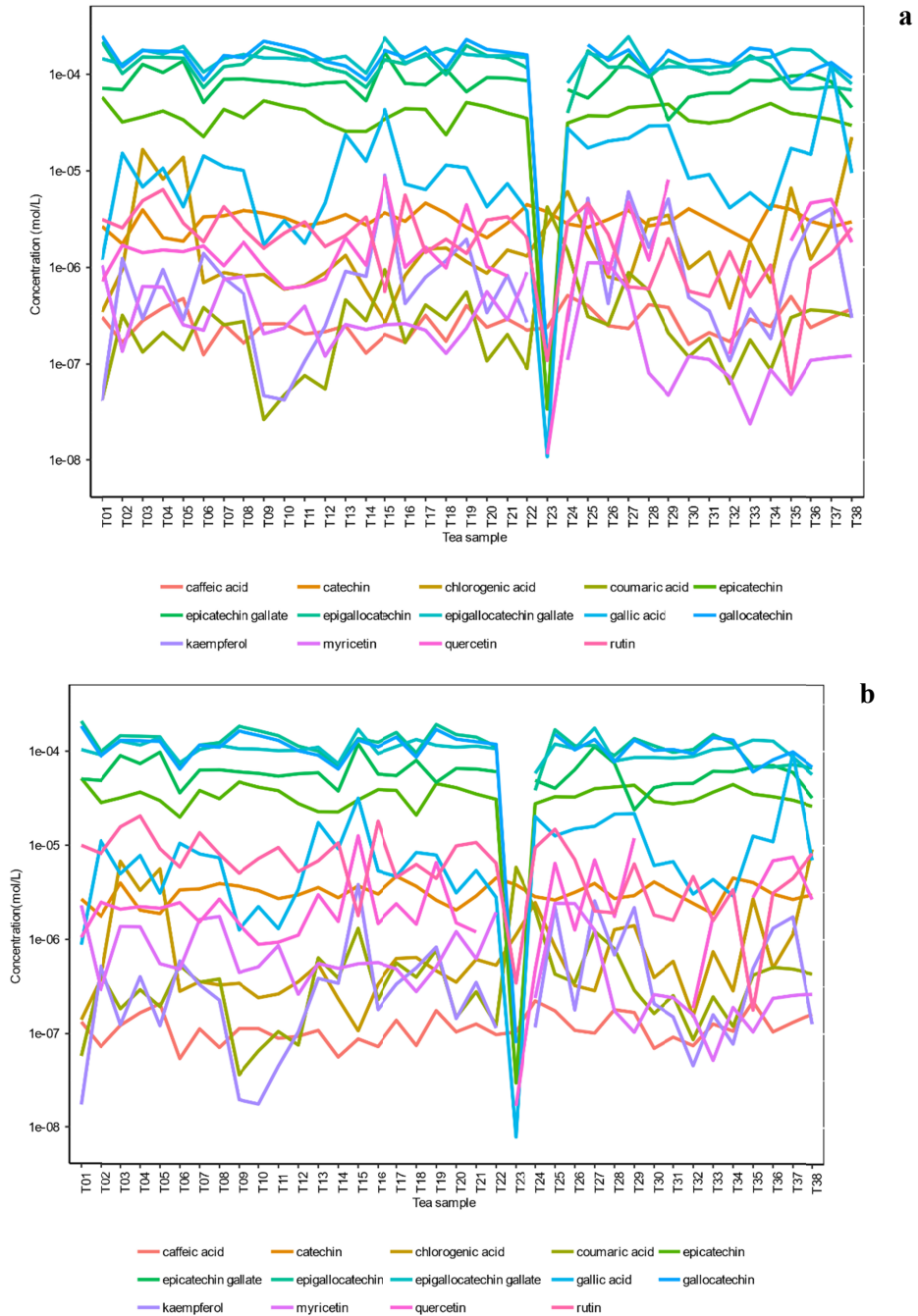
Acidic: $\text{pH} < 5$. **Neutral:** $5 \leq \text{pH} < 8$. **Basic:** $\text{pH} \geq 8$. **Pure water:** organic modifier percentage = 0%. **Water rich:** $0\% < \text{organic modifier percentage} < 40\%$. **1/1 mixture:** $40\% \leq \text{organic modifier percentage} < 60\%$. **Organic rich:** $60\% \leq \text{organic modifier percentage} < 100\%$.

Figure S 7 Comparison of the prediction error of ionization efficiencies in acetonitrile containing solvents in ESI negative mode. Results are divided into groups by water phase pH and organic modifier content. Comparison based on the intersection of compounds measured in all pH groups. The compared results are measured on one instrument.



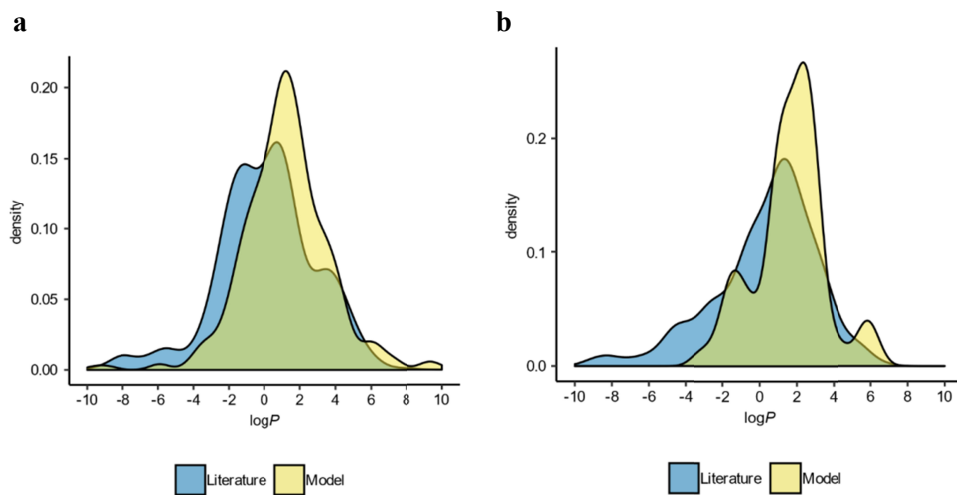
- 1 - acetonitrile 52 mM ammonia.
- 2 - acetonitrile/ water phase 20/80 4 mM ammonium acetate pH(aq) = 5.0
- 3 - acetonitrile/ water phase 80/20 0.2 mM ammonium acetate pH(aq) = 5.0
- 4 - acetonitrile/ water phase 80/20 1 mM ammonium acetate pH(aq) = 3.45
- 5 - acetonitrile/ water phase 80/20 1 mM ammonium acetate pH(aq) = 5.0
- 6 - acetonitrile/ water phase 80/20 1 mM ammonium acetate pH(aq) = 7.0
- 7 - acetonitrile/ water phase 80/20 1 mM ammonium acetate pH(aq) = 7.8
- 8 - acetonitrile/ water phase 20/80 21 mM formic acid pH(aq) = 2.78
- 9 - acetonitrile/ water phase 80/20 5 mM formic acid pH(aq) = 2.78
- 10 - acetonitrile/ water phase 20/80 41 mM ammonia pH(aq) = 10.5
- 11 - acetonitrile/ water phase 40/60 31 mM ammonia pH(aq) = 10.5
- 12 - acetonitrile/ water phase 50/50 26 mM ammonia pH(aq) = 10.5
- 13 - acetonitrile/ water phase 60/40 21 mM ammonia pH(aq) = 10.5
- 14 - acetonitrile/ water phase 80/20 10 mM ammonia pH(aq) = 10.5
- 15 - 52 mM ammonia pH(aq) = 10.5

Figure S 8 Comparison of the prediction error of ionization efficiency between different eluents in ESI negative mode. Compared with the intersection of compounds in studied eluent compositions.



a: concentrations estimated using predicted ionization efficiencies, **b:** concentrations determined with the targeted method.

Figure S 9 Comparison of predicted and measured concentration in the example of metabolites in green tea. T23 is non-green tea negative control.



a: ESI positive mode, **b:** ESI negative mode.

Figure S 10 Comparison of compounds studied previously in the literature (Table S 1) and used for ionization efficiency prediction model development based on calculated $\log P^{152}$ values.

PUBLICATIONS

CURRICULUM VITAE

Name: Jaanus Liigand
Date of birth: February 5, 1990
Citizenship: Estonian
Address: Aardla 140–50, Tartu, 50415, Estonia
Phone, e-mail: +372 53812419, jaanus.liigand@ut.ee

Education:

2018 University of Liege, Prof. Dr Edwin De Pauw research group, ‘Developing a method to differentiate permethylated glycans with α 2,3 linked sialic acid from glycans with α 2,6 linked sialic acid’
2015–present University of Tartu, PhD, ‘Standard substance free quantification for LC/ESI/MS analysis based on the predicted ionization efficiencies’
2013–2014 University of Konstanz, chemistry, exchange student
2013 1st University of Lyon, Rodolphe Antoine group, ‘Optical profiling of electrospray plume with laser-induced-fluorescence’
2012–2015 University of Tartu, M.Sc ‘Electrospray ionisation efficiency scales: mobile phase effects and transferability- cum laude’
2009–2012 University of Tartu, B.Sc ‘Fabrication of nickel oxide gadolinium doped ceria oxide anode for solid oxide fuel cell via tape-casting’ cum laude

List of Publications

1. Liigand, J., de Vries, R., Cuyckens, F. Optimization of flow splitting and make-up flow conditions in liquid chromatography-electrospray ionization-mass spectrometry Rapid. Commun. Mass Spectrum **33**(3), 314–322 (2018)
2. Liigand, P., Liigand, J., Cuyckens, F., Vreeken, R.J., Kruve A. Ionisation efficiencies can be predicted in complicated biological matrices: a proof of concept. Anal. Chim. Acta **1032**, 68–74 (2018)
3. Gornischeff, A., Liigand, J., Rebane, R. A systematic approach toward comparing electrospray ionization efficiencies of derivatized and non-derivatized amino acids and biogenic amines. J. Mass Spectrom. **53**(10), 997–1004 (2018)
4. Ojakivi, M., Liigand, J., Kruve, A. Modifying the Acidity of Charged Droplets. ChemistrySelect **3**(1),12394–12397 (2018)
5. Liigand, P., Kaupmees, K., Haav, K., Liigand, J., Leito, I., Girod, M., Antoine, R., Kruve, A. Think negative: Finding the Best Ionization/MS Mode for Your Analyte. Anal. Chem. **89**, 5665–5668 (2017)

6. Liigand, J., Laaniste, A., Kruve, A. pH effects on Electrospray Ionization Efficiency. *J. Am. Soc. Mass Spectrom.* **28**, 461–469 (2017)
7. Rebane, R., Kruve, A., Liigand, P., Liigand J., Herodes, K., Leito I. Establishing APCI ionization efficiency scale. *Anal. Chem.* **88**(7) 3435–3439 (2016)
8. Liigand, J., Kruve, A., Liigand, P., Laaniste, Asko, Girod, M., Antoine, R., Leito, I. Transferability of the Electrospray Ionization Efficiency Scale between Different Instruments. *J. Am. Soc. Mass Spectrom.* **26**(11), 1923–1930 (2015)
9. Suu, A., Jalukse, L., Liigand, J., Kruve, A., Himmel, D., Krossing, I., Roses, M., Leito, I. Unified pH Values of Liquid Chromatography Mobile Phases. *Anal. Chem.* **87**(5), 2623–2630 (2015)
10. Liigand, J., Kruve, A., Leito, I., Girod, M., Antoine, R. Effect of Mobile Phase on Electrospray Ionization Efficiency. *J. Am. Soc. Mass Spectrom.* **25**(11), 1853–1861 (2014)
11. Kruve, A., Kaupmees, K., Liigand, J., Leito, I. Negative Electrospray Ionization via Deprotonation: Predicting the Ionization Efficiency. *Anal. Chem.* **86**(10), 4822–4830 (2014)
12. Kruve, A., Kaupmees, K., Liigand, J., Oss, M., Leito, I. Sodium adduct formation efficiency in ESI source. *J. Mass Spectrom.* **48**(6), 695–702 (2013)

ELULOOKIRJELDUS

Nimi: Jaanus Liigand
Sünniaeg: 5. veebruar 1990
Kodakondsus: Eesti
Aadress: Aardla 140–50, Tartu, 50415, Estonia
Telefon, e-mail: +372 53812419, jaanus.liigand@ut.ee

Haridus:

- 2018 Liege Ülikool, Prof. Dr. Edwin De Pauw research group, “Developing a method to differentiate permethylated glycans with α 2,3 linked sialic acid from glycans with α 2,6 linked sialic acid”
- 2015–praegu Tartu Ülikool, PhD, “Standard substance free quantification for LC/ESI/MS analysis based on the predicted ionization efficiencies”
- 2013–2014 Konstanzi Ülikool, keemia, vahetusüliõpilane
2013 Lyon 1 Ülikool, Rodolphe Antoine uurimisrühm, “Optical profiling of electrospray plume with laser-induced-fluorescence”
- 2012–2015 Tartu Ülikool, M.Sc “Electrospray ionisation efficiency scales: mobile phase effects and transferability” – cum laude
- 2009–2012 Tartu Ülikool, B.Sc “Tahkeoksiidse kütuseelemendi Ni-GdC anoodi valmistamine *tape* casting meetodil” cum laude

Publikatsioonide loetelu

1. Liigand, J., de Vries, R., Cuyckens, F. Optimization of flow splitting and make-up flow conditions in liquid chromatography-electrospray ionization-mass spectrometry Rapid. Commun. Mass Spectrum **33**(3), 314–322 (2018)
2. Liigand, P., Liigand, J., Cuyckens, F., Vreeken, R.J., Kruve A. Ionisation efficiencies can be predicted in complicated biological matrices: a proof of concept. Anal. Chim. Acta **1032**, 68–74 (2018)
3. Gornischeff, A., Liigand, J., Rebane, R. A systematic approach toward comparing electrospray ionization efficiencies of derivatized and non-derivatized amino acids and biogenic amines. J. Mass Spectrom. **53**(10), 997–1004 (2018)
4. Ojakivi, M., Liigand, J., Kruve, A. Modifying the Acidity of Charged Droplets. ChemistrySelect **3**(1),12394–12397 (2018)
5. Liigand, P., Kaupmees, K., Haav, K., Liigand, J., Leito, I., Girod, M., Antoine, R., Kruve, A. Think negative: Finding the Best Ionization/MS Mode for Your Analyte. Anal. Chem. **89**, 5665–5668 (2017)
6. Liigand, J., Laaniste, A., Kruve, A. pH effects on Electrospray Ionization Efficiency. J. Am. Soc. Mass Spectrom. **28**, 461–469 (2017)

7. Rebane, R., Kruve, A., Liigand, P., Liigand J., Herodes, K., Leito I. Establishing APCI ionization efficiency scale. *Anal. Chem.* **88**(7) 3435–3439 (2016)
8. Liigand, J., Kruve, A., Liigand, P., Laaniste, Asko, Girod, M., Antoine, R., Leito, I. Transferability of the Electrospray Ionization Efficiency Scale between Different Instruments. *J. Am. Soc. Mass Spectrom.* **26**(11), 1923–1930 (2015)
9. Suu, A., Jalukse, L., Liigand, J., Kruve, A., Himmel, D., Krossing, I., Roses, M., Leito, I. Unified pH Values of Liquid Chromatography Mobile Phases. *Anal. Chem.* **87**(5), 2623–2630 (2015)
10. Liigand, J., Kruve, A., Leito, I., Girod, M., Antoine, R. Effect of Mobile Phase on Electrospray Ionization Efficiency. *J. Am. Soc. Mass Spectrom.* **25**(11), 1853–1861 (2014)
11. Kruve, A., Kaupmees, K., Liigand, J., Leito, I. Negative Electrospray Ionization via Deprotonation: Predicting the Ionization Efficiency. *Anal. Chem.* **86**(10), 4822–4830 (2014)
12. Kruve, A., Kaupmees, K., Liigand, J., Oss, M., Leito, I. Sodium adduct formation efficiency in ESI source. *J. Mass Spectrom.* **48**(6), 695–702 (2013)

DISSERTATIONES CHIMICAE UNIVERSITATIS TARTUENSIS

1. **Toomas Tamm.** Quantum-chemical simulation of solvent effects. Tartu, 1993, 110 p.
2. **Peeter Burk.** Theoretical study of gas-phase acid-base equilibria. Tartu, 1994, 96 p.
3. **Victor Lobanov.** Quantitative structure-property relationships in large descriptor spaces. Tartu, 1995, 135 p.
4. **Vahur Mäemets.** The ^{17}O and ^1H nuclear magnetic resonance study of H_2O in individual solvents and its charged clusters in aqueous solutions of electrolytes. Tartu, 1997, 140 p.
5. **Andrus Metsala.** Microcanonical rate constant in nonequilibrium distribution of vibrational energy and in restricted intramolecular vibrational energy redistribution on the basis of Slater's theory of unimolecular reactions. Tartu, 1997, 150 p.
6. **Uko Maran.** Quantum-mechanical study of potential energy surfaces in different environments. Tartu, 1997, 137 p.
7. **Alar Jänes.** Adsorption of organic compounds on antimony, bismuth and cadmium electrodes. Tartu, 1998, 219 p.
8. **Kaido Tammeveski.** Oxygen electroreduction on thin platinum films and the electrochemical detection of superoxide anion. Tartu, 1998, 139 p.
9. **Ivo Leito.** Studies of Brønsted acid-base equilibria in water and non-aqueous media. Tartu, 1998, 101 p.
10. **Jaan Leis.** Conformational dynamics and equilibria in amides. Tartu, 1998, 131 p.
11. **Toonika Rinke.** The modelling of amperometric biosensors based on oxidoreductases. Tartu, 2000, 108 p.
12. **Dmitri Panov.** Partially solvated Grignard reagents. Tartu, 2000, 64 p.
13. **Kaja Orupõld.** Treatment and analysis of phenolic wastewater with microorganisms. Tartu, 2000, 123 p.
14. **Jüri Ivask.** Ion Chromatographic determination of major anions and cations in polar ice core. Tartu, 2000, 85 p.
15. **Lauri Vares.** Stereoselective Synthesis of Tetrahydrofuran and Tetrahydropyran Derivatives by Use of Asymmetric Horner-Wadsworth-Emmons and Ring Closure Reactions. Tartu, 2000, 184 p.
16. **Martin Lepiku.** Kinetic aspects of dopamine D_2 receptor interactions with specific ligands. Tartu, 2000, 81 p.
17. **Katrin Sak.** Some aspects of ligand specificity of P2Y receptors. Tartu, 2000, 106 p.
18. **Vello Pällin.** The role of solvation in the formation of iotsitch complexes. Tartu, 2001, 95 p.
19. **Katrin Kollist.** Interactions between polycyclic aromatic compounds and humic substances. Tartu, 2001, 93 p.

20. **Ivar Koppel.** Quantum chemical study of acidity of strong and superstrong Brønsted acids. Tartu, 2001, 104 p.
21. **Viljar Pihl.** The study of the substituent and solvent effects on the acidity of OH and CH acids. Tartu, 2001, 132 p.
22. **Natalia Palm.** Specification of the minimum, sufficient and significant set of descriptors for general description of solvent effects. Tartu, 2001, 134 p.
23. **Sulev Sild.** QSPR/QSAR approaches for complex molecular systems. Tartu, 2001, 134 p.
24. **Ruslan Petrukhin.** Industrial applications of the quantitative structure-property relationships. Tartu, 2001, 162 p.
25. **Boris V. Rogovoy.** Synthesis of (benzotriazolyl)carboximidamides and their application in relations with *N*- and *S*-nucleophiles. Tartu, 2002, 84 p.
26. **Koit Herodes.** Solvent effects on UV-vis absorption spectra of some solvatochromic substances in binary solvent mixtures: the preferential solvation model. Tartu, 2002, 102 p.
27. **Anti Perkson.** Synthesis and characterisation of nanostructured carbon. Tartu, 2002, 152 p.
28. **Ivari Kaljurand.** Self-consistent acidity scales of neutral and cationic Brønsted acids in acetonitrile and tetrahydrofuran. Tartu, 2003, 108 p.
29. **Karmen Lust.** Adsorption of anions on bismuth single crystal electrodes. Tartu, 2003, 128 p.
30. **Mare Piirsalu.** Substituent, temperature and solvent effects on the alkaline hydrolysis of substituted phenyl and alkyl esters of benzoic acid. Tartu, 2003, 156 p.
31. **Meeri Sassian.** Reactions of partially solvated Grignard reagents. Tartu, 2003, 78 p.
32. **Tarmo Tamm.** Quantum chemical modelling of polypyrrole. Tartu, 2003. 100 p.
33. **Erik Teinmaa.** The environmental fate of the particulate matter and organic pollutants from an oil shale power plant. Tartu, 2003. 102 p.
34. **Jaana Tammiku-Taul.** Quantum chemical study of the properties of Grignard reagents. Tartu, 2003. 120 p.
35. **Andre Lomaka.** Biomedical applications of predictive computational chemistry. Tartu, 2003. 132 p.
36. **Kostyantyn Kirichenko.** Benzotriazole – Mediated Carbon–Carbon Bond Formation. Tartu, 2003. 132 p.
37. **Gunnar Nurk.** Adsorption kinetics of some organic compounds on bismuth single crystal electrodes. Tartu, 2003, 170 p.
38. **Mati Arulepp.** Electrochemical characteristics of porous carbon materials and electrical double layer capacitors. Tartu, 2003, 196 p.
39. **Dan Cornel Fara.** QSPR modeling of complexation and distribution of organic compounds. Tartu, 2004, 126 p.
40. **Riina Mahlapuu.** Signalling of galanin and amyloid precursor protein through adenylate cyclase. Tartu, 2004, 124 p.

41. **Mihkel Kerikmäe.** Some luminescent materials for dosimetric applications and physical research. Tartu, 2004, 143 p.
42. **Jaanus Kruusma.** Determination of some important trace metal ions in human blood. Tartu, 2004, 115 p.
43. **Urmas Johanson.** Investigations of the electrochemical properties of polypyrrole modified electrodes. Tartu, 2004, 91 p.
44. **Kaido Sillar.** Computational study of the acid sites in zeolite ZSM-5. Tartu, 2004, 80 p.
45. **Aldo Oras.** Kinetic aspects of dATP α S interaction with P2Y₁ receptor. Tartu, 2004, 75 p.
46. **Erik Mölder.** Measurement of the oxygen mass transfer through the air-water interface. Tartu, 2005, 73 p.
47. **Thomas Thomborg.** The kinetics of electroreduction of peroxodisulfate anion on cadmium (0001) single crystal electrode. Tartu, 2005, 95 p.
48. **Olavi Loog.** Aspects of condensations of carbonyl compounds and their imine analogues. Tartu, 2005, 83 p.
49. **Siim Salmar.** Effect of ultrasound on ester hydrolysis in aqueous ethanol. Tartu, 2006, 73 p.
50. **Ain Uustare.** Modulation of signal transduction of heptahelical receptors by other receptors and G proteins. Tartu, 2006, 121 p.
51. **Sergei Yurchenko.** Determination of some carcinogenic contaminants in food. Tartu, 2006, 143 p.
52. **Kaido Tämm.** QSPR modeling of some properties of organic compounds. Tartu, 2006, 67 p.
53. **Olga Tšubrik.** New methods in the synthesis of multisubstituted hydrazines. Tartu, 2006, 183 p.
54. **Lilli Sooväli.** Spectrophotometric measurements and their uncertainty in chemical analysis and dissociation constant measurements. Tartu, 2006, 125 p.
55. **Eve Koort.** Uncertainty estimation of potentiometrically measured pH and pK_a values. Tartu, 2006, 139 p.
56. **Sergei Kopanchuk.** Regulation of ligand binding to melanocortin receptor subtypes. Tartu, 2006, 119 p.
57. **Silvar Kallip.** Surface structure of some bismuth and antimony single crystal electrodes. Tartu, 2006, 107 p.
58. **Kristjan Saal.** Surface silanization and its application in biomolecule coupling. Tartu, 2006, 77 p.
59. **Tanel Tätte.** High viscosity Sn(OBu)₄ oligomeric concentrates and their applications in technology. Tartu, 2006, 91 p.
60. **Dimitar Atanasov Dobchev.** Robust QSAR methods for the prediction of properties from molecular structure. Tartu, 2006, 118 p.
61. **Hannes Hagu.** Impact of ultrasound on hydrophobic interactions in solutions. Tartu, 2007, 81 p.
62. **Rutha Jäger.** Electroreduction of peroxodisulfate anion on bismuth electrodes. Tartu, 2007, 142 p.

63. **Kaido Viht.** Immobilizable bisubstrate-analogue inhibitors of basophilic protein kinases: development and application in biosensors. Tartu, 2007, 88 p.
64. **Eva-Ingrid Rõõm.** Acid-base equilibria in nonpolar media. Tartu, 2007, 156 p.
65. **Sven Tamp.** DFT study of the cesium cation containing complexes relevant to the cesium cation binding by the humic acids. Tartu, 2007, 102 p.
66. **Jaak Nerut.** Electroreduction of hexacyanoferrate(III) anion on Cadmium (0001) single crystal electrode. Tartu, 2007, 180 p.
67. **Lauri Jalukse.** Measurement uncertainty estimation in amperometric dissolved oxygen concentration measurement. Tartu, 2007, 112 p.
68. **Aime Lust.** Charge state of dopants and ordered clusters formation in CaF₂:Mn and CaF₂:Eu luminophors. Tartu, 2007, 100 p.
69. **Iiris Kahn.** Quantitative Structure-Activity Relationships of environmentally relevant properties. Tartu, 2007, 98 p.
70. **Mari Reinik.** Nitrates, nitrites, N-nitrosamines and polycyclic aromatic hydrocarbons in food: analytical methods, occurrence and dietary intake. Tartu, 2007, 172 p.
71. **Heili Kasuk.** Thermodynamic parameters and adsorption kinetics of organic compounds forming the compact adsorption layer at Bi single crystal electrodes. Tartu, 2007, 212 p.
72. **Erki Enkvist.** Synthesis of adenosine-peptide conjugates for biological applications. Tartu, 2007, 114 p.
73. **Svetoslav Hristov Slavov.** Biomedical applications of the QSAR approach. Tartu, 2007, 146 p.
74. **Eneli Härk.** Electroreduction of complex cations on electrochemically polished Bi(*hkl*) single crystal electrodes. Tartu, 2008, 158 p.
75. **Priit Möller.** Electrochemical characteristics of some cathodes for medium temperature solid oxide fuel cells, synthesized by solid state reaction technique. Tartu, 2008, 90 p.
76. **Signe Viggor.** Impact of biochemical parameters of genetically different pseudomonads at the degradation of phenolic compounds. Tartu, 2008, 122 p.
77. **Ave Sarapuu.** Electrochemical reduction of oxygen on quinone-modified carbon electrodes and on thin films of platinum and gold. Tartu, 2008, 134 p.
78. **Agnes Kütt.** Studies of acid-base equilibria in non-aqueous media. Tartu, 2008, 198 p.
79. **Rouvim Kadis.** Evaluation of measurement uncertainty in analytical chemistry: related concepts and some points of misinterpretation. Tartu, 2008, 118 p.
80. **Valter Reedo.** Elaboration of IVB group metal oxide structures and their possible applications. Tartu, 2008, 98 p.
81. **Aleksei Kuznetsov.** Allosteric effects in reactions catalyzed by the cAMP-dependent protein kinase catalytic subunit. Tartu, 2009, 133 p.

82. **Aleksei Bredihhin.** Use of mono- and polyanions in the synthesis of multisubstituted hydrazine derivatives. Tartu, 2009, 105 p.
83. **Anu Ploom.** Quantitative structure-reactivity analysis in organosilicon chemistry. Tartu, 2009, 99 p.
84. **Argo Vonk.** Determination of adenosine A_{2A}- and dopamine D₁ receptor-specific modulation of adenylate cyclase activity in rat striatum. Tartu, 2009, 129 p.
85. **Indrek Kivi.** Synthesis and electrochemical characterization of porous cathode materials for intermediate temperature solid oxide fuel cells. Tartu, 2009, 177 p.
86. **Jaanus Eskusson.** Synthesis and characterisation of diamond-like carbon thin films prepared by pulsed laser deposition method. Tartu, 2009, 117 p.
87. **Marko Lätt.** Carbide derived microporous carbon and electrical double layer capacitors. Tartu, 2009, 107 p.
88. **Vladimir Stepanov.** Slow conformational changes in dopamine transporter interaction with its ligands. Tartu, 2009, 103 p.
89. **Aleksander Trummal.** Computational Study of Structural and Solvent Effects on Acidities of Some Brønsted Acids. Tartu, 2009, 103 p.
90. **Eerold Vellemäe.** Applications of mischmetal in organic synthesis. Tartu, 2009, 93 p.
91. **Sven Parkel.** Ligand binding to 5-HT_{1A} receptors and its regulation by Mg²⁺ and Mn²⁺. Tartu, 2010, 99 p.
92. **Signe Vahur.** Expanding the possibilities of ATR-FT-IR spectroscopy in determination of inorganic pigments. Tartu, 2010, 184 p.
93. **Tavo Romann.** Preparation and surface modification of bismuth thin film, porous, and microelectrodes. Tartu, 2010, 155 p.
94. **Nadežda Aleksejeva.** Electrocatalytic reduction of oxygen on carbon nanotube-based nanocomposite materials. Tartu, 2010, 147 p.
95. **Marko Kullapere.** Electrochemical properties of glassy carbon, nickel and gold electrodes modified with aryl groups. Tartu, 2010, 233 p.
96. **Liis Siinor.** Adsorption kinetics of ions at Bi single crystal planes from aqueous electrolyte solutions and room-temperature ionic liquids. Tartu, 2010, 101 p.
97. **Angela Vaasa.** Development of fluorescence-based kinetic and binding assays for characterization of protein kinases and their inhibitors. Tartu 2010, 101 p.
98. **Indrek Tulp.** Multivariate analysis of chemical and biological properties. Tartu 2010, 105 p.
99. **Aare Selberg.** Evaluation of environmental quality in Northern Estonia by the analysis of leachate. Tartu 2010, 117 p.
100. **Darja Lavõgina.** Development of protein kinase inhibitors based on adenosine analogue-oligoarginine conjugates. Tartu 2010, 248 p.
101. **Laura Herm.** Biochemistry of dopamine D₂ receptors and its association with motivated behaviour. Tartu 2010, 156 p.

102. **Terje Raudsepp.** Influence of dopant anions on the electrochemical properties of polypyrrole films. Tartu 2010, 112 p.
103. **Margus Marandi.** Electroformation of Polypyrrole Films: *In-situ* AFM and STM Study. Tartu 2011, 116 p.
104. **Kairi Kivirand.** Diamine oxidase-based biosensors: construction and working principles. Tartu, 2011, 140 p.
105. **Anneli Kruve.** Matrix effects in liquid-chromatography electrospray mass-spectrometry. Tartu, 2011, 156 p.
106. **Gary Urb.** Assessment of environmental impact of oil shale fly ash from PF and CFB combustion. Tartu, 2011, 108 p.
107. **Nikita Oskolkov.** A novel strategy for peptide-mediated cellular delivery and induction of endosomal escape. Tartu, 2011, 106 p.
108. **Dana Martin.** The QSPR/QSAR approach for the prediction of properties of fullerene derivatives. Tartu, 2011, 98 p.
109. **Säde Viirlaid.** Novel glutathione analogues and their antioxidant activity. Tartu, 2011, 106 p.
110. **Ülis Sõukand.** Simultaneous adsorption of Cd²⁺, Ni²⁺, and Pb²⁺ on peat. Tartu, 2011, 124 p.
111. **Lauri Lipping.** The acidity of strong and superstrong Brønsted acids, an outreach for the “limits of growth”: a quantum chemical study. Tartu, 2011, 124 p.
112. **Heisi Kurig.** Electrical double-layer capacitors based on ionic liquids as electrolytes. Tartu, 2011, 146 p.
113. **Marje Kasari.** Bisubstrate luminescent probes, optical sensors and affinity adsorbents for measurement of active protein kinases in biological samples. Tartu, 2012, 126 p.
114. **Kalev Takkis.** Virtual screening of chemical databases for bioactive molecules. Tartu, 2012, 122 p.
115. **Ksenija Kisseljova.** Synthesis of aza-β³-amino acid containing peptides and kinetic study of their phosphorylation by protein kinase A. Tartu, 2012, 104 p.
116. **Riin Rebane.** Advanced method development strategy for derivatization LC/ESI/MS. Tartu, 2012, 184 p.
117. **Vladislav Ivaništšev.** Double layer structure and adsorption kinetics of ions at metal electrodes in room temperature ionic liquids. Tartu, 2012, 128 p.
118. **Irja Helm.** High accuracy gravimetric Winkler method for determination of dissolved oxygen. Tartu, 2012, 139 p.
119. **Karin Kipper.** Fluoroalcohols as Components of LC-ESI-MS Eluents: Usage and Applications. Tartu, 2012, 164 p.
120. **Arno Ratas.** Energy storage and transfer in dosimetric luminescent materials. Tartu, 2012, 163 p.
121. **Reet Reinart-Okugbeni.** Assay systems for characterisation of subtype-selective binding and functional activity of ligands on dopamine receptors. Tartu, 2012, 159 p.

122. **Lauri Sikk.** Computational study of the Sonogashira cross-coupling reaction. Tartu, 2012, 81 p.
123. **Karita Raudkivi.** Neurochemical studies on inter-individual differences in affect-related behaviour of the laboratory rat. Tartu, 2012, 161 p.
124. **Indrek Saar.** Design of GalR2 subtype specific ligands: their role in depression-like behavior and feeding regulation. Tartu, 2013, 126 p.
125. **Ann Laheäär.** Electrochemical characterization of alkali metal salt based non-aqueous electrolytes for supercapacitors. Tartu, 2013, 127 p.
126. **Kerli Tõnurist.** Influence of electrospun separator materials properties on electrochemical performance of electrical double-layer capacitors. Tartu, 2013, 147 p.
127. **Kaija Põhako-Esko.** Novel organic and inorganic ionogels: preparation and characterization. Tartu, 2013, 124 p.
128. **Ivar Kruusenberg.** Electroreduction of oxygen on carbon nanomaterial-based catalysts. Tartu, 2013, 191 p.
129. **Sander Piiskop.** Kinetic effects of ultrasound in aqueous acetonitrile solutions. Tartu, 2013, 95 p.
130. **Ilona Faustova.** Regulatory role of L-type pyruvate kinase N-terminal domain. Tartu, 2013, 109 p.
131. **Kadi Tamm.** Synthesis and characterization of the micro-mesoporous anode materials and testing of the medium temperature solid oxide fuel cell single cells. Tartu, 2013, 138 p.
132. **Iva Bozhidarova Stoyanova-Slavova.** Validation of QSAR/QSPR for regulatory purposes. Tartu, 2013, 109 p.
133. **Vitali Grozovski.** Adsorption of organic molecules at single crystal electrodes studied by *in situ* STM method. Tartu, 2014, 146 p.
134. **Santa Veikšina.** Development of assay systems for characterisation of ligand binding properties to melanocortin 4 receptors. Tartu, 2014, 151 p.
135. **Jüri Liiv.** PVDF (polyvinylidene difluoride) as material for active element of twisting-ball displays. Tartu, 2014, 111 p.
136. **Kersti Vaarmets.** Electrochemical and physical characterization of pristine and activated molybdenum carbide-derived carbon electrodes for the oxygen electroreduction reaction. Tartu, 2014, 131 p.
137. **Lauri Tõntson.** Regulation of G-protein subtypes by receptors, guanine nucleotides and Mn²⁺. Tartu, 2014, 105 p.
138. **Aiko Adamson.** Properties of amine-boranes and phosphorus analogues in the gas phase. Tartu, 2014, 78 p.
139. **Elo Kibena.** Electrochemical grafting of glassy carbon, gold, highly oriented pyrolytic graphite and chemical vapour deposition-grown graphene electrodes by diazonium reduction method. Tartu, 2014, 184 p.
140. **Teemu Näykki.** Novel Tools for Water Quality Monitoring – From Field to Laboratory. Tartu, 2014, 202 p.
141. **Karl Kaupmees.** Acidity and basicity in non-aqueous media: importance of solvent properties and purity. Tartu, 2014, 128 p.

142. **Oleg Lebedev.** Hydrazine polyanions: different strategies in the synthesis of heterocycles. Tartu, 2015, 118 p.
143. **Geven Piir.** Environmental risk assessment of chemicals using QSAR methods. Tartu, 2015, 123 p.
144. **Olga Mazina.** Development and application of the biosensor assay for measurements of cyclic adenosine monophosphate in studies of G protein-coupled receptor signaling. Tartu, 2015, 116 p.
145. **Sandip Ashokrao Kadam.** Anion receptors: synthesis and accurate binding measurements. Tartu, 2015, 116 p.
146. **Indrek Tallo.** Synthesis and characterization of new micro-mesoporous carbide derived carbon materials for high energy and power density electrical double layer capacitors. Tartu, 2015, 148 p.
147. **Heiki Erikson.** Electrochemical reduction of oxygen on nanostructured palladium and gold catalysts. Tartu, 2015, 204 p.
148. **Erik Anderson.** *In situ* Scanning Tunnelling Microscopy studies of the interfacial structure between Bi(111) electrode and a room temperature ionic liquid. Tartu, 2015, 118 p.
149. **Girinath G. Pillai.** Computational Modelling of Diverse Chemical, Biochemical and Biomedical Properties. Tartu, 2015, 140 p.
150. **Piret Pikma.** Interfacial structure and adsorption of organic compounds at Cd(0001) and Sb(111) electrodes from ionic liquid and aqueous electrolytes: an *in situ* STM study. Tartu, 2015, 126 p.
151. **Ganesh babu Manoharan.** Combining chemical and genetic approaches for photoluminescence assays of protein kinases. Tartu, 2016, 126 p.
152. **Carolyn Siimenson.** Electrochemical characterization of halide ion adsorption from liquid mixtures at Bi(111) and pyrolytic graphite electrode surface. Tartu, 2016, 110 p.
153. **Asko Laaniste.** Comparison and optimisation of novel mass spectrometry ionisation sources. Tartu, 2016, 156 p.
154. **Hanno Evard.** Estimating limit of detection for mass spectrometric analysis methods. Tartu, 2016, 224 p.
155. **Kadri Ligi.** Characterization and application of protein kinase-responsive organic probes with triplet-singlet energy transfer. Tartu, 2016, 122 p.
156. **Margarita Kagan.** Biosensing penicillins' residues in milk flows. Tartu, 2016, 130 p.
157. **Marie Kriisa.** Development of protein kinase-responsive photoluminescent probes and cellular regulators of protein phosphorylation. Tartu, 2016, 106 p.
158. **Mihkel Vestli.** Ultrasonic spray pyrolysis deposited electrolyte layers for intermediate temperature solid oxide fuel cells. Tartu, 2016, 156 p.
159. **Silver Sepp.** Influence of porosity of the carbide-derived carbon on the properties of the composite electrocatalysts and characteristics of polymer electrolyte fuel cells. Tartu, 2016, 137 p.
160. **Kristjan Haav.** Quantitative relative equilibrium constant measurements in supramolecular chemistry. Tartu, 2017, 158 p.

161. **Anu Teearu.** Development of MALDI-FT-ICR-MS methodology for the analysis of resinous materials. Tartu, 2017, 205 p.
162. **Taavi Ivan.** Bifunctional inhibitors and photoluminescent probes for studies on protein complexes. Tartu, 2017, 140 p.
163. **Maarja-Liisa Oldekop.** Characterization of amino acid derivatization reagents for LC-MS analysis. Tartu, 2017, 147 p.
164. **Kristel Jukk.** Electrochemical reduction of oxygen on platinum- and palladium-based nanocatalysts. Tartu, 2017, 250 p.
165. **Siim Kukk.** Kinetic aspects of interaction between dopamine transporter and *N*-substituted nortropine derivatives. Tartu, 2017, 107 p.
166. **Birgit Viira.** Design and modelling in early drug development in targeting HIV-1 reverse transcriptase and Malaria. Tartu, 2017, 172 p.
167. **Rait Kivi.** Allostery in cAMP dependent protein kinase catalytic subunit. Tartu, 2017, 115 p.
168. **Agnes Heering.** Experimental realization and applications of the unified acidity scale. Tartu, 2017, 123 p.
169. **Delia Juronen.** Biosensing system for the rapid multiplex detection of mastitis-causing pathogens in milk. Tartu, 2018, 85 p.
170. **Hedi Rahnel.** ARC-inhibitors: from reliable biochemical assays to regulators of physiology of cells. Tartu, 2018, 176 p.
171. **Anton Ruzanov.** Computational investigation of the electrical double layer at metal–aqueous solution and metal–ionic liquid interfaces. Tartu, 2018, 129 p.
172. **Katrin Kestav.** Crystal Structure-Guided Development of Bisubstrate-Analogue Inhibitors of Mitotic Protein Kinase Haspin. Tartu, 2018, 166 p.
173. **Mihkel Ilisson.** Synthesis of novel heterocyclic hydrazine derivatives and their conjugates. Tartu, 2018, 101 p.
174. **Anni Allikalt.** Development of assay systems for studying ligand binding to dopamine receptors. Tartu, 2018, 160 p.
175. **Ove Oll.** Electrical double layer structure and energy storage characteristics of ionic liquid based capacitors. Tartu, 2018, 187 p.
176. **Rasmus Palm.** Carbon materials for energy storage applications. Tartu, 2018, 114 p.
177. **Jürgen Metsik.** Preparation and stability of poly(3,4-ethylenedioxythiophene) thin films for transparent electrode applications. Tartu, 2018, 111 p.
178. **Sofja Tšepelevitš.** Experimental studies and modeling of solute-solvent interactions. Tartu, 2018, 109 p.
179. **Märt Lõkov.** Basicity of some nitrogen, phosphorus and carbon bases in acetonitrile. Tartu, 2018, 104 p.
180. **Anton Mastitski.** Preparation of α -aza-amino acid precursors and related compounds by novel methods of reductive one-pot alkylation and direct alkylation. Tartu, 2018, 155 p.
181. **Jürgen Vahter.** Development of bisubstrate inhibitors for protein kinase CK2. Tartu, 2019, 186 p.

182. **Piia Liigand.** Expanding and improving methodology and applications of ionization efficiency measurements. Tartu, 2019, 189 p.
183. **Sigrid Selberg.** Synthesis and properties of lipophilic phosphazene-based indicator molecules. Tartu, 2019, 74 p.